

Instrumentation for High Energy Physics

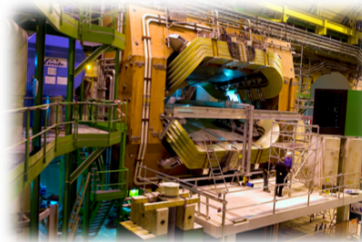
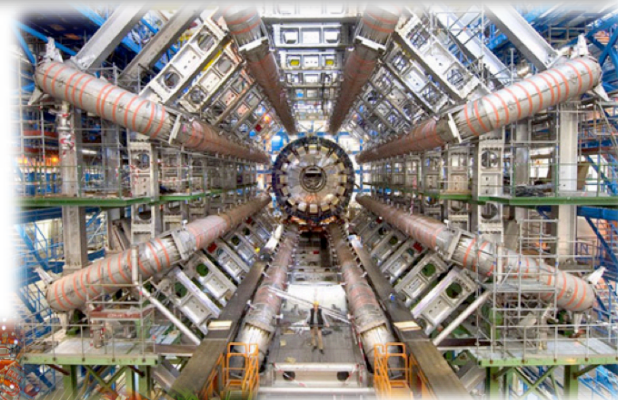
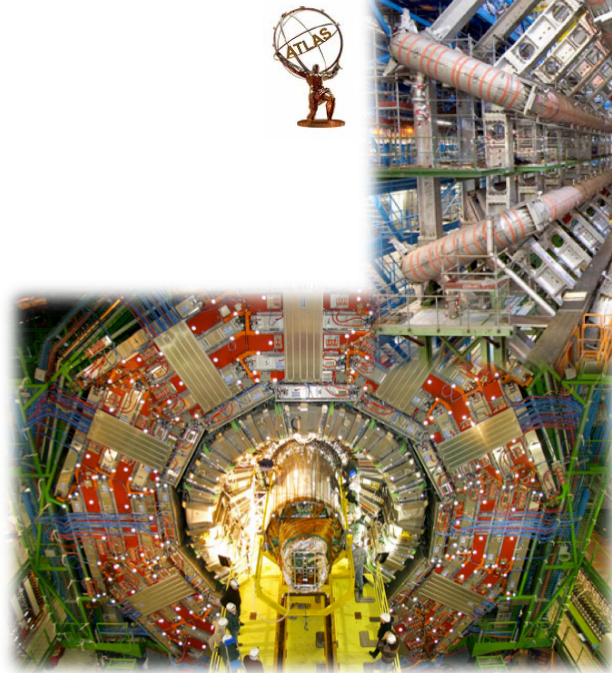
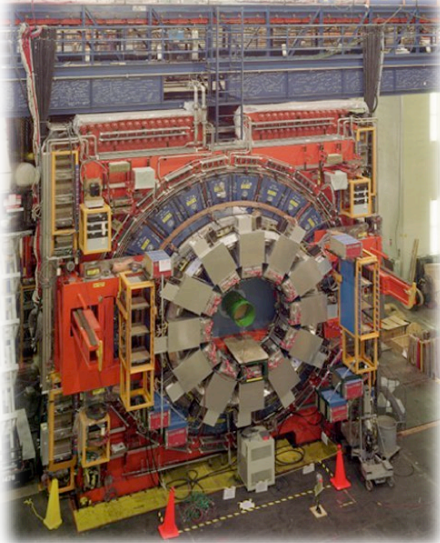
- *Introduction*
- *Particle ID*
- **Particle momenta measurement**
- *Particle Energy measurement*

Ludwik Dobrzynski

Laboratoire Leprince Ringuet - Ecole polytechnique - CNRS - IN2P3

Cairo April 2014

Hadron Colliders: Detectors



■ Multipurpose detectors have similar components :

- **Inner trackers**
- **Calorimeters**
- Outer **muon detectors**

Note: CDF and D0 have ~1 million channels. ATLAS and CMS much larger in magnitude, about 100 million electronic channels !

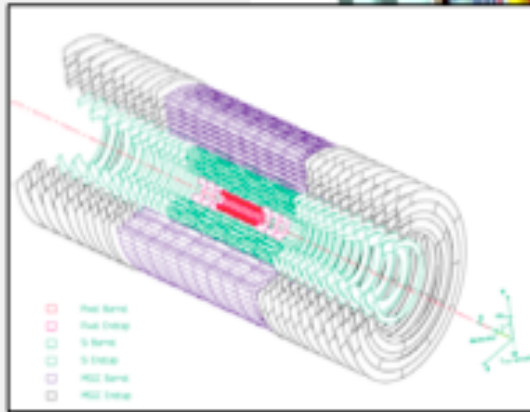
SUPERCONDUCTING COIL

Total weight : 12,500 t
 Overall diameter : 15 m
 Overall length : 21.6 m
 Magnetic field : 4 Tesla

CALORIMETERS
 ECAL Scintillating $PbWO_4$ Crystals
 HCAL Plastic scintillator copper sandwich

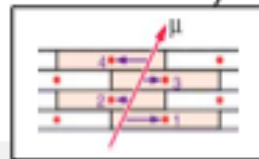
IRON YOKE

TRACKERS

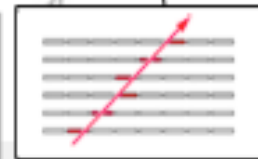


Silicon Microstrips
 Pixels

MUON BARREL

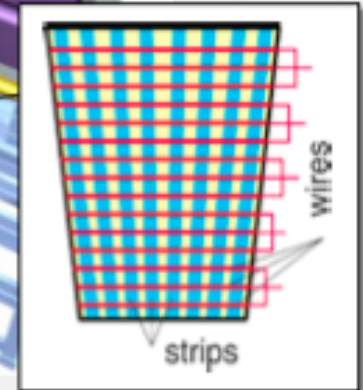


Drift Tube
 Chambers (DT)

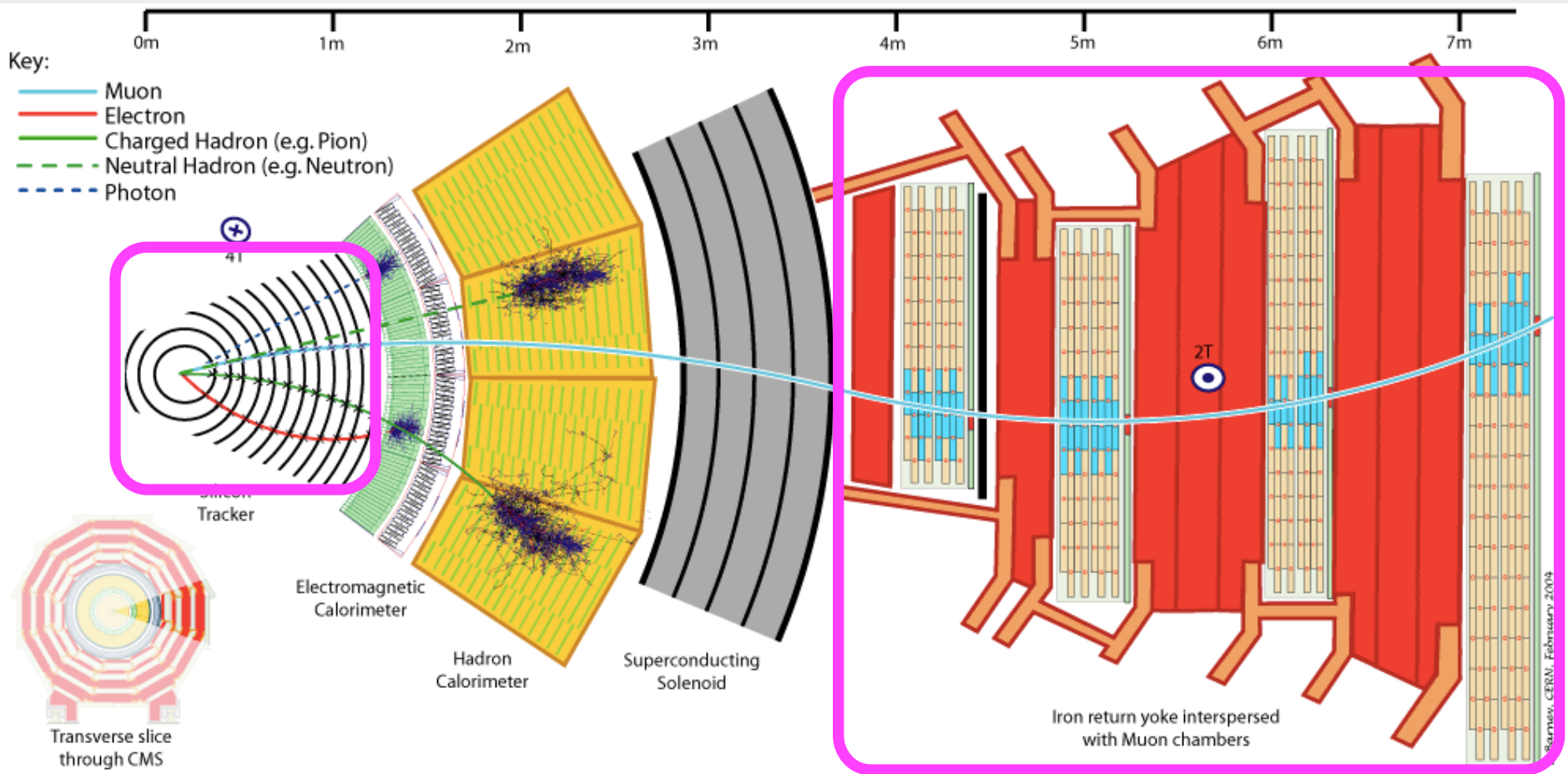


Resistive Plate
 Chambers (RPC)

MUON ENDCAPS



Cathode Strip Chambers (CSC)
 Resistive Plate Chambers (RPC)





Tracking basic concepts

LMR

- In HEP, tracking is the act of measuring the direction and magnitude of *charged particle* momentum, and determining the particle position
- It is a well established process, very complex due to the high track density in modern experiments. It needs specific implementation adapted to the detector type and geometry
- A good tracking performance is critical to allow
 - Precise momentum measurement
 - invariant mass determination
 - Identification of multiple vertices / track impact parameter (long-life particles)
- Track reconstruction requires track finding (pattern recognition) and estimation of track parameters (fitting)
- Alignment is a prerequisite for tracking

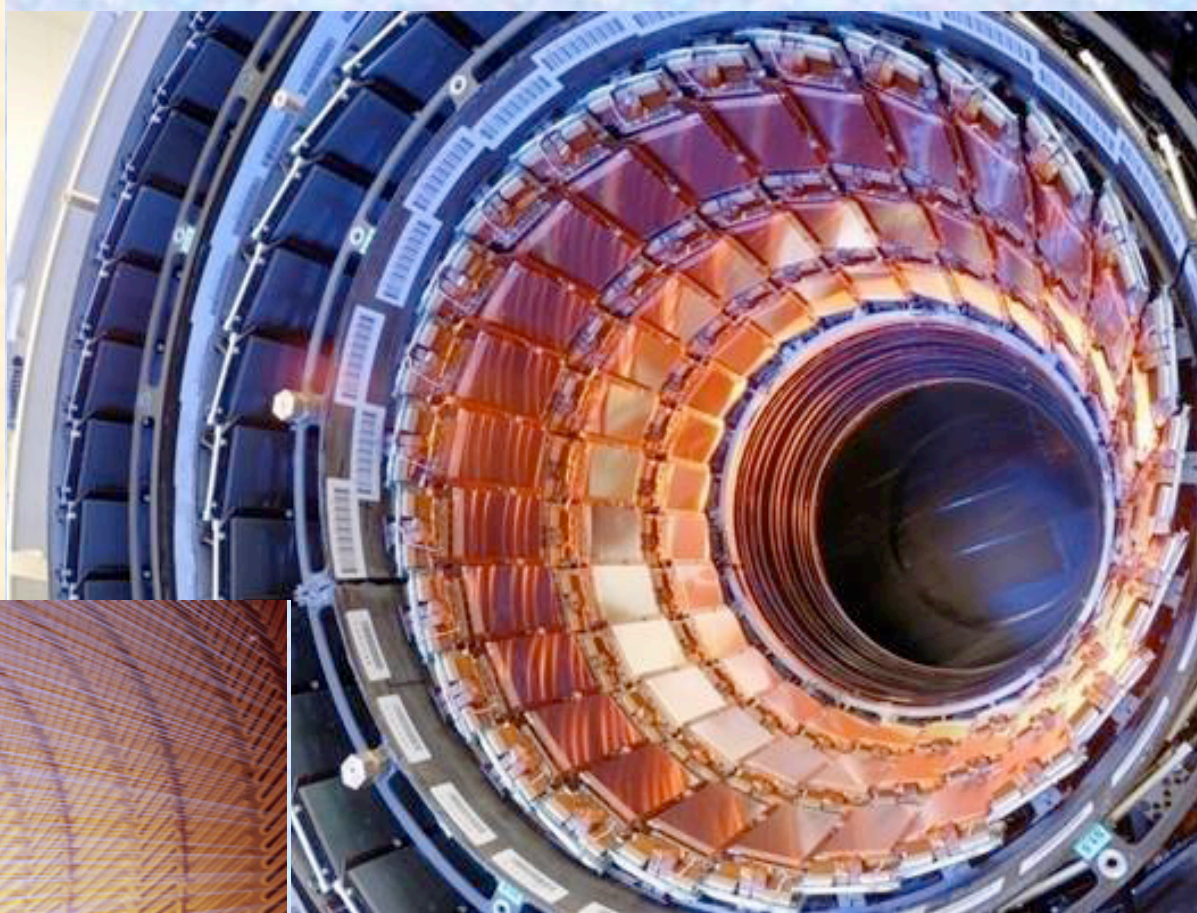
Gaseous detectors

Measure: hit and/or drift time

- Position resolution: $\sim 50 \mu\text{m}$
 - Tracks reconstruction
- + Magnetic field
 - Momentum

Measure also: energy loss dE/dx

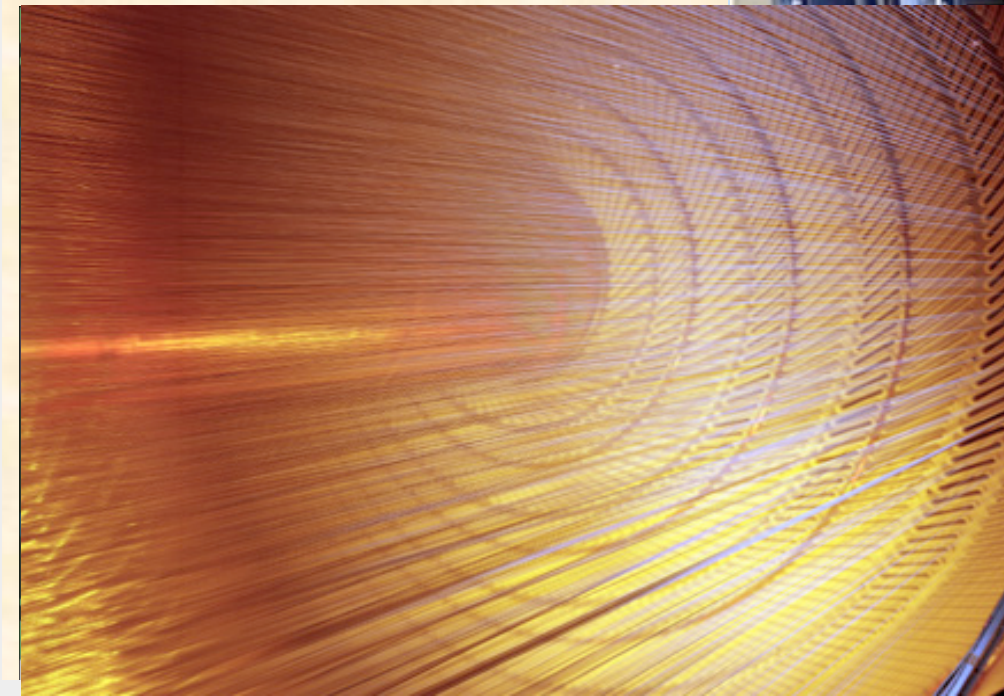
- Particle ID



Silicon detectors

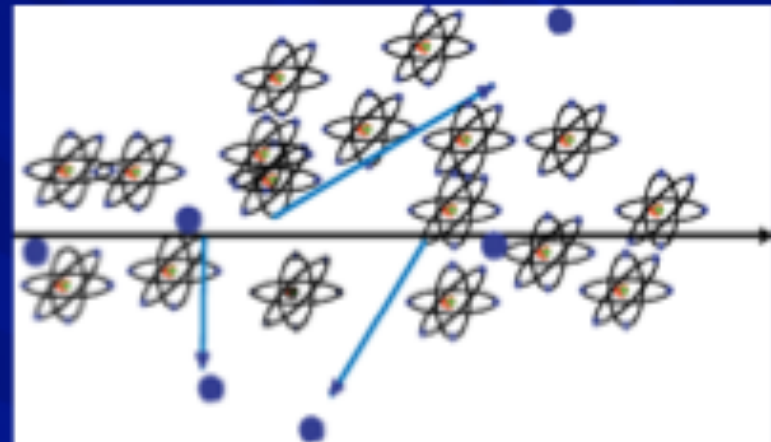
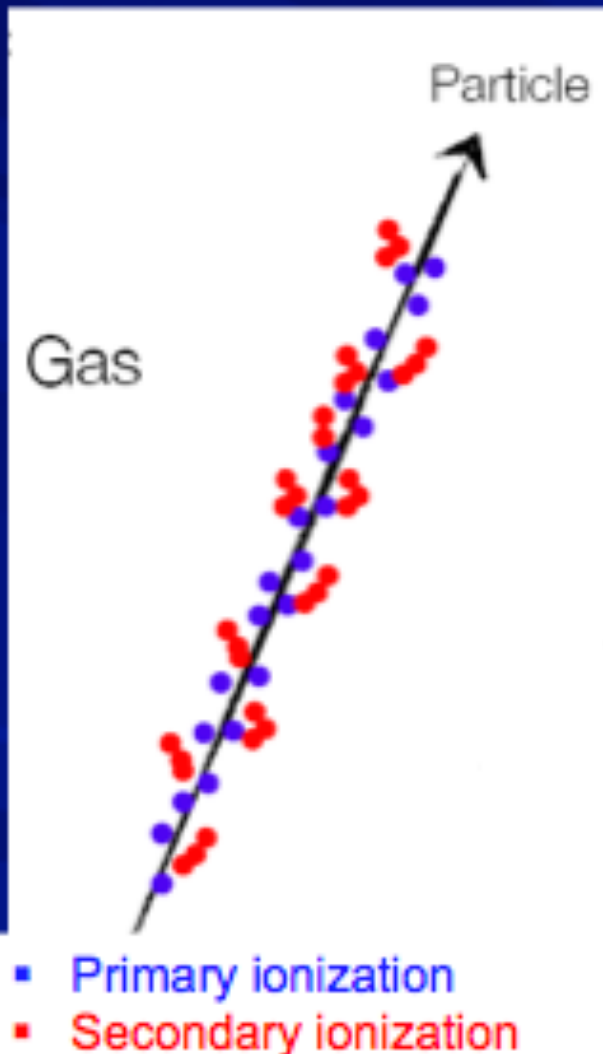
Measure: hits and/or amplitude

- Position resolution: $\sim 5 \mu\text{m}$
- Tracks & **Vertices** reconstruction



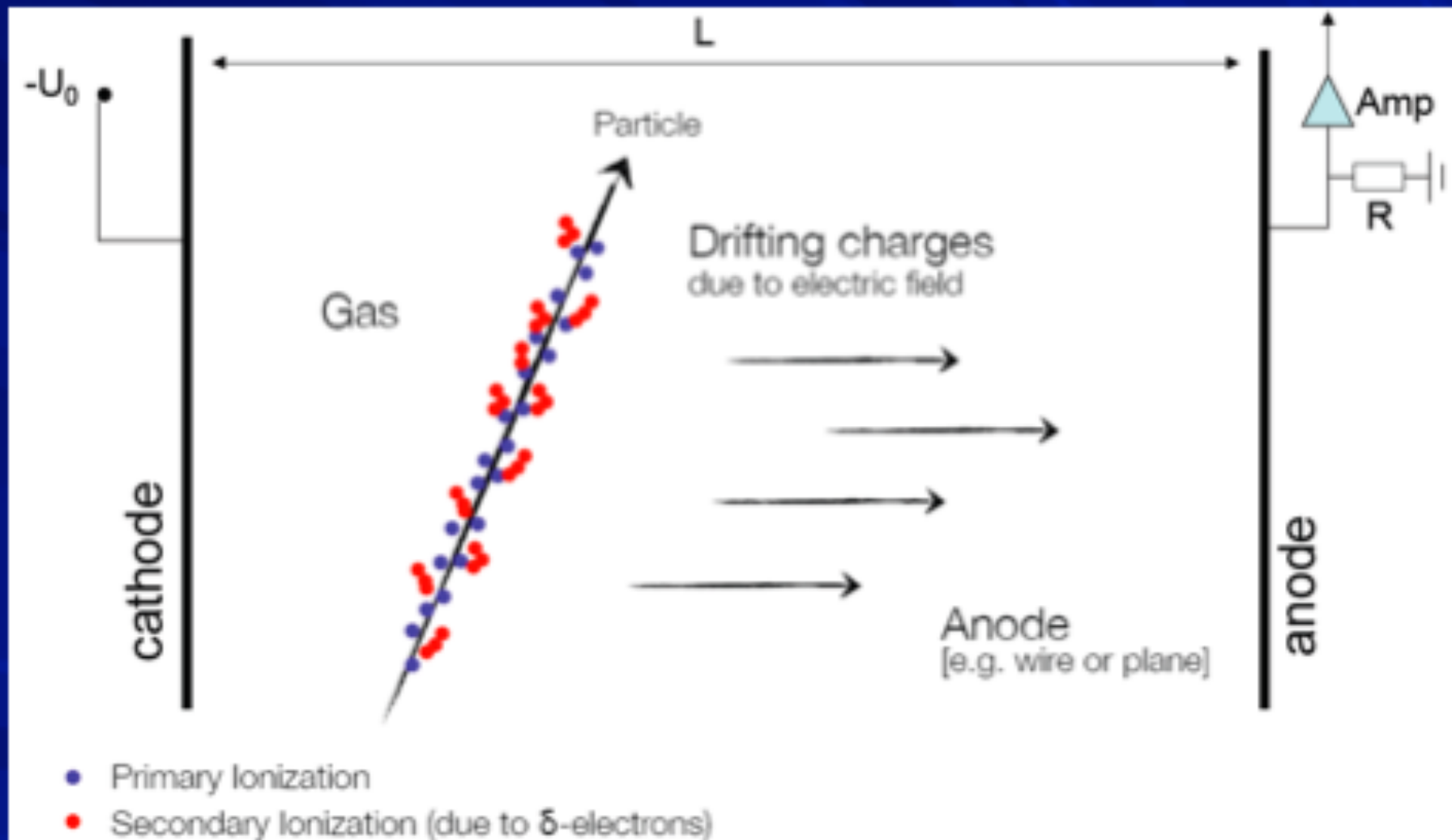
Signal creation

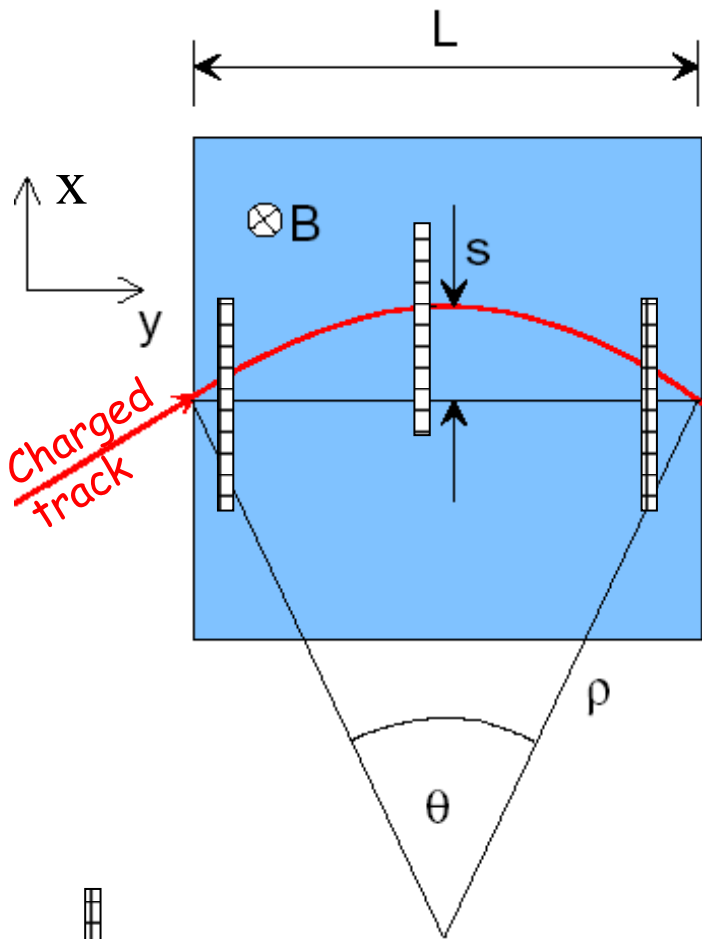
- Charged particle traversing matter leave excited atoms, electron-ion pairs (gases) and electrons-hole pairs (solids)



- Excitation: The photons emitted by the excited atoms in transparent materials can be detected with photon detectors
- Ionization: By applying an electric field in the detector volume, the ionization electrons and ions can be collected on electrodes and readout

Gas Detectors: primary





$$p_T \text{ (GeV/c)} = 0.3 B \rho \quad (\text{T} \cdot \text{m})$$

$$\frac{L}{2\rho} = \sin \theta/2 \approx \theta/2 \quad \rightarrow \quad \theta \approx \frac{0.3 L \cdot B}{p_T}$$

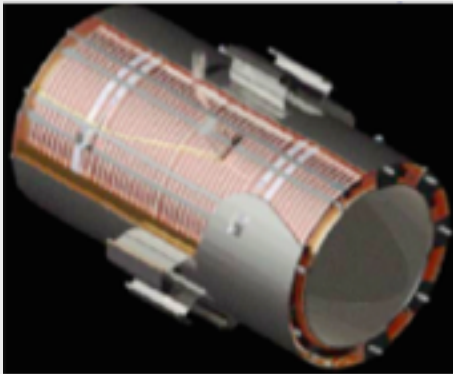
$$s = \rho(1 - \cos \theta/2) \approx \rho \frac{\theta^2}{8} \approx \frac{0.3 L^2 B}{8 p_T}$$

Resolution degrades because of
 → Multiple scattering (material in the detector)
 → Misalignment

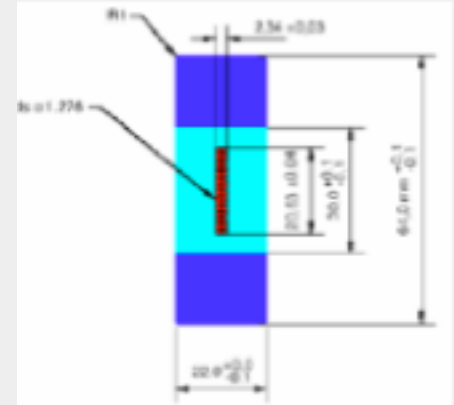
• In more realistic detector with N points (equally spaced):

$$\frac{\sigma(p_T)}{p_T} \approx \sqrt{\frac{720}{N+4}} \sigma_x \frac{p_T}{0.3 B L^2}$$

- **Basic goal : measure 1 TeV muons with 10% resolution**
 - CMS choice $B=4T$ ($E=2.7GJ$) offer 10-20 μm resolution



Challenge : 4 turns winding to carry enough current what imply to have a design to reinforce the superconducting cable

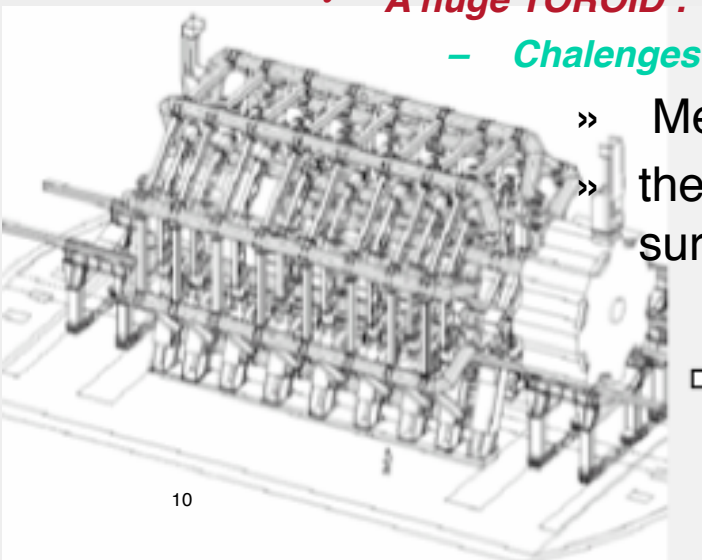


- ATLAS choice require (50 μm resolution):

- **A central solenoid**
- **A huge TOROID :**

– **Challenges :**

- » Mechanics should resist to a store of 1.5 GJ if quench
- » the spacial and alignment precision over a large surface area



Two main classes of detectors :

- Gaseous detectors : *(for more details see )*

well adapted as low material density : small amount of X0 and so small multiple scattering.

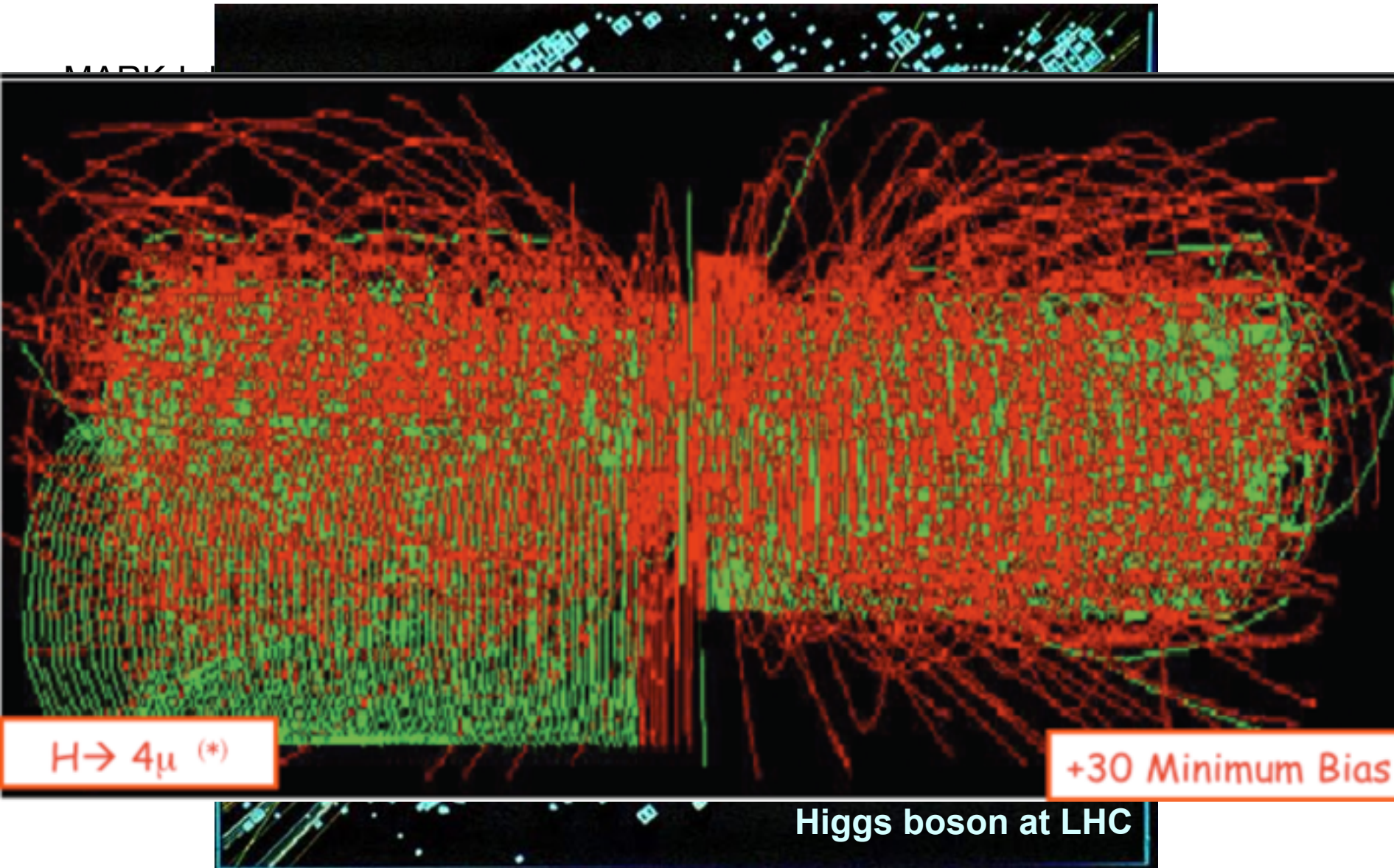
- proportional counter,
- Multi Wire Proportional Chamber,
- TPC,
- microgaseous detectors like GEM,
- MicroMegas...

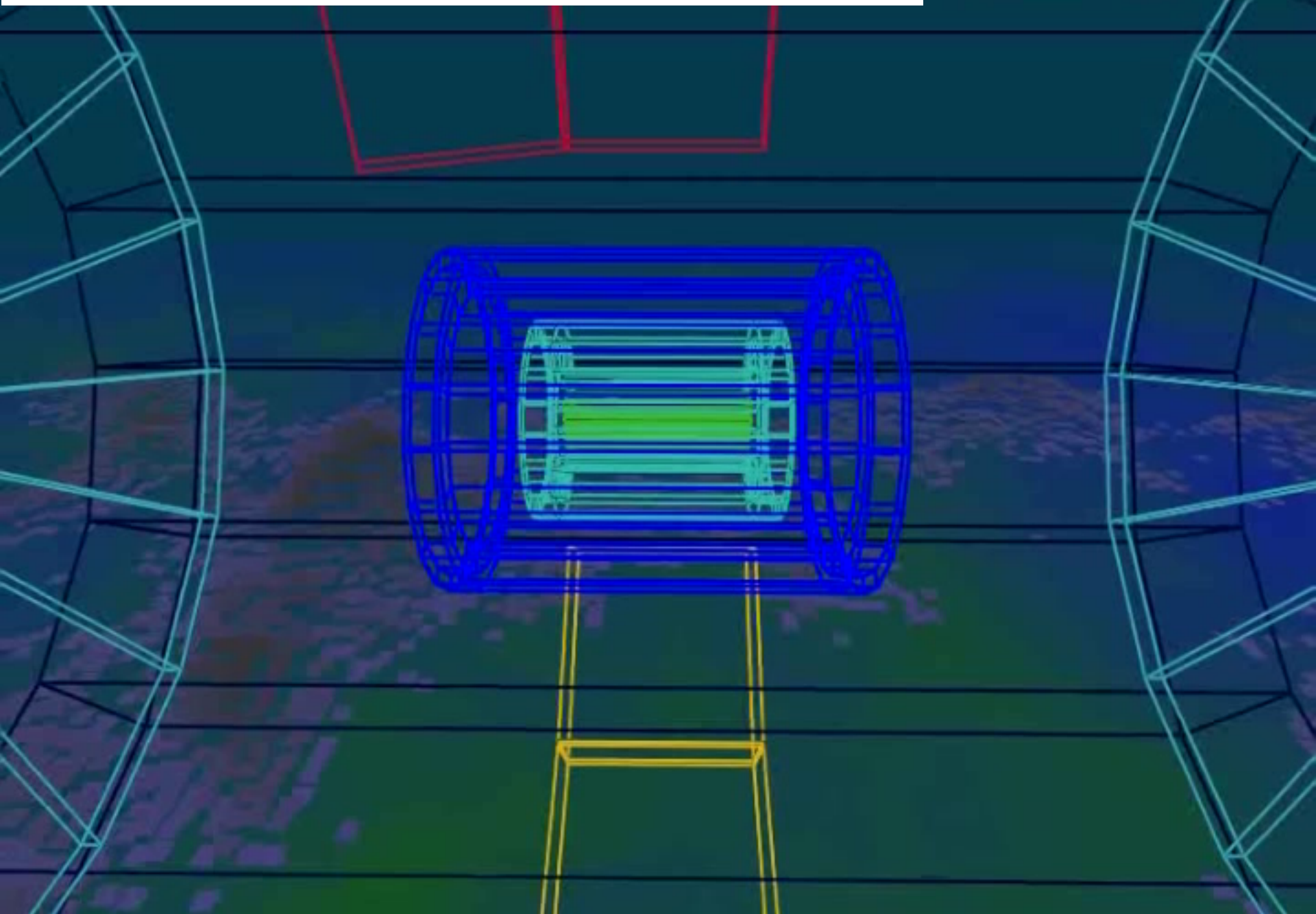
Not always suited for high rate environment (too slow)

-Solid state detectors : *(for more details see )*

- Used for energy measurement (Si, Ge, Ge(Li)) since long time at low energy (nuclear physics).
- **Precision device** in High Energy physics (due to advance in micro electronic techniques) : very small granularity and small device
- **Drawback : no charge multiplication mechanism! and quite dense**

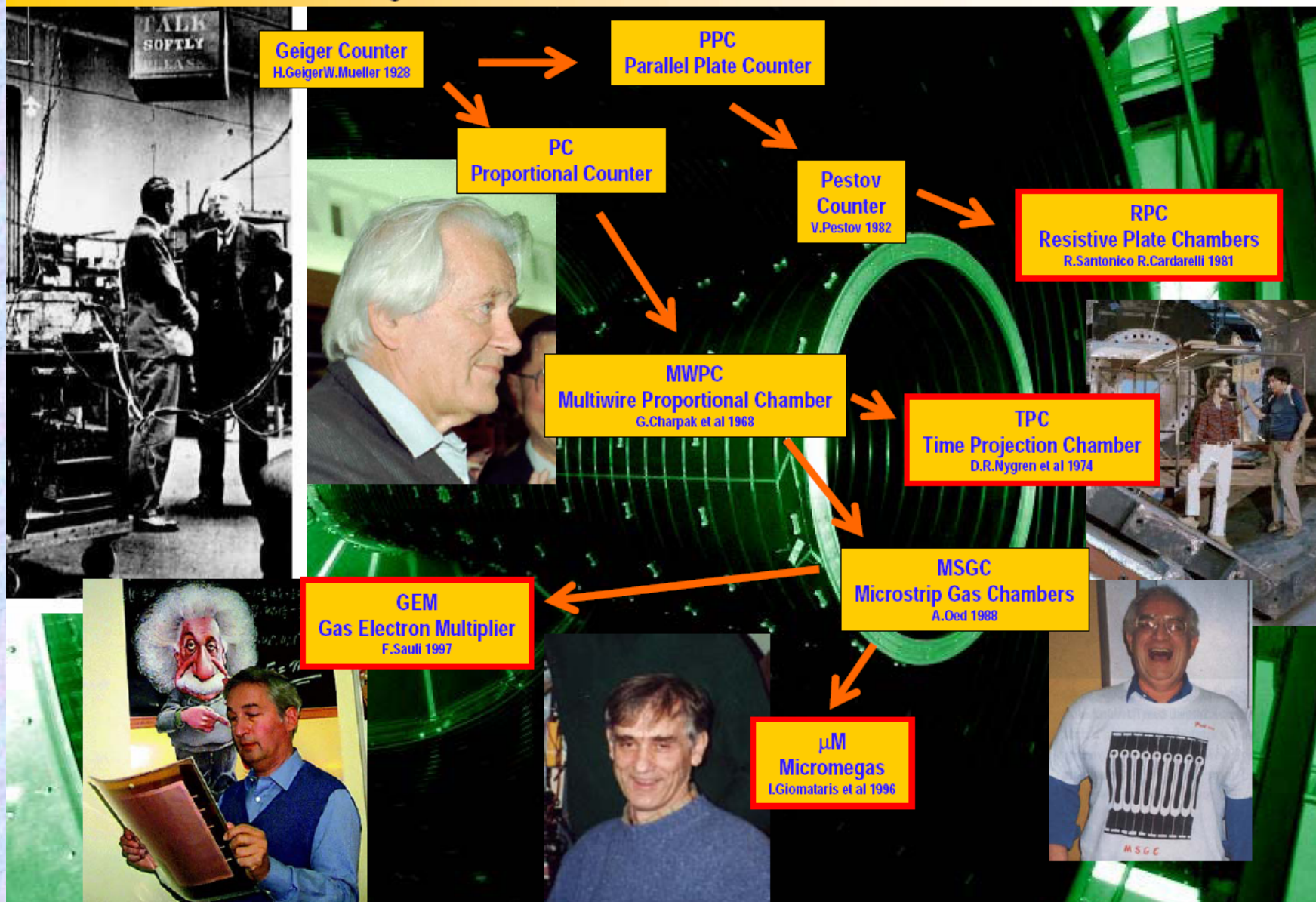
Increasing challenges





History of Gaseous Detector Developments

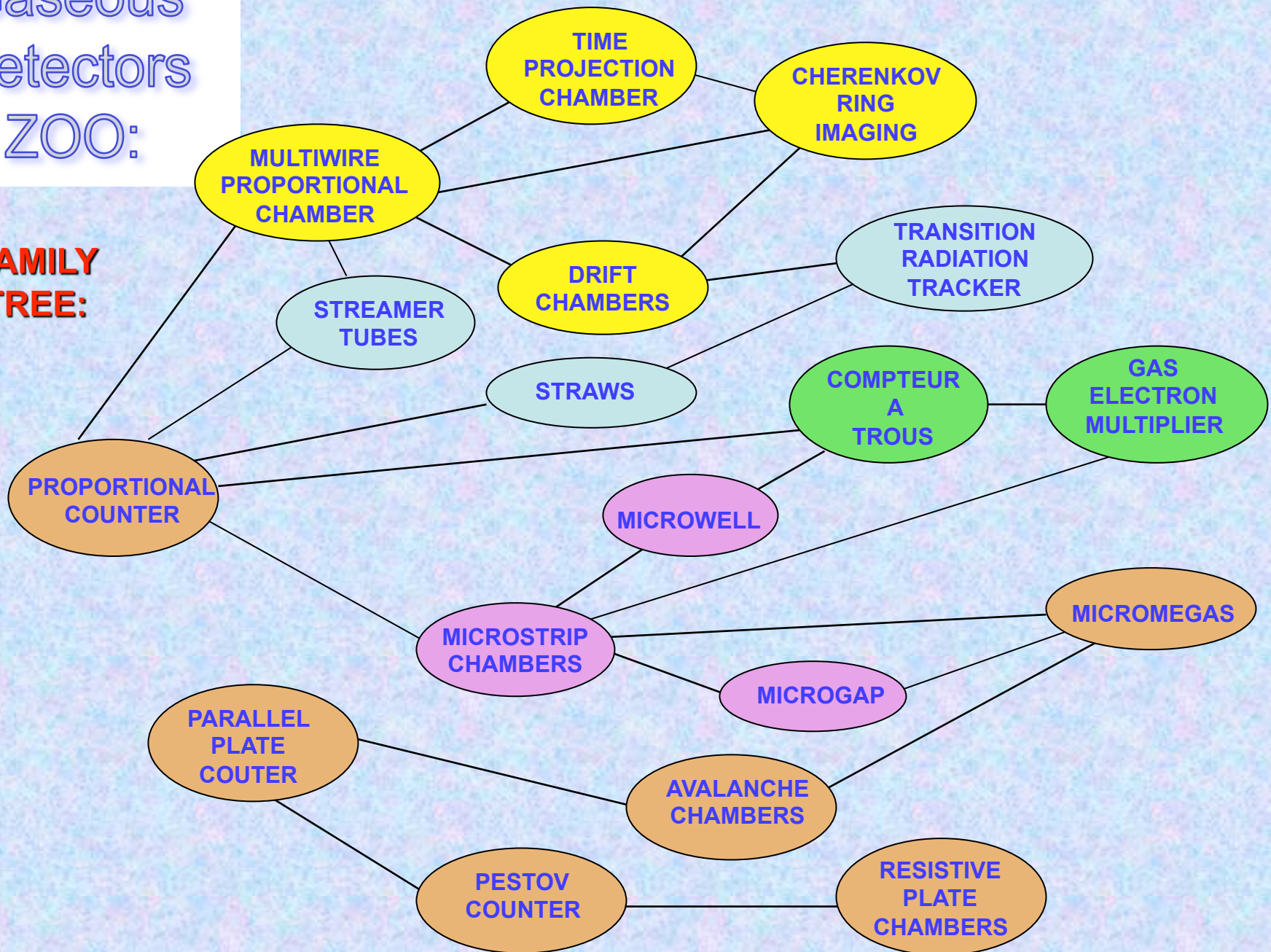
Gas Detector History



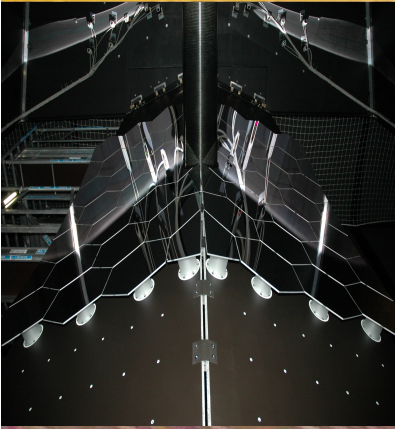
Gaseous Detectors ZOO:

(for more details see )

FAMILY TREE:



Example: Gaseous Detector in the LHC Experiments

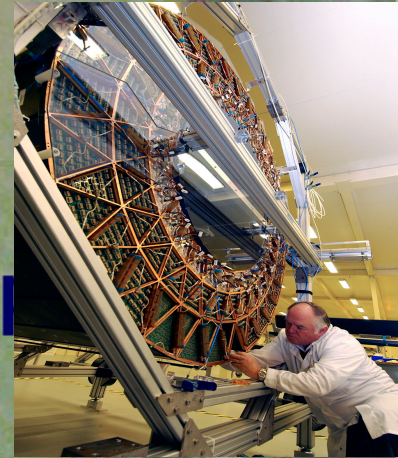


ALICE: TPC (tracker), TRD (transition rad.), TOF (MRPC), HMPID (RICH-pad chamber), Muon tracking (pad chamber), Muon trigger (RPC)

ATLAS: TRD (straw tubes), MDT (muon drift tubes), Muon trigger (RPC, thin gap chambers)

CMS: Muon detector (drift tubes, CSC), RPC (muon trigger)

LHCb: Tracker (straw tubes), Muon detector (MWPC, GEM)



- **Gaseous detectors are still the first choice whenever the large area particle detection and medium precision measurements is required**
- **Advances in photolithography and micro-processing techniques in the chip industry during the past decade triggered a major transition in the field of gas detectors from wire structures to micro-pattern devices.**
- **MPGDs became a wide-spread tool for experiments at the ENERGY, INTENSITY and COSMIC FRONTIERS: for high-rate tracking over large sensitive areas, precision reconstruction of charged particles in the TPC, X-ray, UV and visible photon detection and neutron spectroscopy.**
- **Industrial methods of MPGD production allows to extend technology to $\sim m^2$ unit detectors \rightarrow many potential MPGD applications within the HEP and beyond**
- **Modern, sensitive & low noise electronics (e.g. Timepix CMOS chip, etc ...) will enlarge the range of applications**

Even if new strips *gas detector* now stands the high flux, *alternative is solid state detectors* :

- Solid state detectors have been intensively used for low energy measurement
- Used as position measurement detectors

Advantages : (example of Si)

- High radiation hardness
- Can accept very large flux and very small segmentation
- Rigid detectors so self “supporting structures”
- Energy to create e-/hole pair is very low 3.6 eV (1/10 of gas)
- High density 2.33 g/cm³ . dE/dx per track is 390 eV/μm
 - 108 e/h pairs
 - High mobility : 1450 cm²/Vs for electron and 450 for holes
 - small size and fast signal
- *Very good single point accuracy*

Disadvantages : No charge multiplication , no continuous tracking

- Needs cooling system to operate at low temperature (less radiation effect)
- High density : radiation length before calorimeter
- Cost but less true taken into account the large area produced for LHC

A semiconductor detector! Also called a solid state detector.

Through going charged particles create electron hole pairs.

These charges drift to the electrodes.

The drift generates a signal.

Semiconductor detectors are used for:

- ***Nuclear Physics***

Energy measurement of charged particles (MeV range), gamma spectroscopy (precise determination of photon energy)

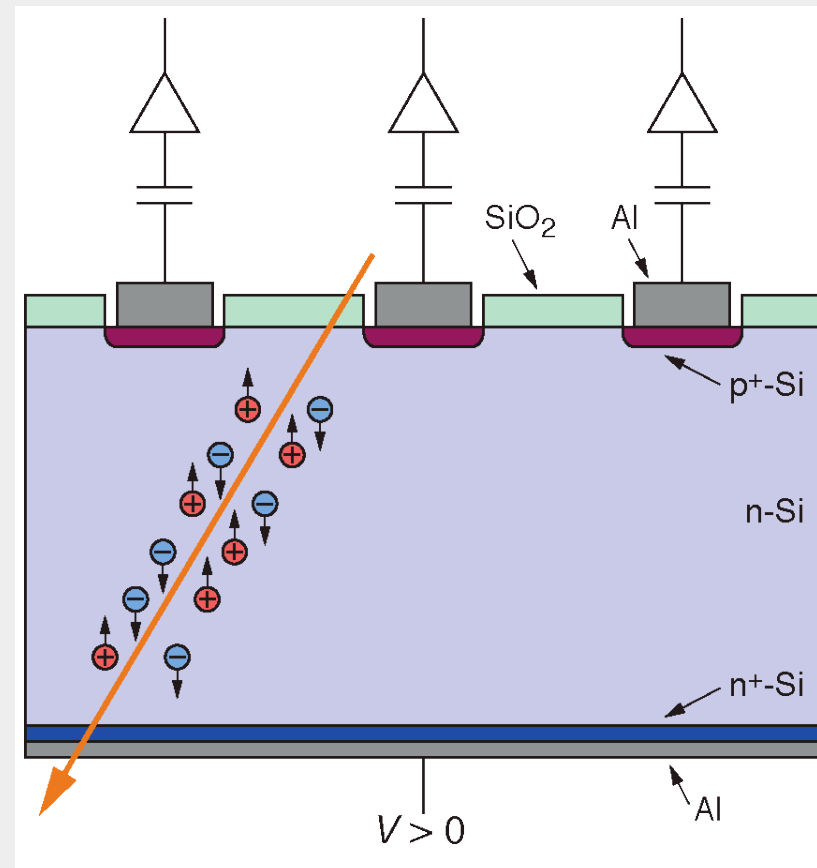
- ***Particle Physics:*** Tracking or vertex detectors, precise determination of particle tracks and decay vertices

- ***Satellite Experiments***

Tracking detectors

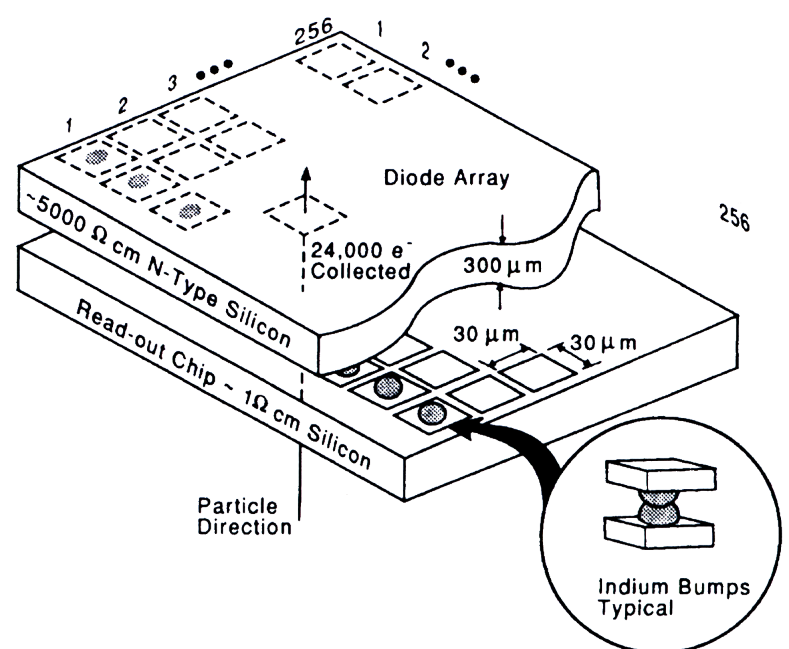
- ***Industrial Applications***

Security, Medicine, Biology,...



Principle

“Flip-Chip” pixel detector: On top the Si detector, below the readout chip, each pixel.

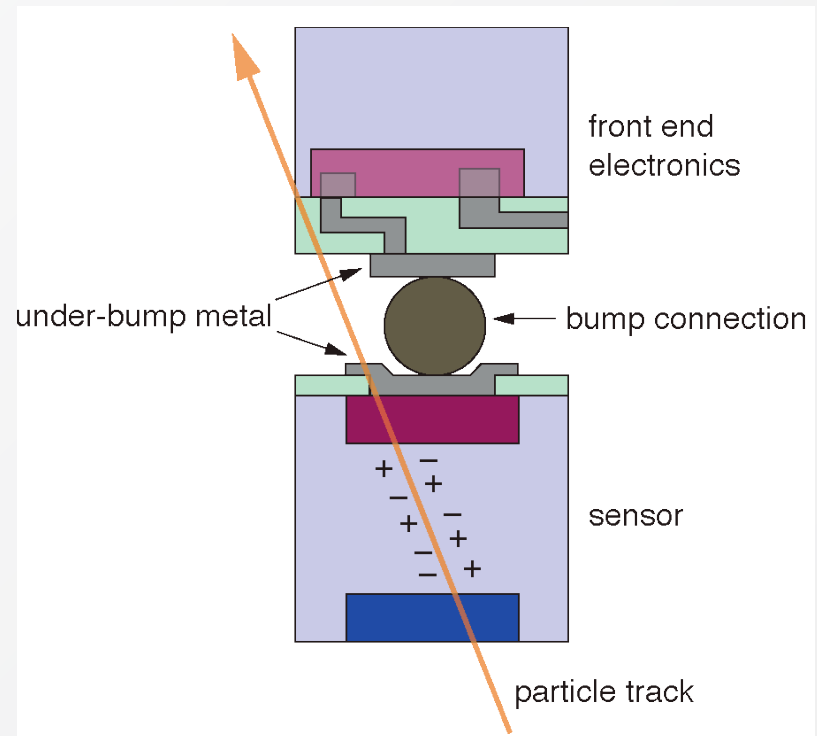


S.L. Shapiro et al., *Si PIN Diode Array Hybrids for Charged Particle Detection*, Nucl. Instr. Meth. A **275**, 580 (1989)

Detail of bump bond connection

Bottom is the detector, on top the bump bonds make the electrical connection for readout chip:

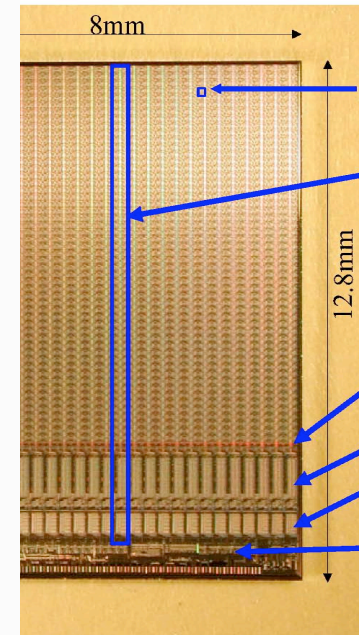
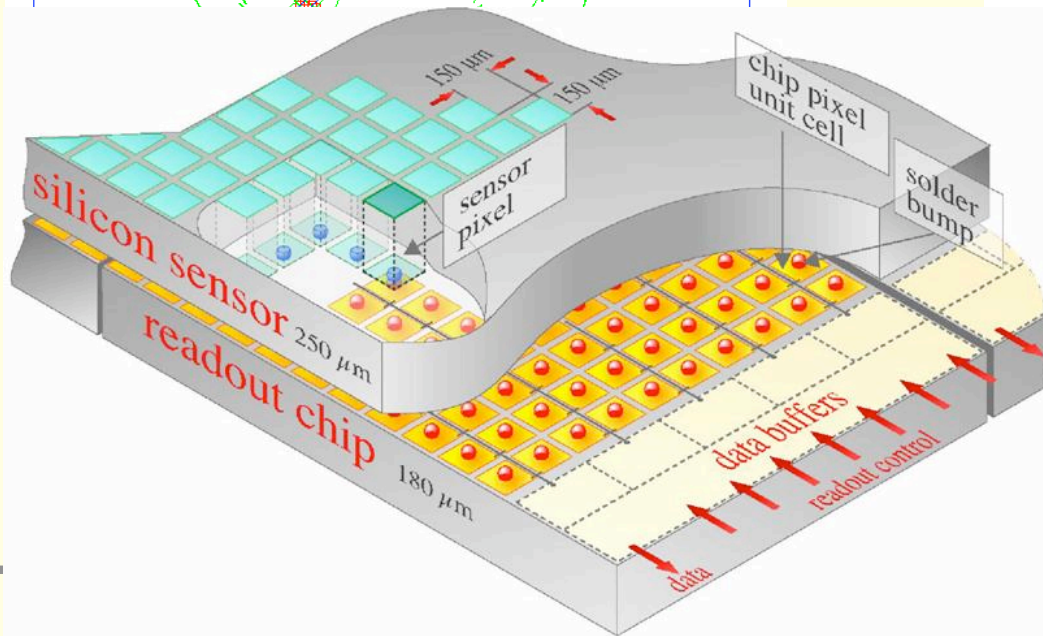
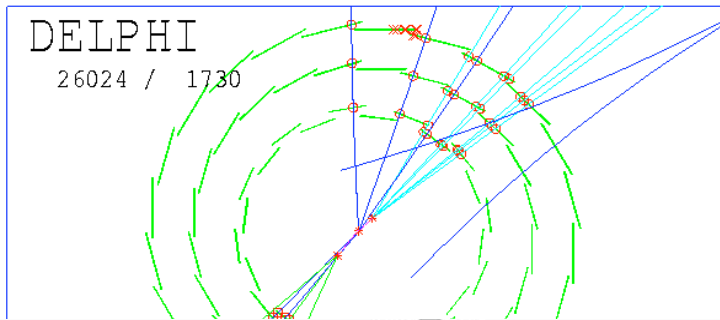
Text



L. Rossi, *Pixel Detectors Hybridisation*, Nucl. Instr. Meth. A **501**, 239 (2003)

Silicon pixel detectors

Silicon sensors and readout electronics with same geometry. First detectors end of 80' (Delphi, H1, Aleph....). Now an unavoidable detectors if one wants to perform b tagging.



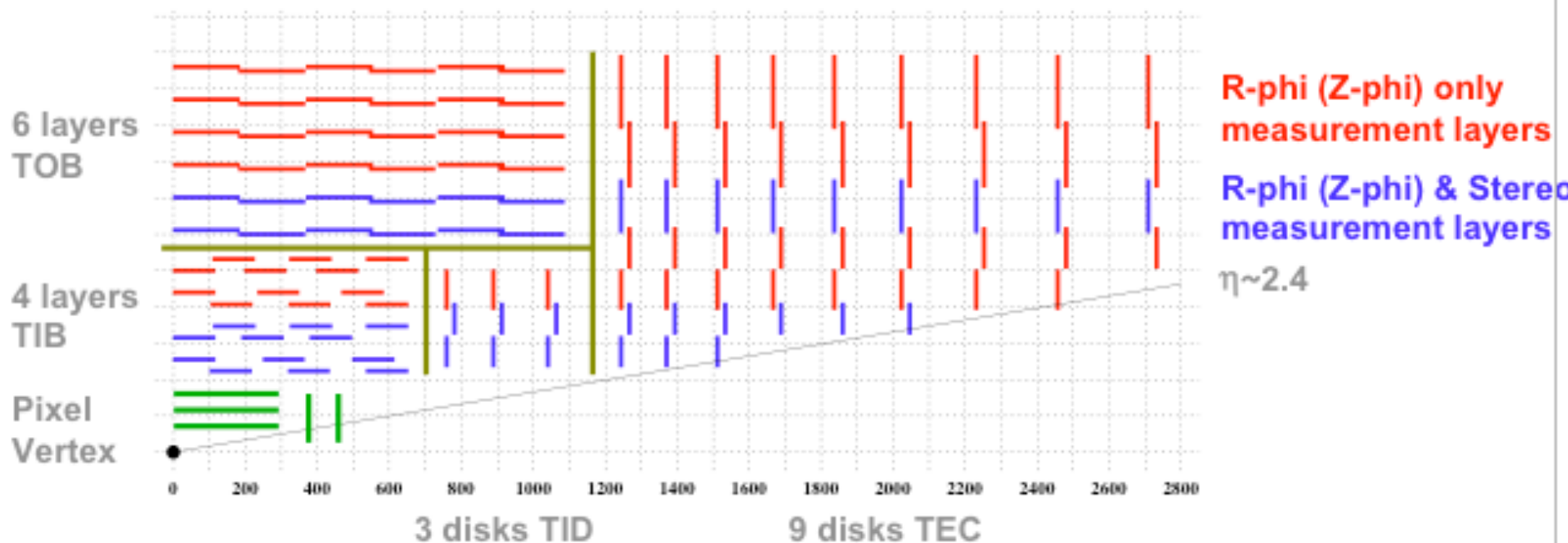
- 150 μm x 150 μm pixel
- 52x53 pixels in 26 double columns
345 k transistors
- Periphery:
78 k transistors
- Pixel-column interface
- Data buffers (4x24 capacitors)
- Timestamp buffers (8x8 bits)
- I2C, DACs, regulators, counters, readout, wirebonds
6 k transistors

Rely on “few” measurement layers, each able to provide robust (clean) and precise coordinate determination

2 to 3 Silicon Pixel, and 10 to 14 Silicon Strip Measurement Layers

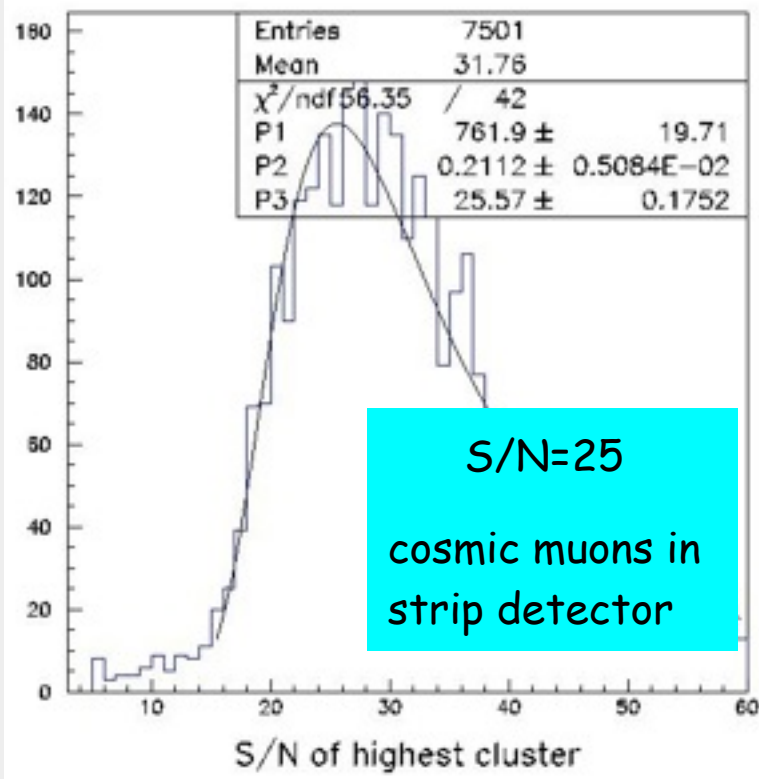
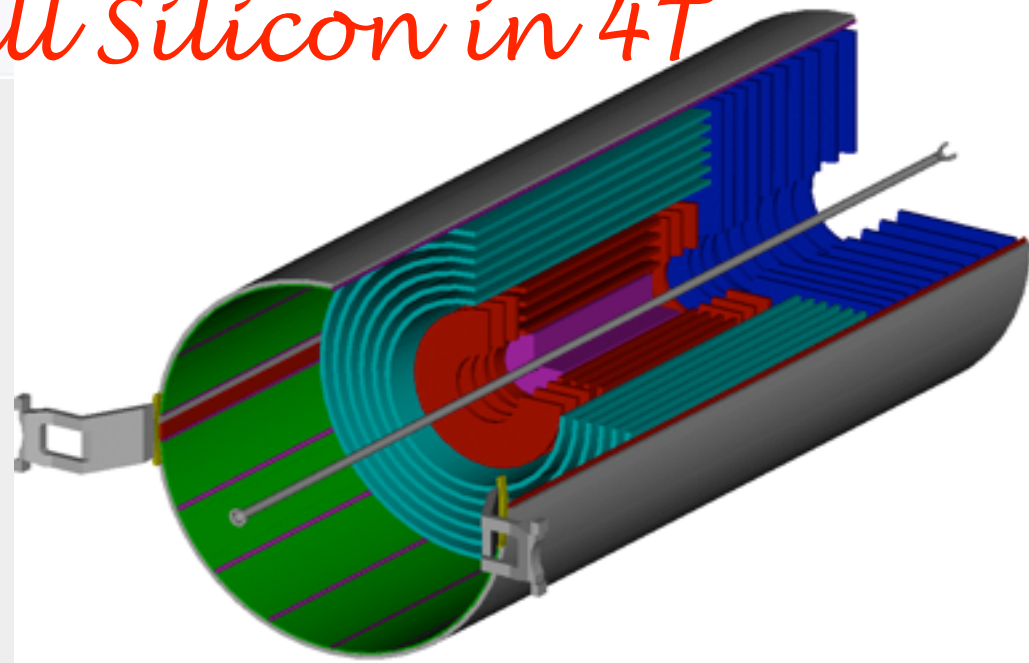
Radius ~ 110cm, Length ~ 270cm

$\eta \sim 1.7$

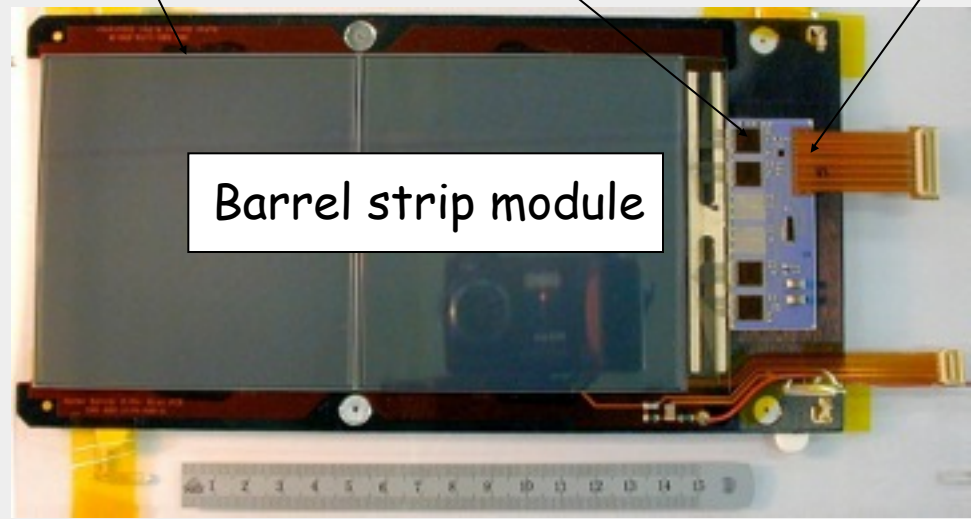


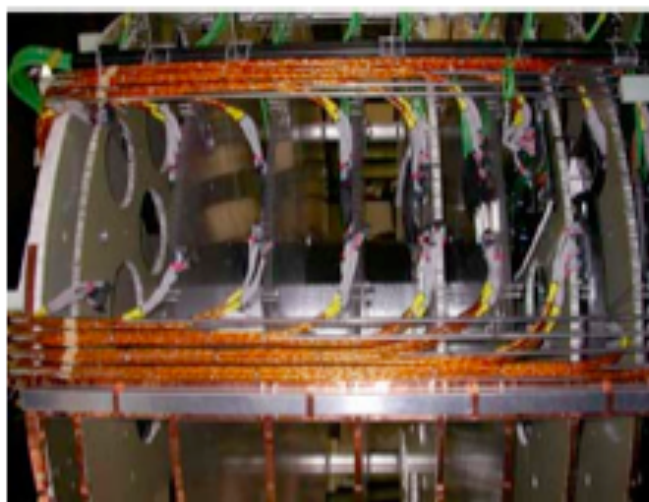
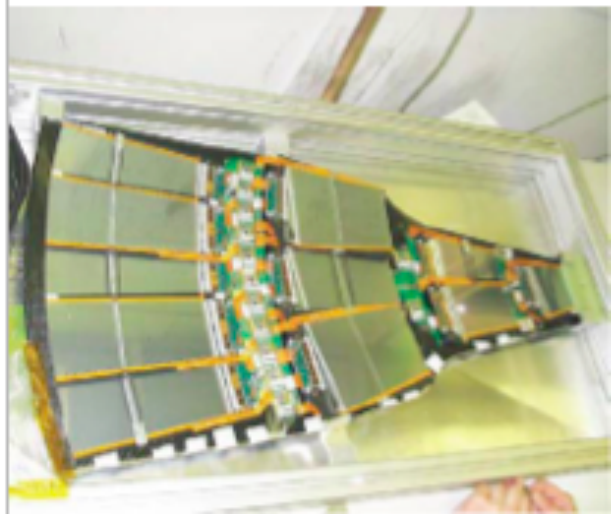
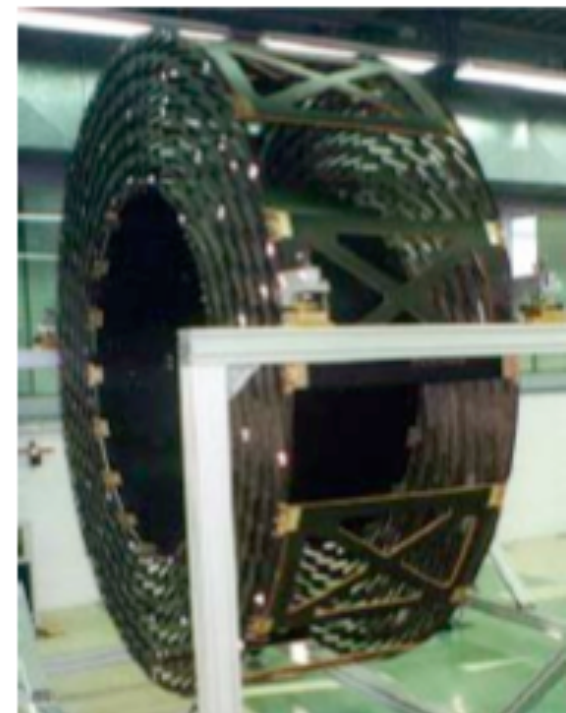
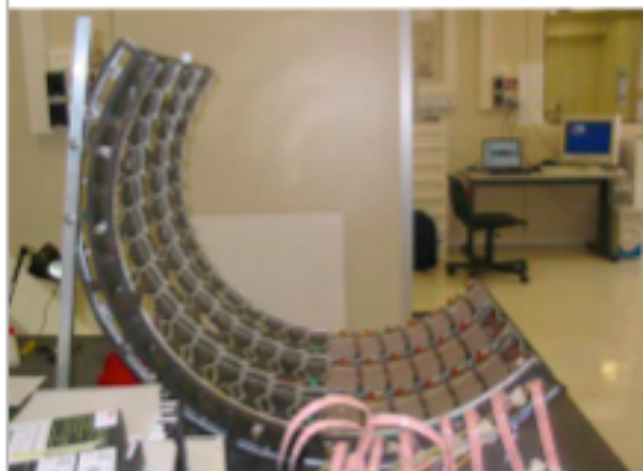
CMS tracker: full Silicon in 4T

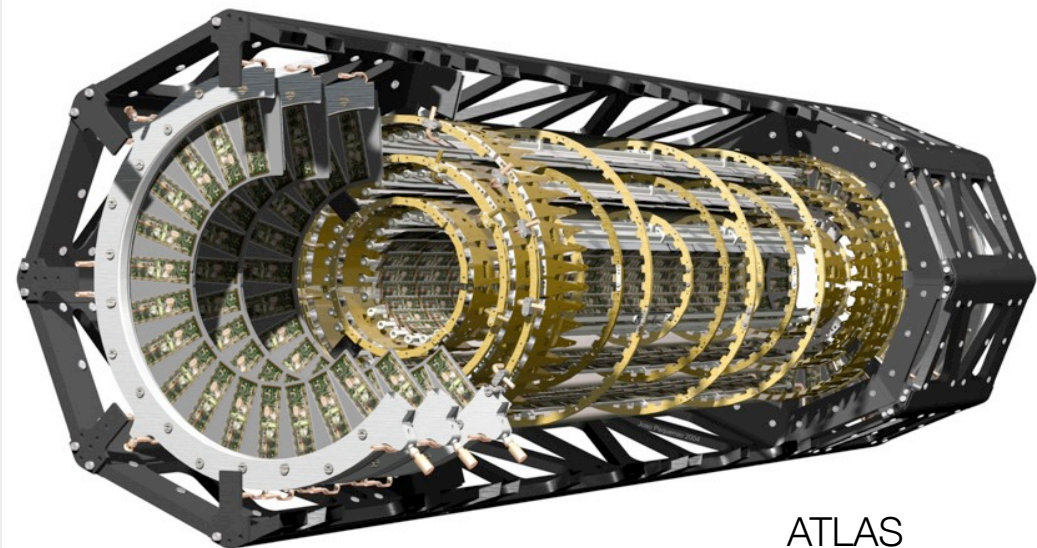
- 5.4 m long, barrel and disks
- 210 m² Si sensors
- Full volume (24 m³) at -10°C
- 10M strips
- 67M pixels (100 x 150 μm)



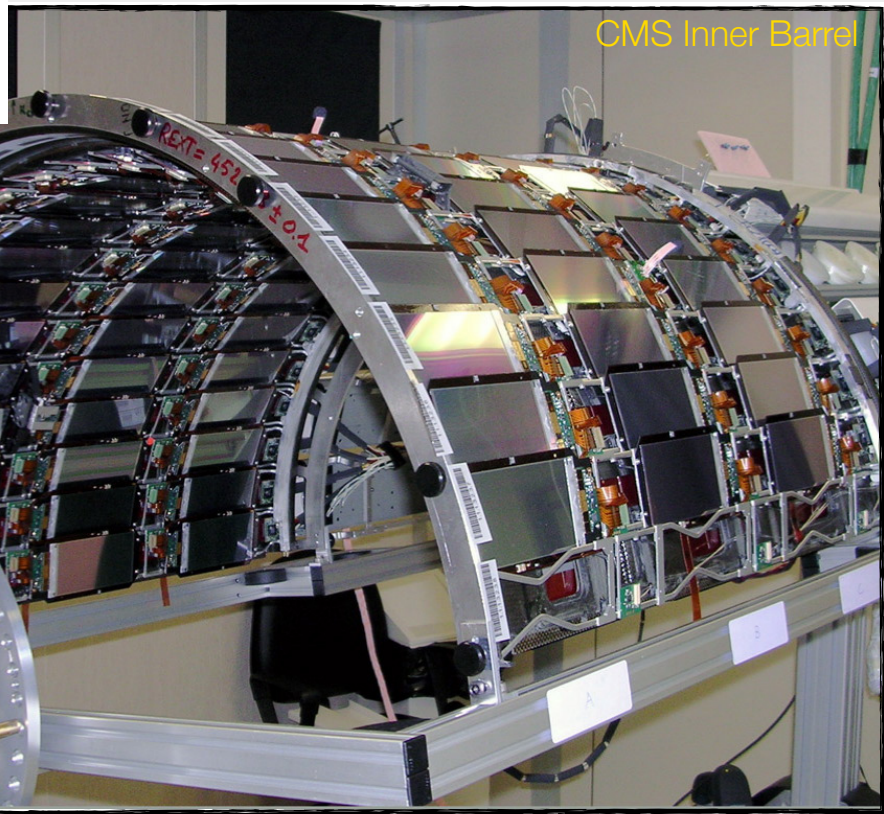
sensor APV 0.25 micron
(128 channels analog) Flex-hybrid







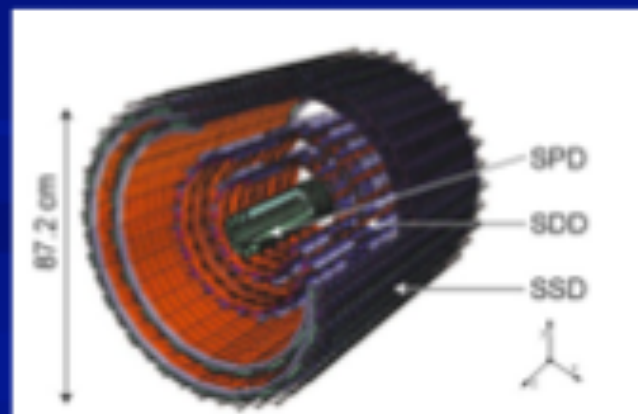
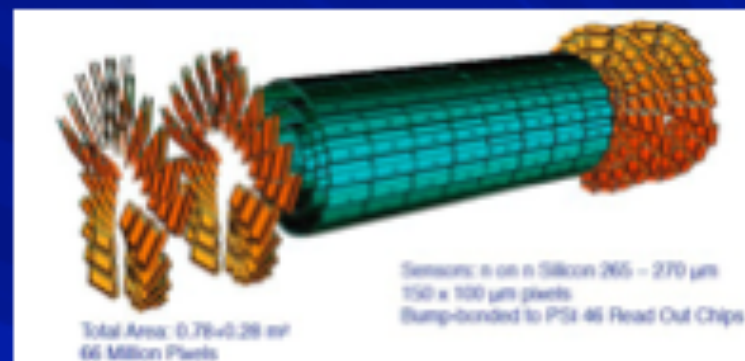
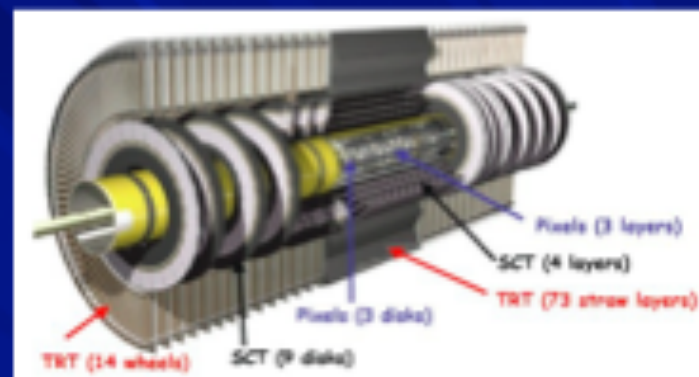
ATLAS
Pixel Detector



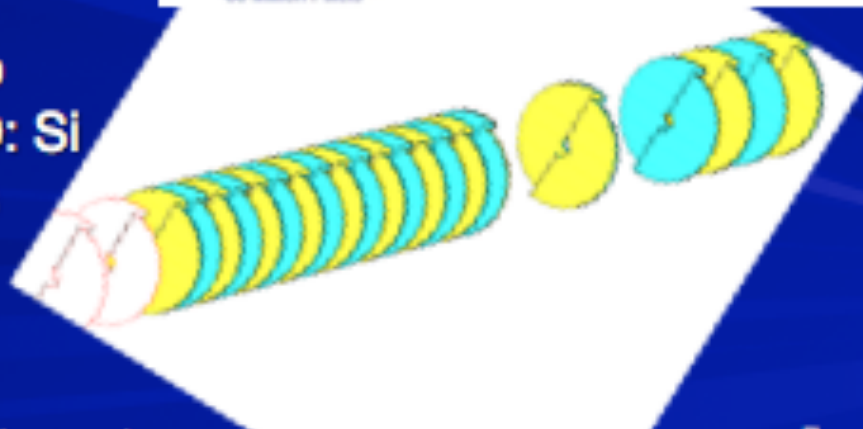
CMS Inner Barrel

The LHC silicon detectors

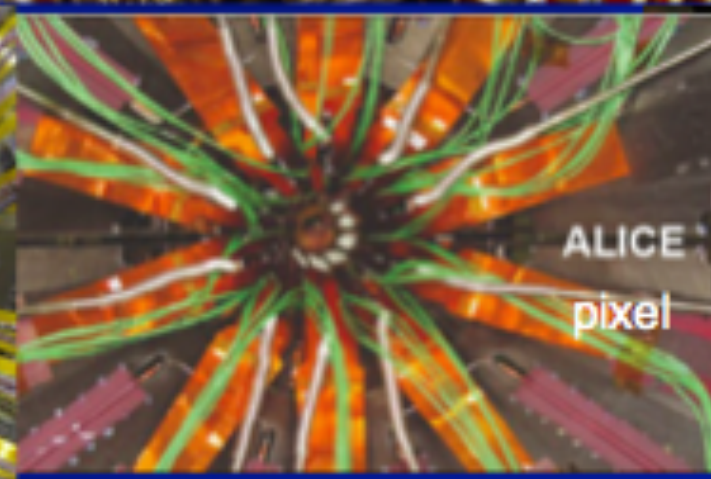
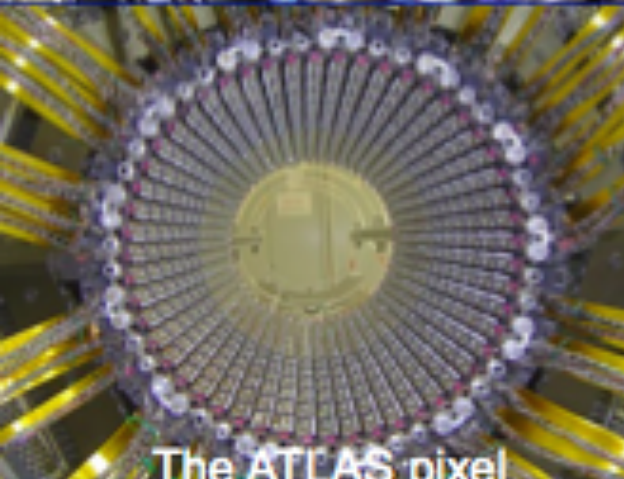
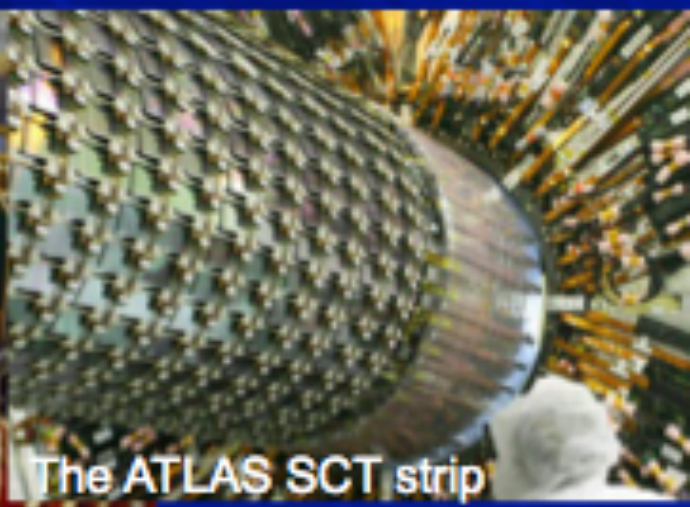
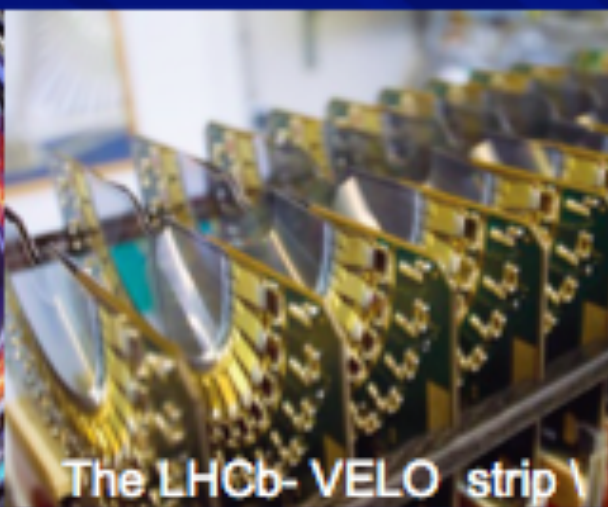
- **ATLAS Strips:** 61 m² of silicon, 4088 modules, 6x10⁶ channels
Pixels: 1744 modules, 80 x 10⁶ channels
- **CMS** the world largest silicon tracker 200 m² of strip sensors (single sided) 11 x 10⁶ readout channels ~1m² of pixel sensors, 60x10⁶ channels
- **ALICE** Pixel sensors Drift detectors
Double sided strip detectors

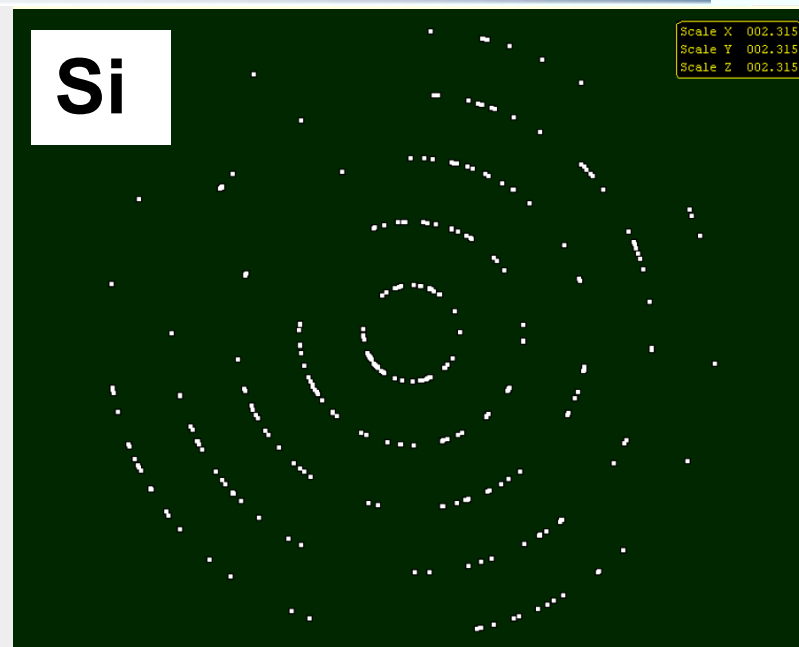
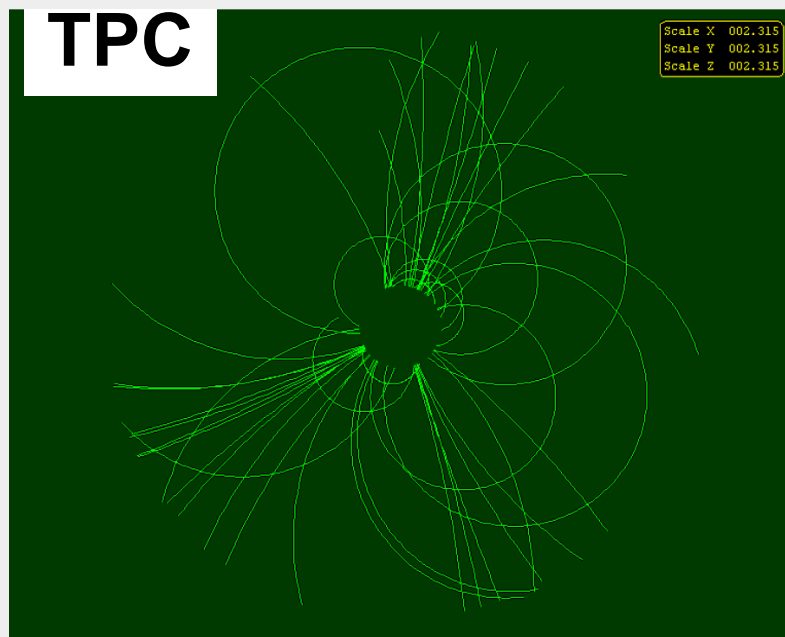


- **LHCb**
VELO: Si
Strips



The LHC detectors





- Charged track detectors have taken full benefit of progress in magnets (supra) (high field, large dimensions and electronics developments). *Whatever technologies B field knowledge + alignment of detectors is very important.*
- **Gaseous** are used since 60' but have really a new revival with the micro strips gas chambers (high flux is no more a problem). Good resolution can be really performant with pixel readout *Many applications, not only in HEP.*
 ==> *New TPC will probably use these readout devices in ILC experiments project*
- **Solid state detectors** : considerable progress in parallel with electronics readout. Their size rises by one order of magnitude in LHC experiment (200 m² in CMS detector of Si) Many R&D to improve radiation hardness, readout speed, material budget.....

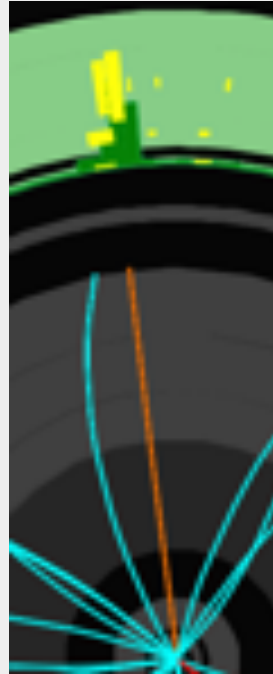
Table 28.1: Typical spatial and temporal resolutions of common detectors.
Revised September 2003 by R. Kadel (LBNL).

Detector Type	Accuracy (rms)	Resolution Time	Dead Time
Bubble chamber	10–150 μm	1 ms	50 ms ^a
Streamer chamber	300 μm	2 μs	100 ms
Proportional chamber	50–300 $\mu\text{m}^{b,c,d}$	2 ns	200 ns
Drift chamber	50–300 μm	2 ns ^e	100 ns
Scintillator	—	100 ps/n ^f	10 ns
Emulsion	1 μm	—	—
Liquid Argon Drift [Ref. 6]	$\sim 175\text{--}450 \mu\text{m}$	$\sim 200 \text{ ns}$	$\sim 2 \mu\text{s}$
Gas Micro Strip [Ref. 7]	30–40 μm	< 10 ns	—
Resistive Plate chamber [Ref. 8]	$\lesssim 10 \mu\text{m}$	1–2 ns	—
Silicon strip	pitch/(3 to 7) ^g	h	h
Silicon pixel	2 μm^i	h	h

h : limitation is given by the readout electronics but intrinsically can be very small

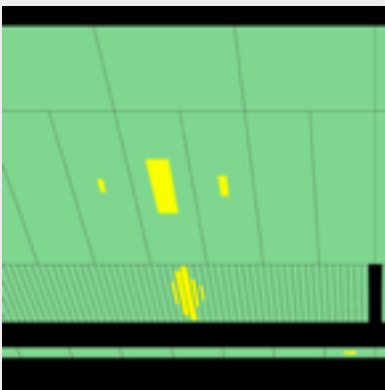
Electron/Photon Identification

- Electron/Photon reconstruction takes as input the tracks and calorimeter clusters already produced
- Electron/Photon leave narrow clusters in the electromagnetic calorimeter
 - Apply selection on the cluster shape to reduce background from jets
- Electron has track pointing at cluster
 - Requires aligning the calorimeter with the tracker
- Photon has no track pointing at its cluster
- Final Electron momentum measurement can come from tracking or calorimeter information (or a combination of both)
 - Often have a final calibration to give the best electron energy
- Often want isolated electrons
 - Require little calorimeter energy or tracks in the region around the electron



Electron/Photon Backgrounds

- Hadronic jets leave energy in the calorimeter which can fake electrons or photons
- Usually a Jet produces energy in the hadronic calorimeter as well as in the electromagnetic calorimeter
- Usually the calorimeter cluster is much wider for jets than for electrons/photons
- So it should be easy to separate electrons from jets
- However have many thousands more jets than electrons, so need the rate of jets faking an electron to be very small $\sim 10^{-4}$
- Need complex identification algorithms to give the rejection whilst keeping a high efficiency



Example of an electron energy deposit in the electromagnetic calorimeter in ATLAS.

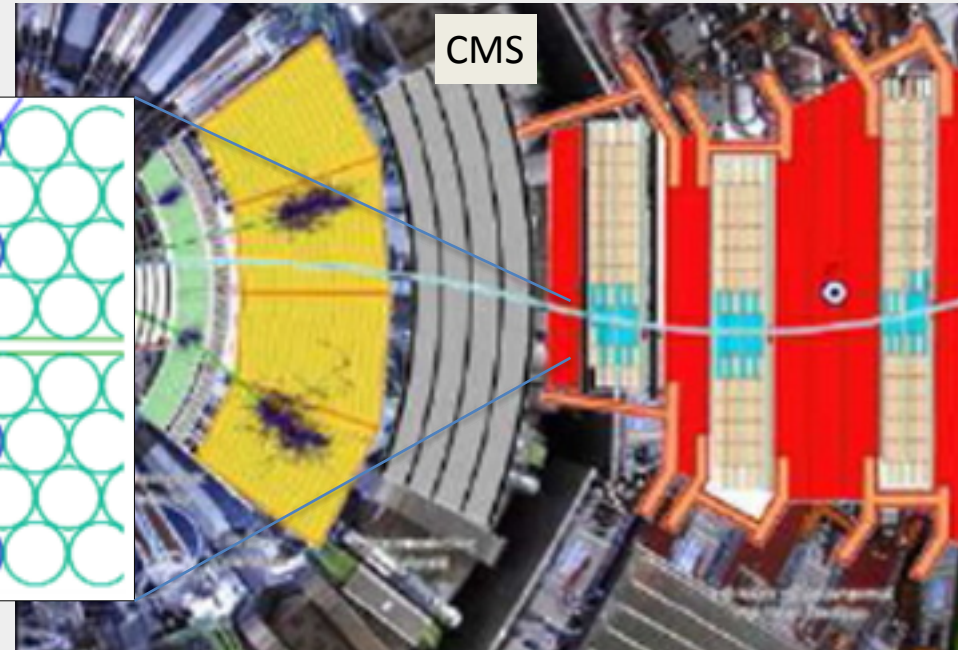
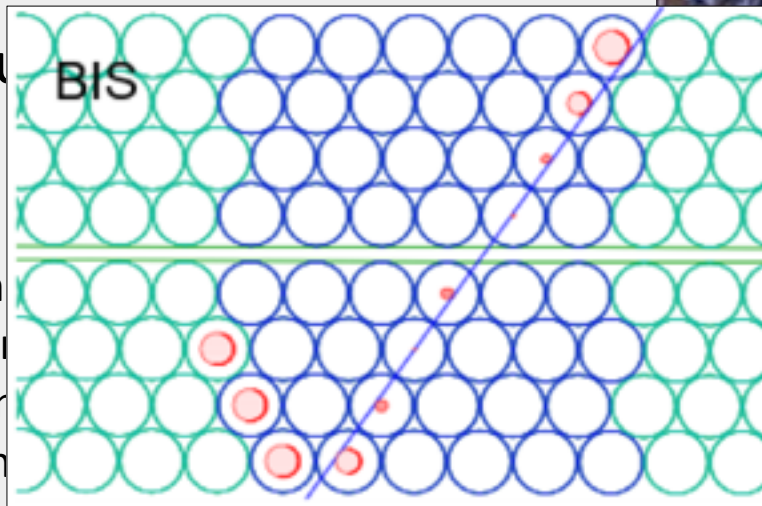
Use shower shape variables based on size of cluster in the radial and longitudinal directions to distinguish from hadronic showers

Muon identification

- Combine the muon segments found in the muon detector with tracks from the tracking detector

• Momentum
Muons segment in
drift tubes
from bend
in tracker

- Combine
resolution
- Need an
field in the
- Alignment of the muon detectors
also very important to get best momentum
resolution



Tracking Steps

Detector Output



Analysis input

Layer-based position measurements

Pixel

Silicon Strip

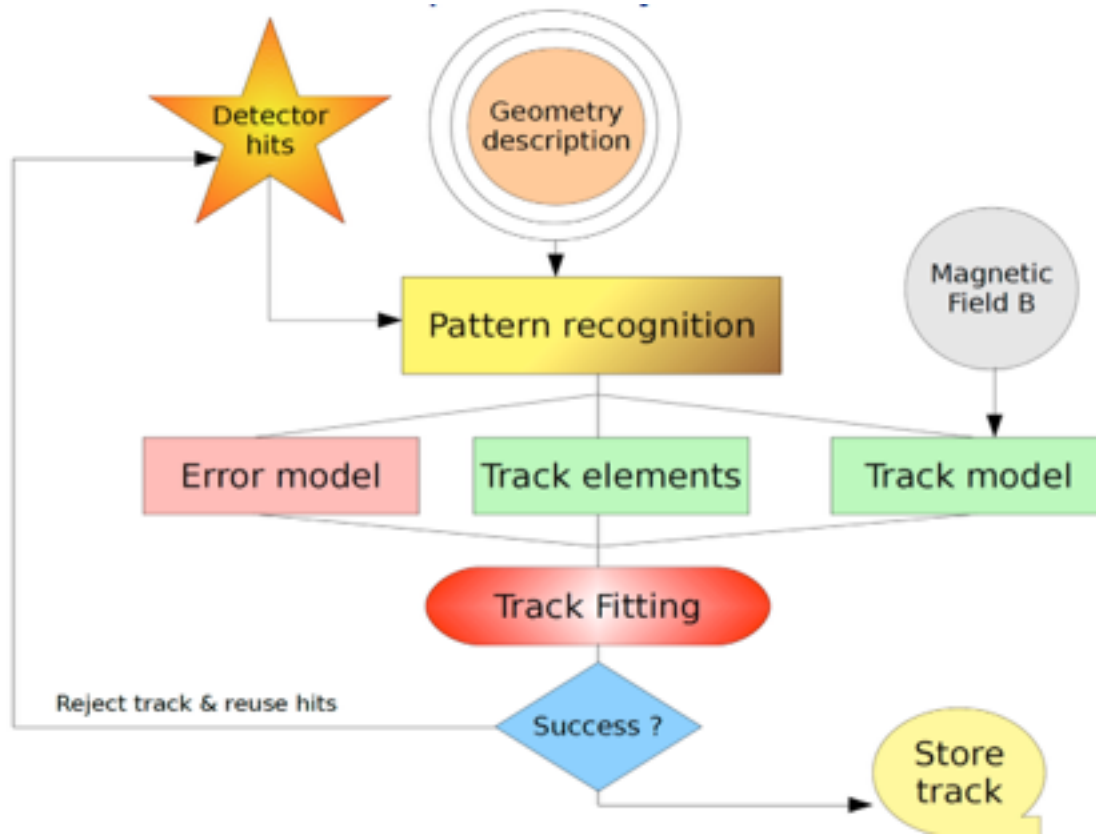
Muon chambers (Drift, Cathode Strip, etc..)

Continuous position measurements: TPC, TRD, etc..



Track reconstruction:
Four momentum of charged particles
Charge sign
ID tags of particles

Event reconstruction:
Collision vertex
Track impact parameter
Secondary vertex



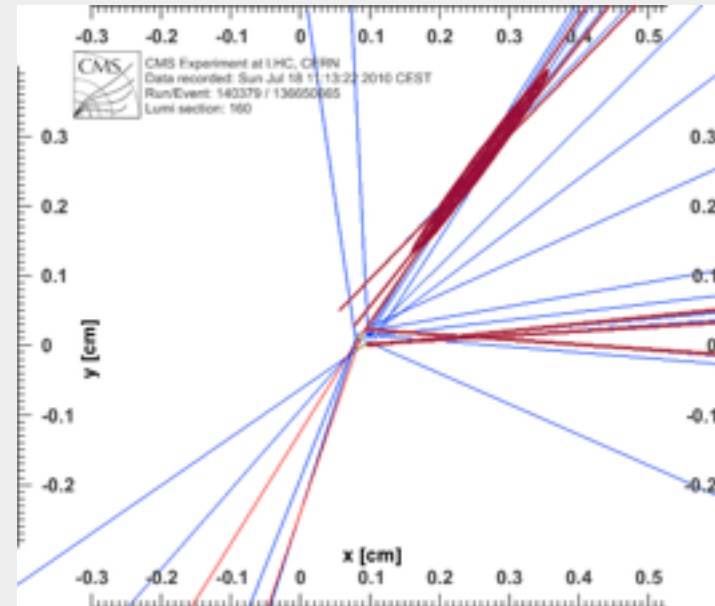
Track finding very important for analysis

Tracks are used directly in the reconstruction of

- Electrons
- Muons
- And to a lesser extent in Tau, Jet and photon reconstruction

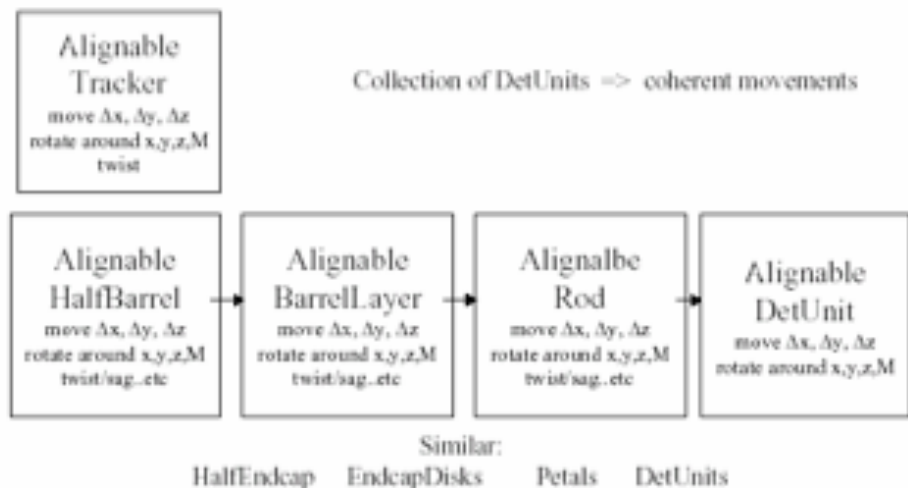
For reconstructed tracks we know

- Momentum
 - straighter the track the higher momentum it is
- Charge
- Point of closest approach to the interaction point



(important to identify particles such as b-quarks which have a long lifetime and so travel a measurable distance before they decay)

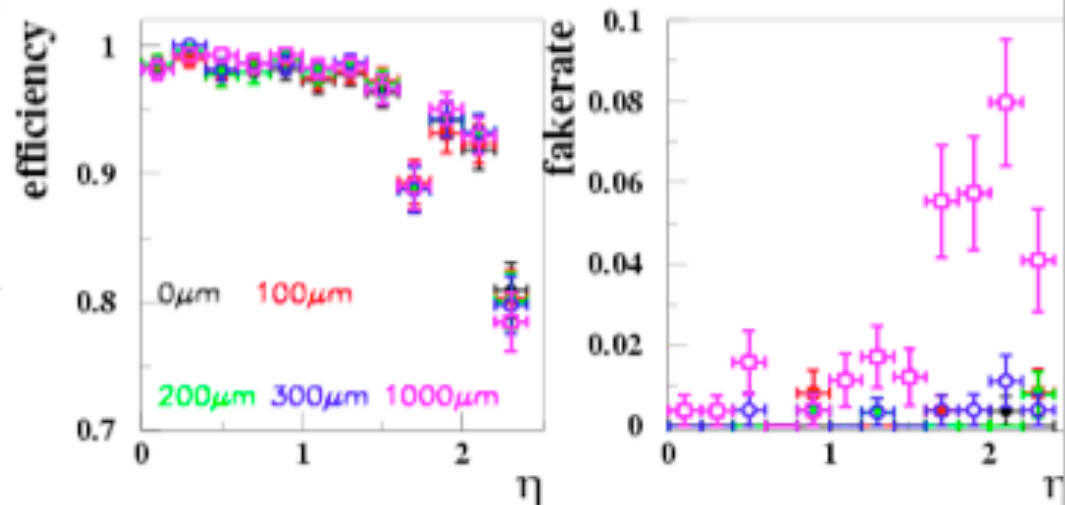
(Mis)Alignment Elements

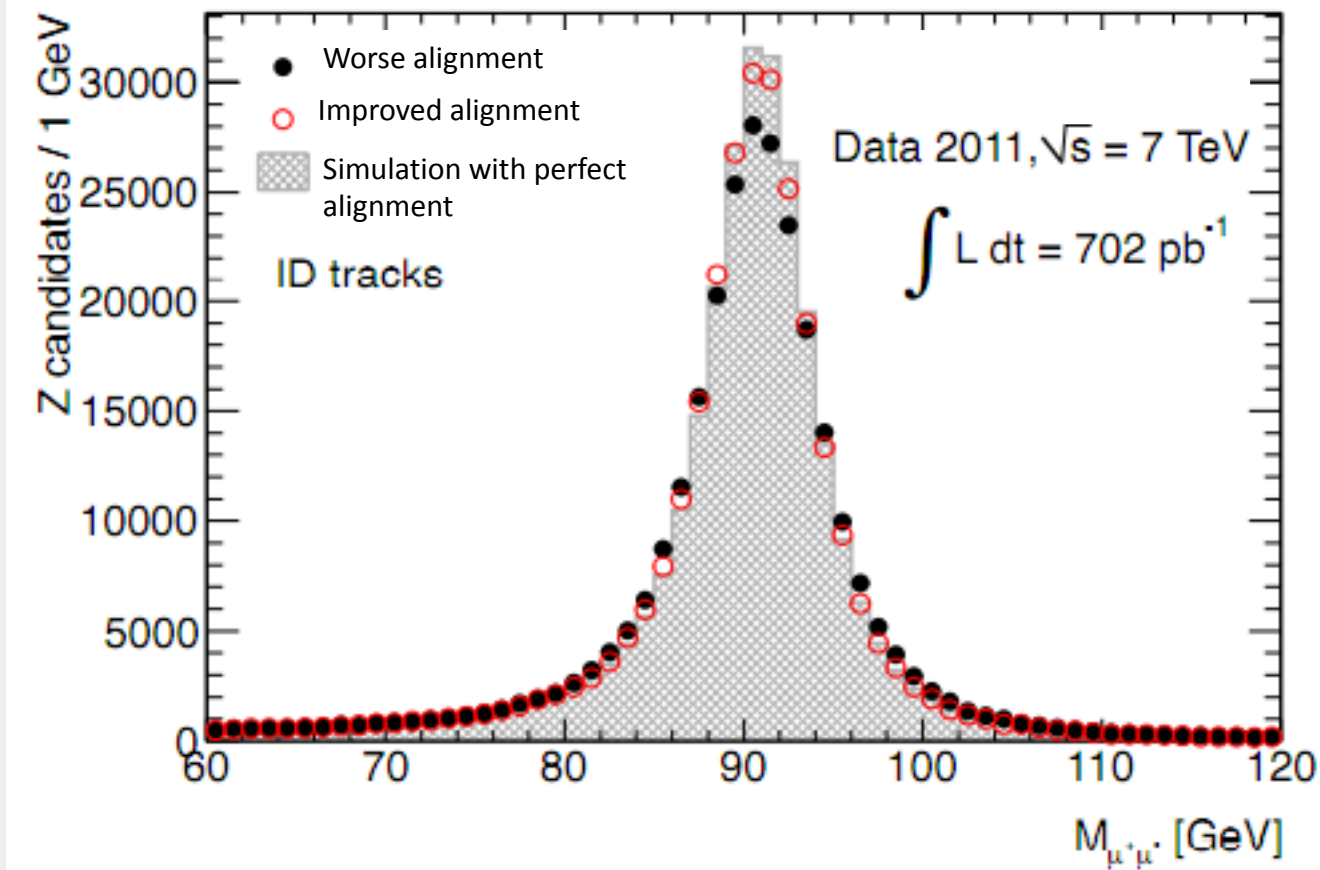


Software tools implemented to introduce, and account for, misalignments following the hierarchical organization of the mechanical degrees of freedom inherent in the support structures

Efficient & clean pattern recognition with misalignments of up to 1mm, for $W \rightarrow \mu\nu$ events at $2 \cdot 10^{33}$

This is the essential starting point for alignment with tracks & sets scale for initial accuracy required





- Improving the tracker alignment description in the reconstruction gives better track momentum resolution which leads to better mass resolution.
- Can see the reconstructed Z width gets narrower if we use better alignment constants. Very important for physics analysis to have good alignment.
- Alignment of detector elements can change with time for example when the detector is opened for repair, or when the magnetic field is turned on and off.

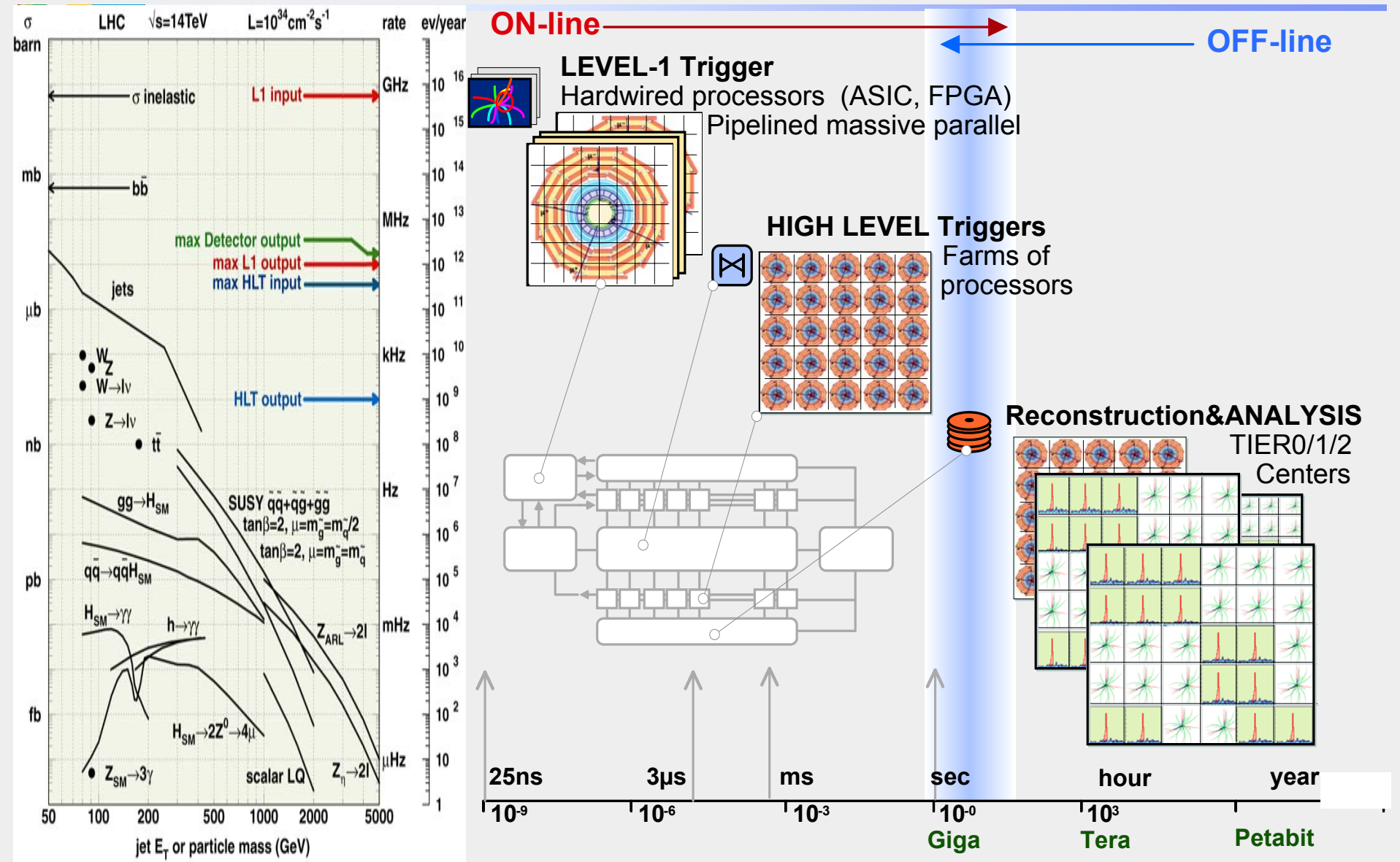
- As particles travel through matter they interact (through the EM force) and transfer part of their energy to the detector.
- At the energies of interest ionization is the dominating mechanism.
- Gaseous detectors measure the ionization of gas to identify the path followed by particles.
- Silicon detectors use the ionization of silicon. They permit a much better accuracy but are more expensive.
- Accurate tracking is important for example to detect displaced vertices (long lived particles such as states with b and c quarks).
- This played an important role in the discovery of the top quark and in the study of CP violation.



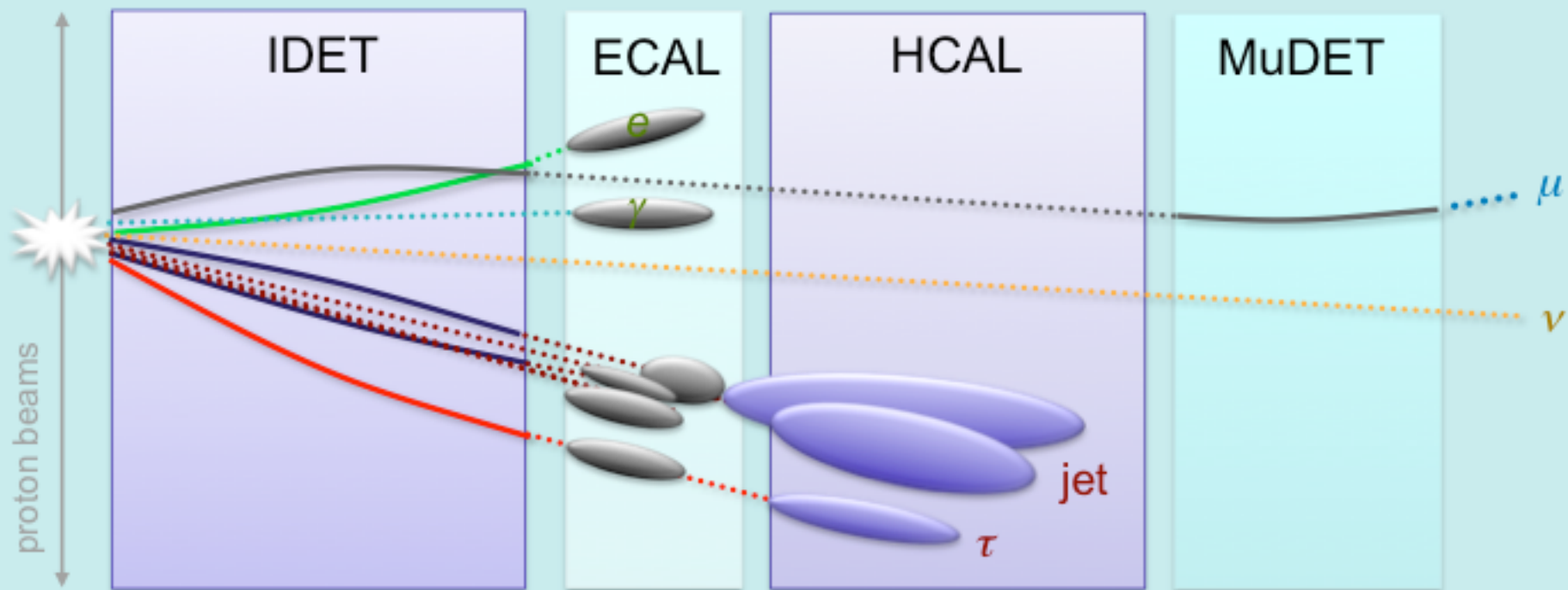
Why do we Need a Trigger

LM

- Experiments in High Energy Physics are different from those in many other areas : *the reactions are measured **collision by collision***
- This means that there is essentially no time integration in the measurement. *Measurements are essentially instantaneous.*
- The detector needs to have an indicator of the **correct time** to read out (typically with a precision of the order of nanoseconds)
- Experiments may need to be **selective** in what they read out **<=== TRIGGER**
- Once an event is selected for readout, a complicated sequence of operations takes place. During this time, the detector **may not be able to register another event**. The status of the detector needs to be monitored.
- The time during which the detector cannot read out is called **BUSY** time, or **dead** time.
- As these functions crucially affect what is analysed (*what is not triggered is LOST*)
 - account needs to be taken of what is kept, and under what conditions,
 - by recording a **summary of the selection decision per event**,
 - and by keeping **statistics** of the numbers of events selected according the selection criteria.
- *The trigger system controls these functions*



Trigger Signatures

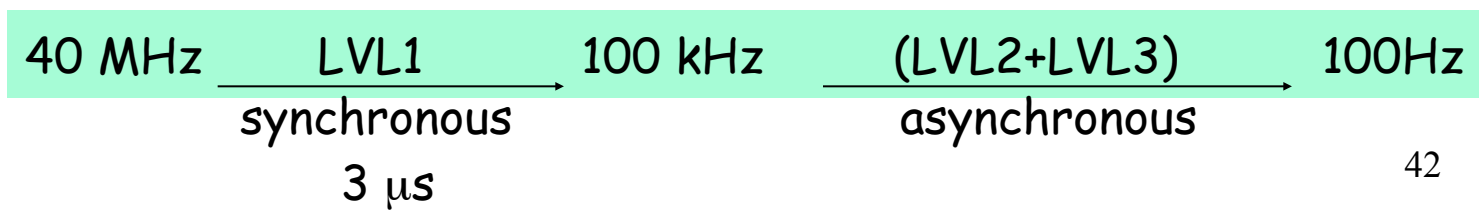
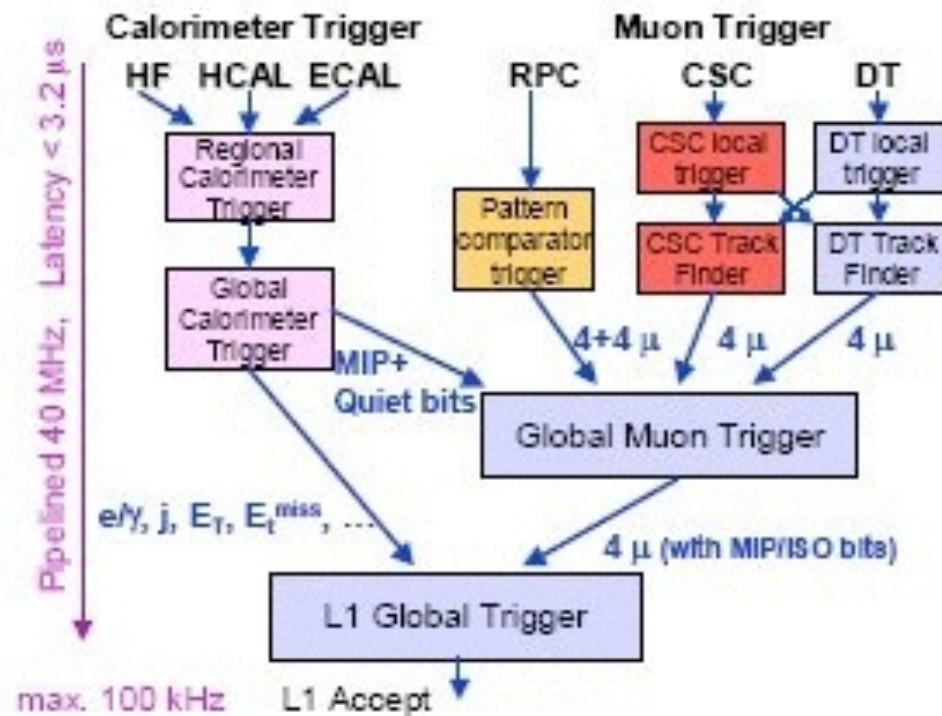
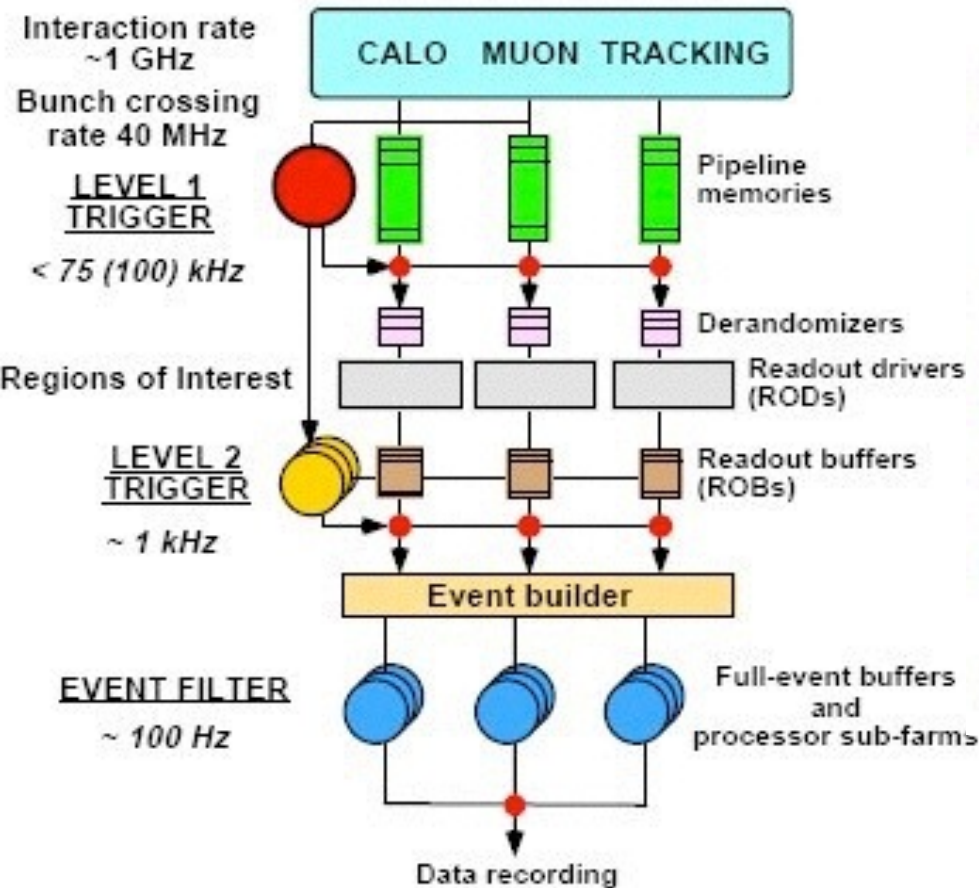


Features distinguishing new physics from the bulk of the SM cross-section

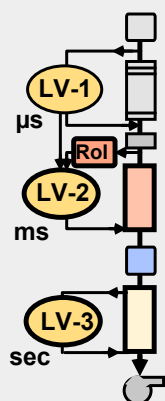
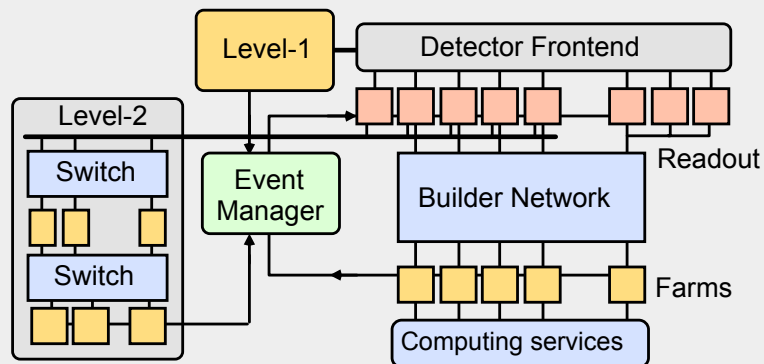
- Presence of high- p_T objects from decays of heavy particles (min. bias $\langle p_T \rangle \sim 0.6$ GeV)
- More specifically, the presence of isolated high- p_T leptons or photons
- The presence of known heavy particles (W , Z)
- Missing transverse energy (either from high- p_T neutrinos, or from new invisible particles)

- *Most experiences (except Alice) have up to 30 interactions per Bunch Crossing (BC), and must be able to process each BC.*
- *The time between 2 BC's (50ns) is far too short to allow a trigger to be processed*
- *Solution is to break the algorithm into tasks that can be processed in one BC, and arrange that data from each successive BC are stored.*
- *When the full algorithm is complete a decision is made*
- *In this way*
 - *a new set of data(for 1 BC) enters the system at each BC, and*
 - *A NEW TRIGGER DECISION IS MADE FOR THAT BC a fixed time (trigger latency) after the data arrived.*
- *Data from non triggering detectors are also stored in shift registers, advancing one position per BC. If when the trigger decision is made, it turns out the no needed which are discarded data.*

Pipelined-multilevel-triggers



- Additional processing in LV-2: reduce network bandwidth requirements**



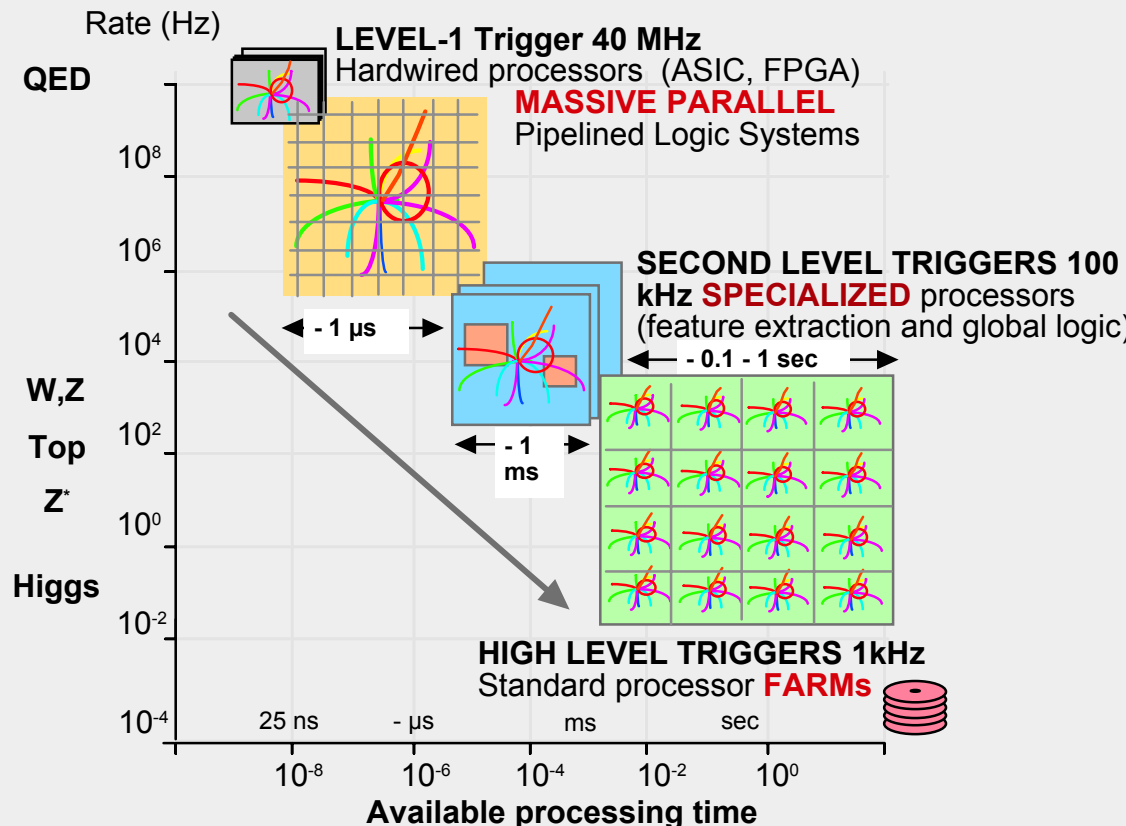
40 MHz

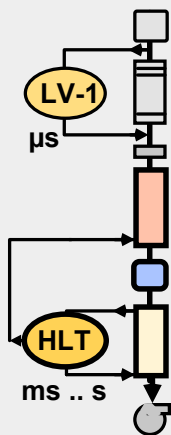
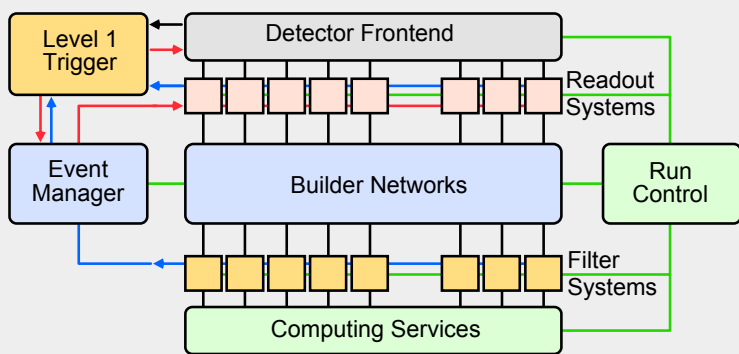
10^5 Hz

10^3 Hz

10 Gb/s

10^2 Hz



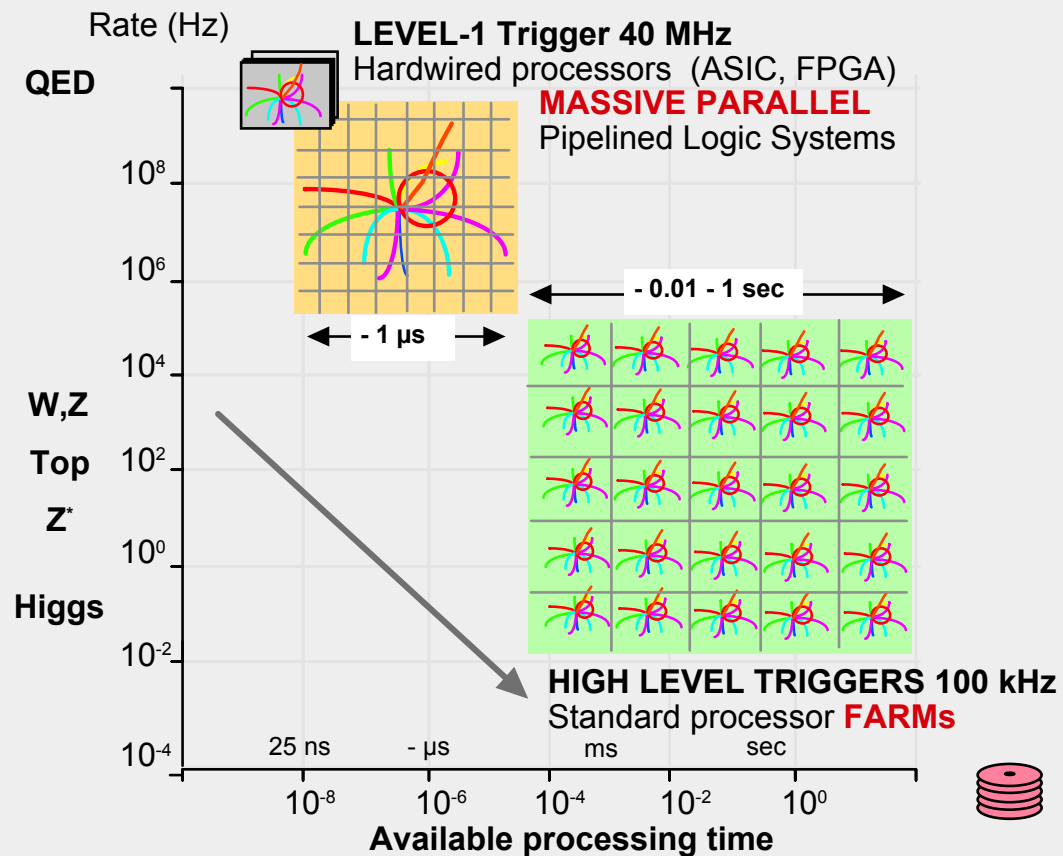


40 MHz

10^5 Hz

1000 Gb/s

10^2 Hz



- Reduce number of building blocks
- Rely on commercial components (especially processing and communications)

Challenges for Future Detectors: Experimental Opportunities

The Energy Frontier

Origin of Mass

Matter/Anti-matter
Asymmetry

Dark Matter

Origin of Universe

Unification of Forces

New Physics
and the Standard Model

Dark Energy

Neutrino Physics

Proton Decay

The Intensity Frontier

The Cosmic Frontier

The Energy Frontier

- Rad hard, low mass vertex sensors
- Triggering at luminosities $> 10^{35}/\text{cm}^2/\text{s}$
- $4 \mu\text{m}$ point tracking resolution
- Hadronic jet energy resolutions of $30\%/\text{sqrt}(E)$

The Intensity Frontier

- Low-cost efficient photo-detectors
- Large volume, long drift LAr TPC with maintained purity and robust readout
- Psec level time-of-flight for rare decays

The Cosmic Frontier

- Background rates in dark matter detectors down to a level of 1 nuclear recoil per ton per year
- Depth of observation of galaxy clusters
- Probe the Planck scale of space-time



Text books (a selection)

- C. Grupen, B. Schwartz, Particle Detectors, 2nd ed., Cambridge University Press, 2008
- G. Knoll, Radiation Detection and Measurement, 3rd ed. Wiley, 2000
- W. R. Leo, Techniques for Nuclear and Particle Physics Experiments, Springer, 1994
- R.S. Gilmore, Single particle detection and measurement, Taylor&Francis, 1992
- K. Kleinknecht, Detectors for particle radiation , 2nd edition, Cambridge Univ. Press, 1998
- W. Blum, W. Reigler, L. Rolandi, Particle Detection with Drift Chambers, Springer, 2008
- R. Wigmans, Calorimetry, Oxford Science Publications, 2000
- G. Lutz, Semiconductor Radiation Detectors, Springer, 1999

Review Articles

- Experimental techniques in high energy physics, T. Ferbel (editor), World Scientific, 1991.
- Instrumentation in High Energy Physics, F. Sauli (editor), World Scientific, 1992.
- Many excellent articles can be found in Ann. Rev. Nucl. Part. Sci.

Other sources

- Particle Data Book Phys. Lett. B592, 1 (2008) <http://pdg.lbl.gov/pdg.html>
- R. Bock, A. Vasilescu, Particle Data Briefbook <http://www.cern.ch/Physics/ParticleDetector/BriefBook/>
- ICFA schools lectures : <http://www.ifm.umich.mx/school/ICFA-2002/>
- O. Ullaland <http://lhcb-doc.web.cern.ch/lhcbdoc/presentations/lectures/Default.htm>
- Proceedings of detector conferences (Vienna VCI, Elba, IEEE, Como)
- Journals: Nucl. Instr. Meth. A, Journal of Instrumentation







Trigger and DAQ

- R. Fernow : Introduction to experimental particle physics (C.U.P. 1986)
- R. Frühwirth, M. Regler, R.K. Bock, H. Grote and D. Notz ; Data Analysis Techniques for High-Energy Physics (2nd ed.) (C.U.P. 2000)
- CERN-⁴⁶Latin American Schools of Physics : Usually an article on trigger and DAQ

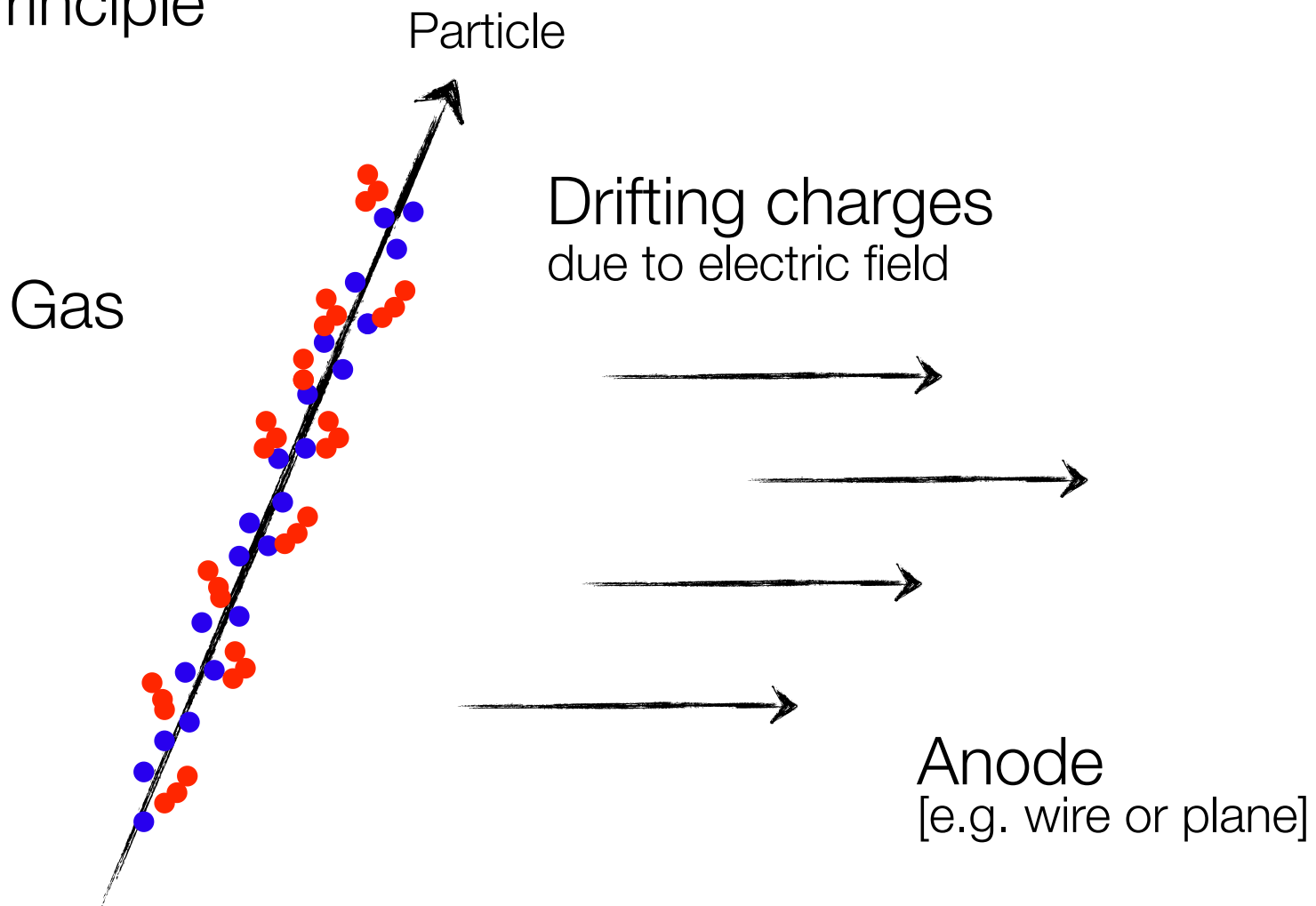
References

- Sze, Physics of semiconductor devices
- Helmuth Spieler lecture notes (www-physics.kbl.gov/~spieler)
- G. Lutz, Semiconductor radiation detectors : Device Physics, Springer (2007)
- Doris Eckstein (DESY lectures)
- Gino Bolla UTEV seminar: http://www.fnal.gov/orgs/utev/past_speakers.html
- R. Lipton Academic lectures: http://www-ppd.fnal.gov/eppoffice-w/Academic_Lectures/Past_Lectures.htm
- Steve Worm notes on Radiation Damage
- Silicon Microstrip Detectors , A. Peisert, in " Instrumentation in High Energy Physics ", F .Sauli (ed), World Scientific, (1992).
- Pixel Detectors, Rossi, Fisher, Rohe, Wermes, Springer
- M. Moll thesis on Radiation Damage

BACKUP

- Gaseous Detectors *for details see* 
- Large volume Particle Tracking *for details see* 
- Exemple of Gaseous detectors *for details see* 
- The Silicon Sensors *for details see* 
- Silicon detectors *for details see* 
- Overview of readout electronics *for details see* 

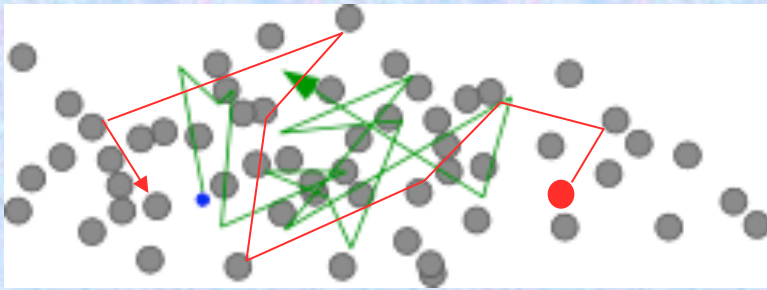
Schematic Principle of gas detectors



- Primary Ionization
- Secondary Ionization (due to δ -electrons)

Drift and Diffusion of Charges in Gases

ELECTRIC FIELD $E = 0$: THERMAL DIFFUSION



Maxwell energy distribution:

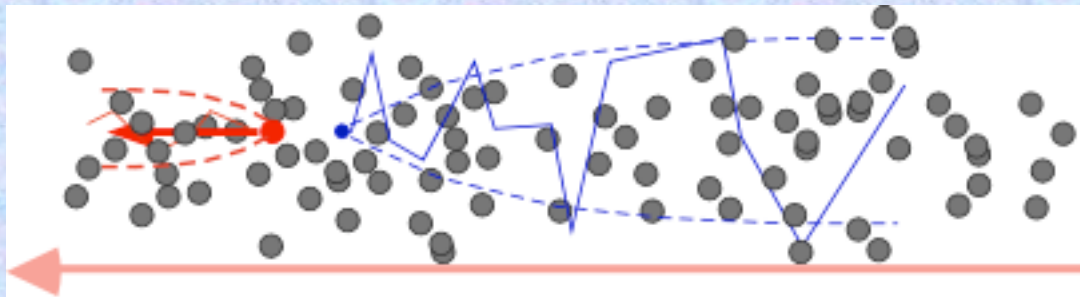
$$F(\epsilon) = C\sqrt{\epsilon} e^{-\frac{\epsilon}{kT}}; \quad \langle \epsilon \rangle \sim kT \sim 0.025 \text{ eV}$$

$$\text{RMS of charge diffusion: } \sigma_x = \sqrt{2Dt}$$

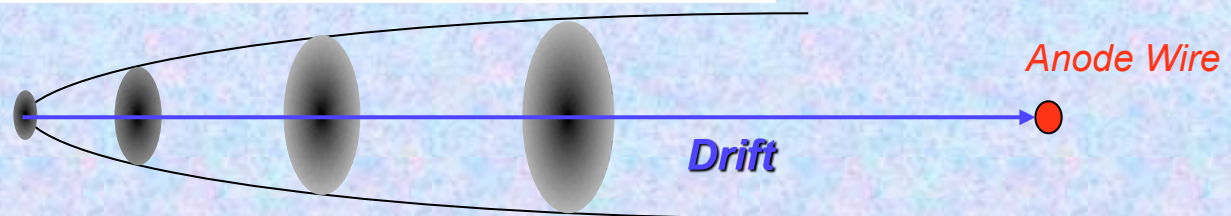
ELECTRIC FIELD $E > 0$: CHARGE TRANSPORT AND DIFFUSION

IONS

ELECTRONS



E



Diffusion in gases (no E-field)

- * In absence of other effects, at thermal energies, the mean speed of the charges (given by the Maxwell distribution of the energies) is:

$$v = \sqrt{\frac{8kT}{\pi m}} \quad \text{where } k \text{ is Boltzmann's constant, } T \text{ the temperature and } m \text{ the mass of the particle}$$

- * The charges diffuse by multiple collisions, and a local distribution follows a Gaussian law:

$$\frac{dN}{dx} = \frac{N_0}{\sqrt{4\pi Dt}} \exp\left(-\frac{x^2}{4Dt}\right) \quad \text{where } N_0 \text{ is the total number of charges, } x \text{ the distance from the point of creation and } D \text{ the diffusion coefficient}$$

- * Then the linear and volume r.m.s. of the spread are:

$$\sigma_x = \sqrt{2Dt}$$

$$\sigma_v = \sqrt{6Dt}$$

For instance, the radial spread of ions in air in normal conditions is about 1 mm after 1 second

Drift and mobility in gas

- * In the presence of an electric field, electrons and ions will drift in the gas. The drift velocity for electrons can be much higher w.r.t. ions since they are much lighter.
- * $\mu = v/E$ is the mobility of a charge where v is the drift velocity and E the electric field.
- * Ions :
 - Mean velocity v^+ is proportional to E/P
 - Mobility μ^+ is constant (average energy of ions almost unmodified up to very high electric fields)
- * Electrons:
 - Drift velocity $v^- = (e/2m).E.\tau$ where τ is the mean time between collision
 - Typical value around 5 cm/ μ s are obtained (ions thousand times slower)

Charge multiplication

- * $\alpha = 1/\lambda$ is the probability of ionization per unit length with λ the mean free path of the electron for a secondary ionizing collision
- * For n electrons, there will be $dn = n\alpha dx$ new electrons created in a path dx
- * Then $n = n_0 e^{\alpha x}$ with α : first Townsend coefficient
- * And we can define a multiplication factor M :

$$M = \frac{n}{n_0} = \exp\left[\int_{r_1}^{r_2} \alpha(x) dx\right] \quad \alpha \text{ is a function of } x \text{ (non uniform electric fields)}$$

- * Limitation of M : above 10^8 , sparks occur (Raether limit)
- * Calculating α (or gas gain) for different gases (model by Rose and Korff):

$$\frac{\alpha}{p} = A \exp\left(\frac{-Bp}{E}\right) \quad \text{where } A \text{ and } B \text{ depend on the gas}$$

Ionization statistics:

Mean distance between two ionizations: $\lambda = 1/(n_e \sigma_I)$

Mean number of ionizations: $\langle n_p \rangle = L/\lambda$

n_p Poissonian distributed:

$$P(n_p, \langle n_p \rangle) = \frac{\langle n_p \rangle^{n_p} e^{-\langle n_p \rangle}}{n_p!}$$

$P(0) = \exp(-L/\lambda)$ yields λ, σ_I
using (in)efficiency of gas-detectors

Mean free path λ :
[typical values]

He 0.25 cm

Air 0.052 cm

Xe 0.023 cm

[$\rightarrow \sigma_I(\text{He}) \approx 100$

σ_I : Ionization x-Section

n_e : Electron density

L : Thickness

Also important:

Mobility of charges:

Influences the timing behavior of gas detectors ...

Diffusion:

Influences the spatial resolution ...

Avalanche process via impact ionization:

Important for the gain factor of the gas detector ...

Recombination and electron attachment:

Admixture of electronegative gases ($\text{O}_2, \text{F}, \text{Cl} \dots$) influences detection efficiency ...

Ion mobility:

With external electric field: ions obtain velocity v_D in addition to thermal motion; on average ions move along field lines of electric field E ...

Kinetic energy:

$$\langle T_{\text{ion}}(E \neq 0) \rangle = \langle T_{\text{ion}}(\text{Therm.}) \rangle = \frac{3}{2}kT$$

Temperature
sorry ...

approximately equal to thermal energy, as the (heavy) ions lose typically half their energy when colliding with the non-ionized gas atoms.

Drift velocity v_D develops only from one interaction to another ...

Assuming $v_D(t=0)=0$ and collision time τ yields:

$$\vec{v} = \vec{a} \cdot \tau = \frac{e\vec{E}}{M} \cdot \tau$$

$$\tau = \lambda(T_{\text{kin}})/v_{\text{therm.}} = \text{const.}$$

$$\vec{v}_D = \langle \vec{v} \rangle = \frac{1}{2}\vec{v} = \frac{e|\vec{E}|}{2M} \cdot \tau = \mu_+ |\vec{E}|$$

since T_{kin} essentially thermal, and $v_{\text{therm.}}$ thus constant ...

Drift velocity v_D for ions
proportional to E !

μ_+ : ion mobility e.g. $\mu_+=0.61 \text{ cm}^2/\text{Vs}$ for C_4H_{10}

[$E = 1 \text{ kV/cm}$; typical drift distances = few cm \rightarrow typical ion drift time = few ms]



Gaseous Detectors



Electron mobility:

Equation of motion:

$$m\ddot{\vec{x}} = e\vec{E} + e(\vec{v} \times \vec{B}) + m\vec{A}(t)$$

[in E, B field]

$\vec{v} = \dot{\vec{x}}$ instantaneous electron velocity

$m\vec{A}(t)$ time-dependent stochastic force
[describes collisions with gas atoms]

Assume:

- E and B field constant between collisions
- Time averaged stochastic term can be represented by friction term
- Time between collisions small with respect to considered time interval: $\Delta t \gg \tau$
- Drift velocity at fixed E constant, i.e. average acceleration vanishes, $\langle \ddot{\vec{x}} \rangle = 0$

$$\vec{v}_D = \langle \vec{v} \rangle$$

$$\langle m\ddot{\vec{x}} \rangle = e\vec{E} + e(\vec{v}_D \times \vec{B}) - \frac{m}{\tau}\vec{v}_D = 0$$

$$\text{with } \mu = \mu_- = \frac{e\tau}{m}$$

$$\omega = \frac{eB}{m}$$

B = 0:

$$\vec{v}_D = \frac{e\tau}{m}\vec{E} = \mu_- \vec{E}$$

B ≠ 0:

$$\vec{v}_D = \mu \cdot \vec{E} + \omega\tau \cdot \vec{v}_D \times \hat{B}$$

$$\rightarrow \vec{v}_D = \frac{\mu|\vec{E}|}{1 + \omega^2\tau^2} \left[\underbrace{\hat{E}}_{\text{Component } \perp \text{ to E,B}} + \underbrace{\omega\tau\hat{E} \times \hat{B} + \omega^2\tau^2(\hat{E} \cdot \hat{B})\hat{B}}_{\text{Component in direction of B}} \right]$$

Remark:

$\mu_+ \ll \mu_-$ as $M \gg m \dots$

Component
 \perp to E,B

Component
in direction of B

Electron mobility: $\vec{v}_D = \mu \vec{E}$
 [B = 0]

Compare:

Electrons: v_D of order cm/ μ s
 Ions: v_D of order cm/ms

Consider two situations:

$T_{\text{kin,e}} \gg kT$

gas atoms have only a few low-lying energy levels such that electrons can lose little energy in collisions [hot gases]

$$\lambda(T_e) \sim \lambda(E) \quad \text{and} \quad \mu \sim \tau \sim 1/\sigma(E)$$

μ not constant!
 [if $\lambda \sim 1/E$; $v_D = \text{const}$]

Electrons accelerated in E-field until sufficient energy is reached ...
 Higher E-field yields smaller mean free path \rightarrow constant v_D possible ...
 [Example: $v_D = 3 - 5$ cm/ μ s for 90% Ar/10% CH₄]

$T_{\text{kin,e}} \approx kT$

gas atoms have many low-lying energy levels such that electrons lose all energy they gain between collisions [cold gases]

$$\mu \approx \text{const.} \quad \text{and} \quad v_D \propto E$$

Similar to situation with ions ...

[Example: $\mu = 7 \cdot 10^{-3}$ cm²/ μ s V for 90% Ne/10% CO₂; $v_D = 2$ cm/ μ s @ 300 V/cm]

Large electric field yields
large kinetic energy of electrons ...

→ Avalanche formation

Larger mobility of electrons results in liquid
drop like avalanche with electrons near head ...

Mean free path: λ_{ion}
[for a secondary ionization]

Probability of an ionization per
unit path length: $\alpha = 1/\lambda_{ion}$ [1st Townsend coefficient]

$$dn = n \cdot \alpha dx$$

$n(x) =$ electrons
at location x

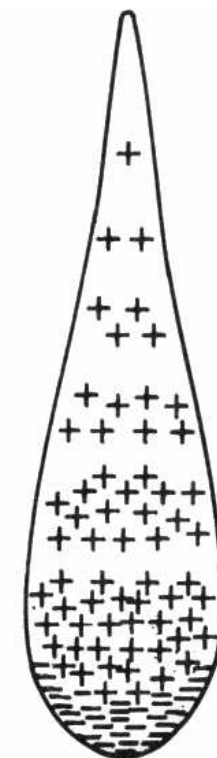
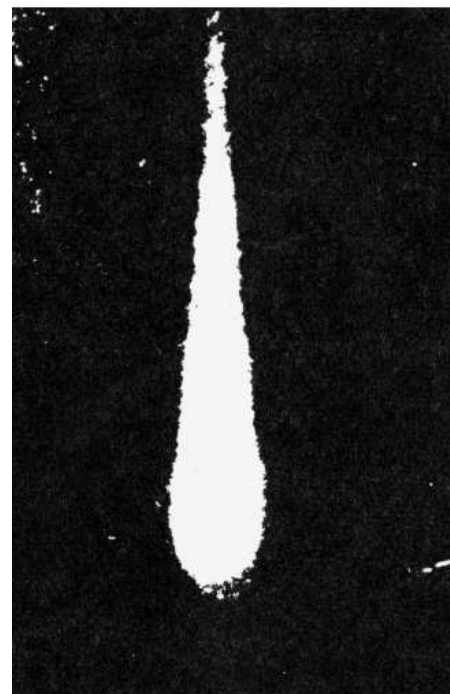
$$n = n_0 e^{\alpha x}$$

Gain:

$$G = \frac{n}{n_0} = e^{\alpha x} \quad \text{and more general for } \alpha = \alpha(x): \quad G = \frac{n}{n_0} = \exp \left[\int_{x_1}^{x_2} \alpha(x) dx \right]$$

[Raether limit: $G \approx 10^8$; $\alpha x = 20$; then sparking sets in ...]

Townsend avalanche

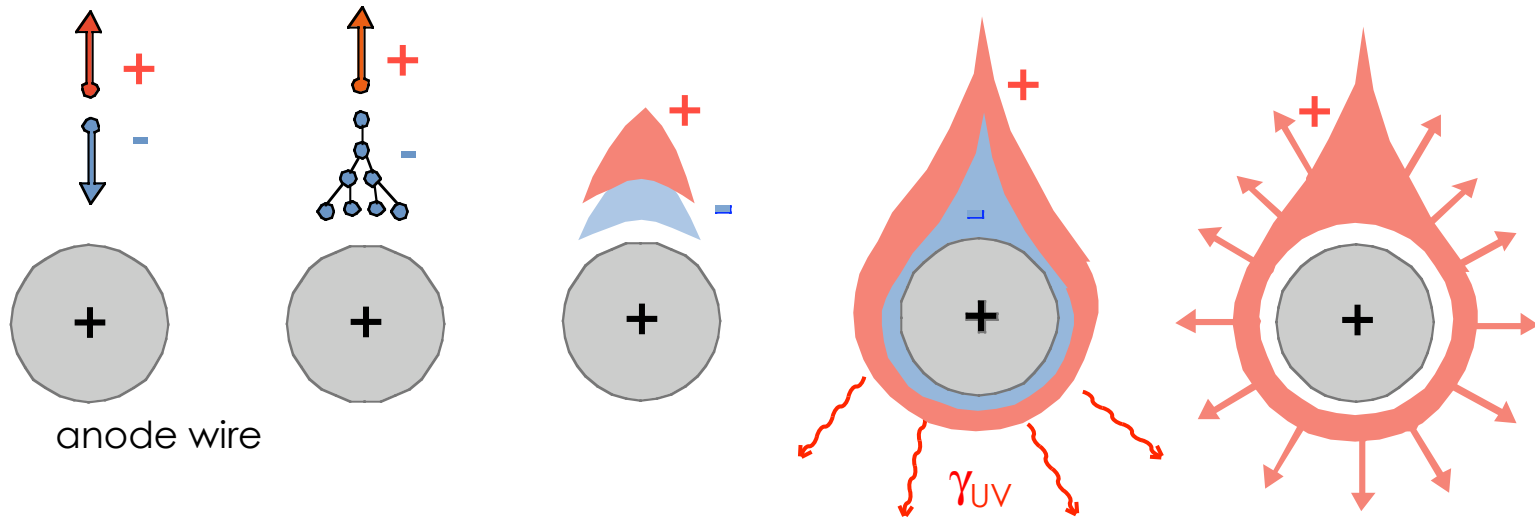


Drop-like shape of an avalanche

Left: cloud chamber picture

Right: schematic view

Avalanche phenomenon

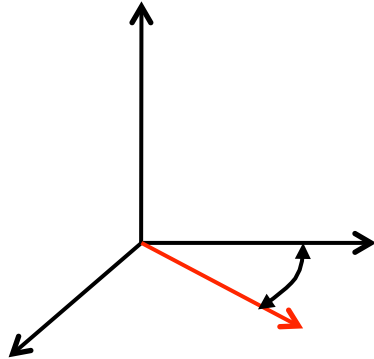


- * One electron drifts towards the anode wire:
 - Electric field is increasing
 - Ionizing collisions → pair multiplication
- * Due to lateral diffusion and difference of velocity of electrons-ions, a drop-like avalanche develops near the wire
- * UV photons are emitted → risk of uncontrolled amplification (spark)
- * Electrons are collected in a very short time (few ns) and ions drift slowly towards the cathode

Magnetic field

The drifting electrons cloud is rotated by an angle θ_B in the plane perpendicular to E and B .

$$\vec{E} \perp \vec{B}$$



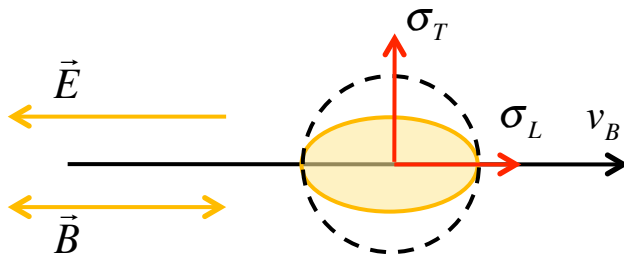
$$\tan \theta_B = \omega \tau$$

τ : mean collision time

$$v_B = \frac{E}{B} \frac{\omega \tau}{\sqrt{1 + \omega^2 \tau^2}}$$

$\omega = eB/m \rightarrow$ Larmor frequency

$$\vec{E} \parallel \vec{B}$$



$$v_B = v_0$$

$$\sigma_L = \sigma_0$$

Drift velocity unchanged

$$\sigma_T = \frac{\sigma_0}{\sqrt{1 + \omega^2 \tau^2}}$$

Transverse diffusion is reduced

Back

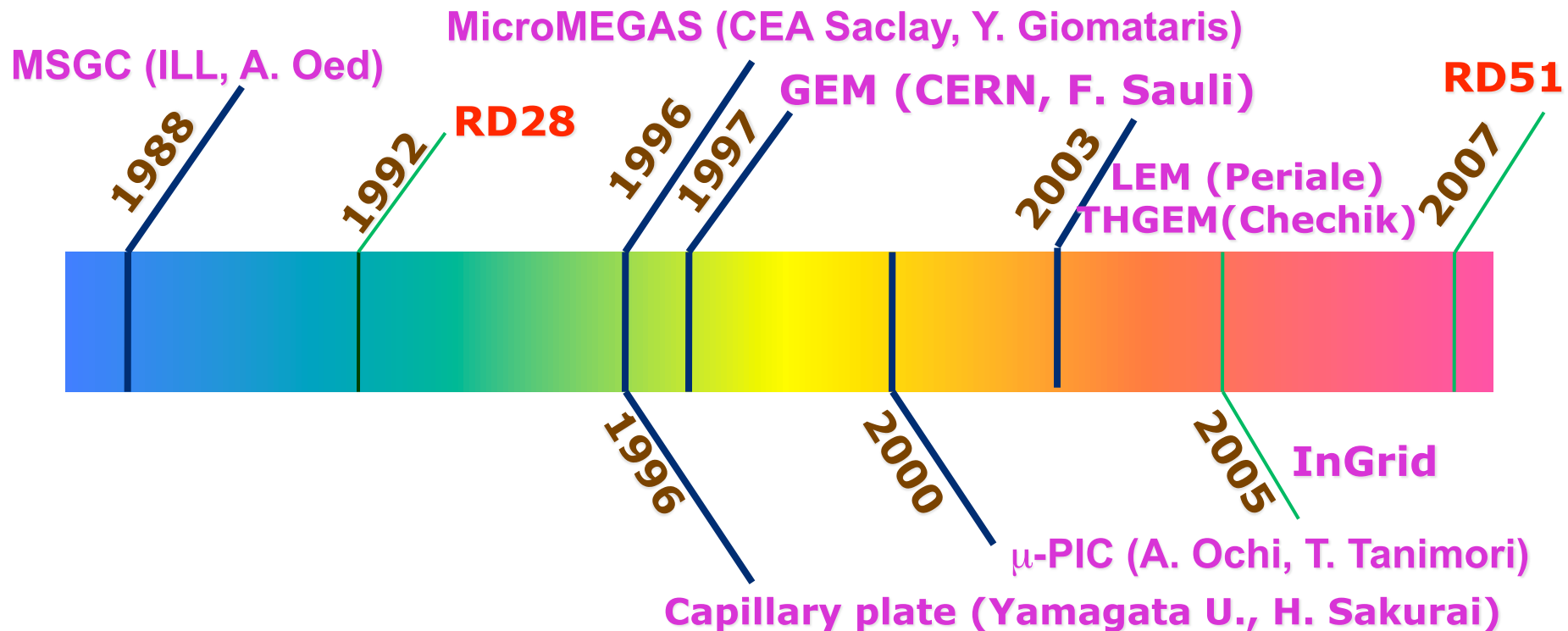
Gas Detectors

Large Volume Particle Tracking



MPGD Developments: Historical Roadmap*

(*Many more micro-pattern structures were developed; shown only those presented in this talk)



EXAMPLE OF GASEOUS DETECTORS

Geiger Counter

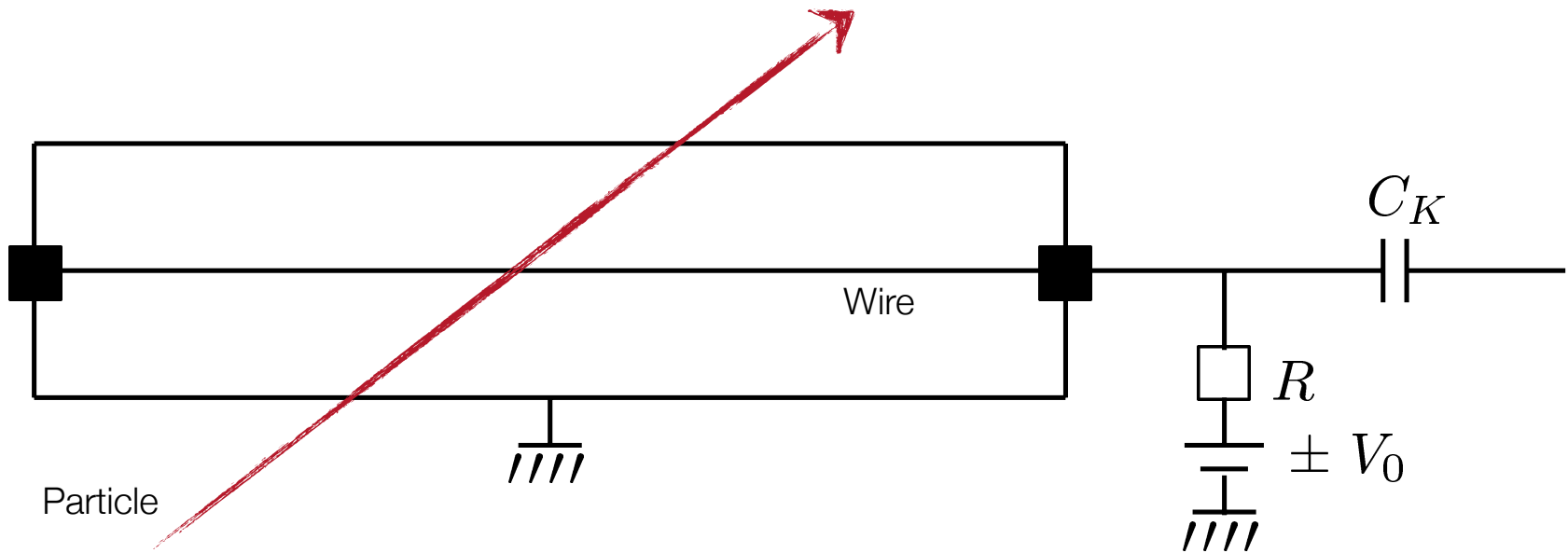
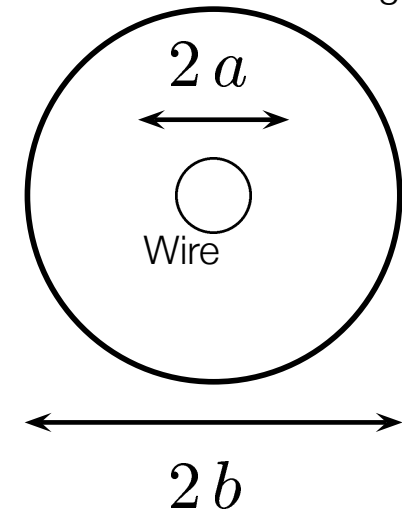
Relations:

E-field: $|\vec{E}| = \frac{\lambda}{2\pi\epsilon_0} \frac{1}{r}$

with:
 $\lambda = Q/L$
 [linear charge density]

Voltage: $V_0 = \frac{\lambda}{2\pi\epsilon_0} \ln \frac{b}{a} = \frac{\lambda}{C}$

Capacity:
 [per unit length] $C = \frac{2\pi\epsilon_0}{\ln \frac{b}{a}}$ [F/m]

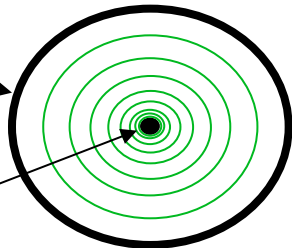


Single Wire Proportional Counter

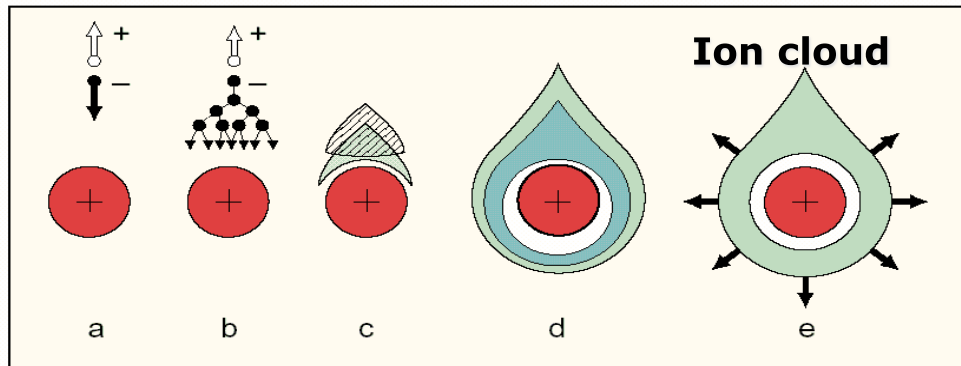
Thin anode wire (~20–50 μm) coaxial with cathode:

Cathode
radius b

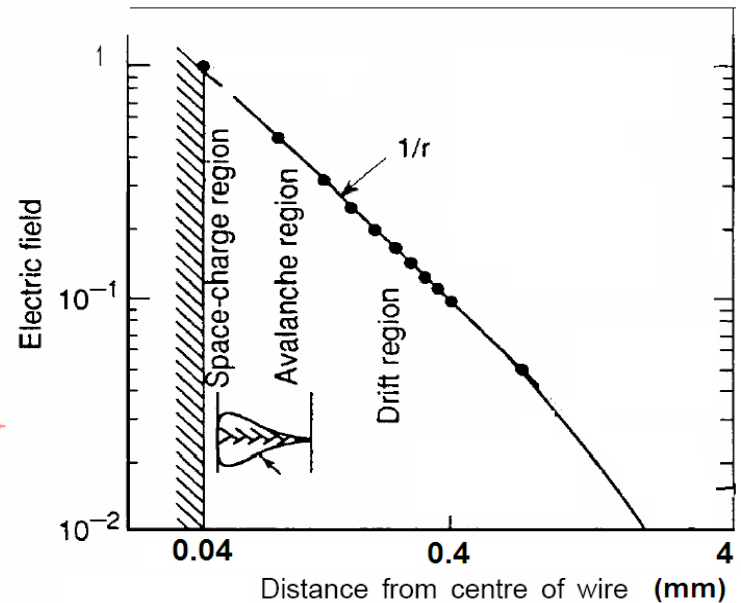
Anode
radius a



$$E(r) = \frac{CV_0}{2\pi\epsilon_0} \frac{1}{r}$$



Avalanche development in the high electric field (~ 250 kV/cm) around a thin wire (multiplication region ~ 100 μm):



Time development of an avalanche in a proportional counter

A single primary electron proceeds towards anode in regions of increasingly high fields, experiencing ionizing collisions; due to the lateral diffusion, a drop-like avalanche, surrounding the wire develops.

Moving charges create signal on nearby electrodes – the electron induced signal is almost negligible !!!

Ionization mode:

full charge collection
no multiplication; gain ≈ 1

Proportional mode:

multiplication of ionization
signal proportional to ionization
measurement of dE/dx
secondary avalanches need quenching;
gain $\approx 10^4 - 10^5$

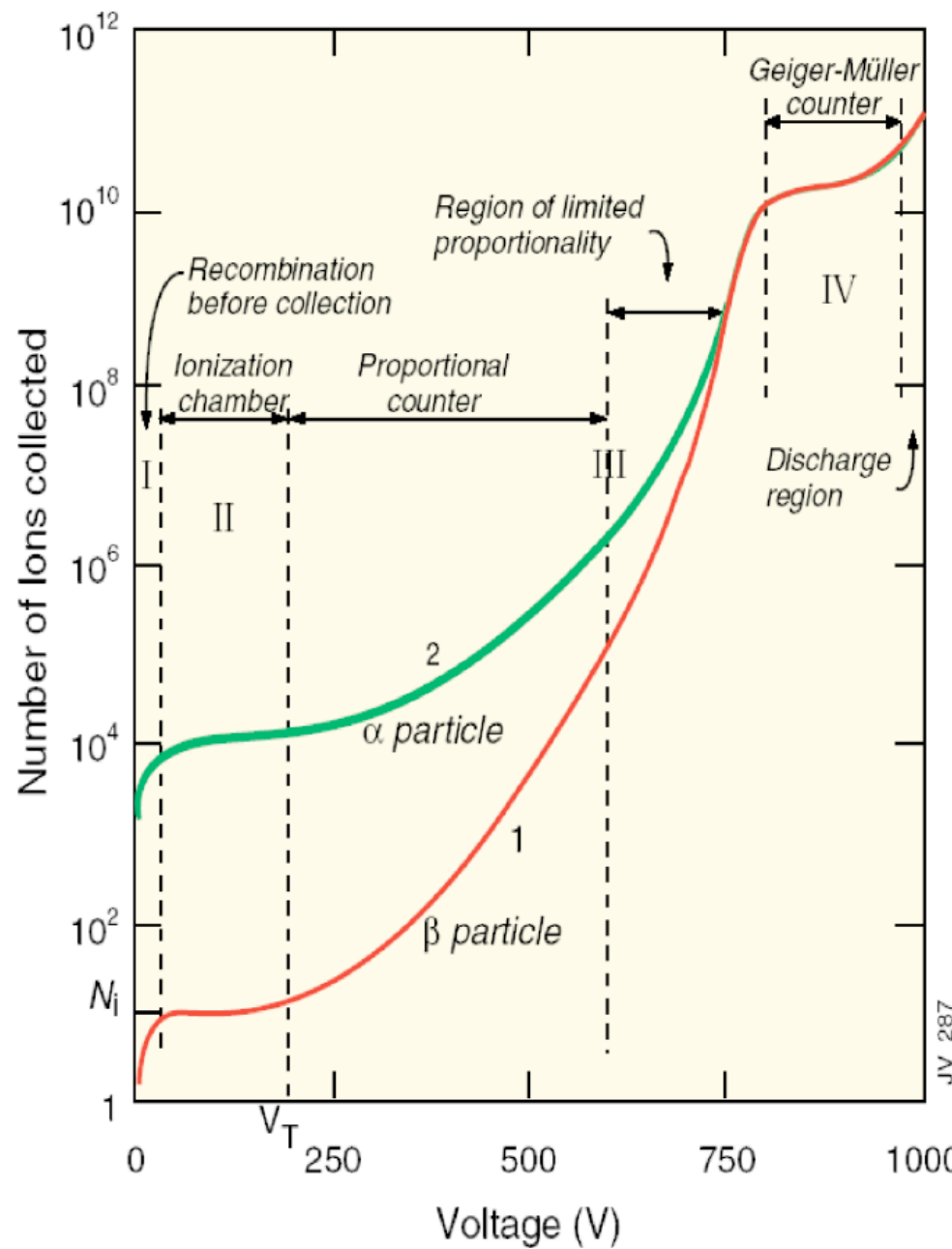
Limited proportional mode:

[saturated, streamer]

strong photoemission
requires strong quenchers or pulsed HV;
gain $\approx 10^{10}$

Geiger mode:

massive photoemission;
full length of the anode wire affected;
discharge stopped by HV cut



Measure drift time t_D
 [need to know t_0 ; fast scintillator, beam timing]

Determine location of original ionization:

$$x = x_0 \pm v_D \cdot t_D$$

$$y = y_0 \pm v_D \cdot t_D$$

If drift velocity changes along path:

$$x = \int_0^{t_D} v_D dt$$

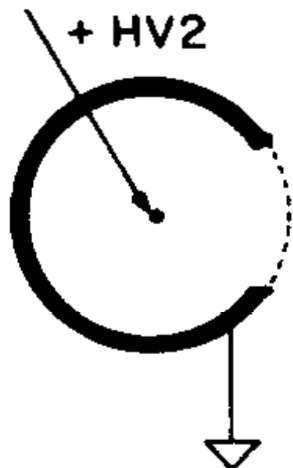
In any case:

Need well-defined drift field ...

Simple Drift Chamber Setup

But: here, uniform drift field requires high-voltages in case of large area detectors

Anode wire
 + HV2



Charged particle



Drift voltage
 -HV1



Drift region

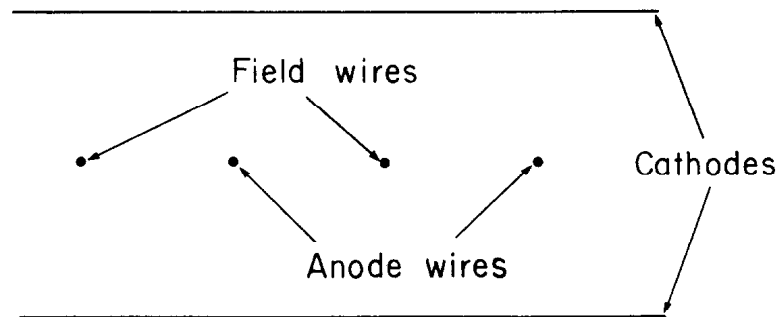


Scintillation counter



Modified MWPC ...

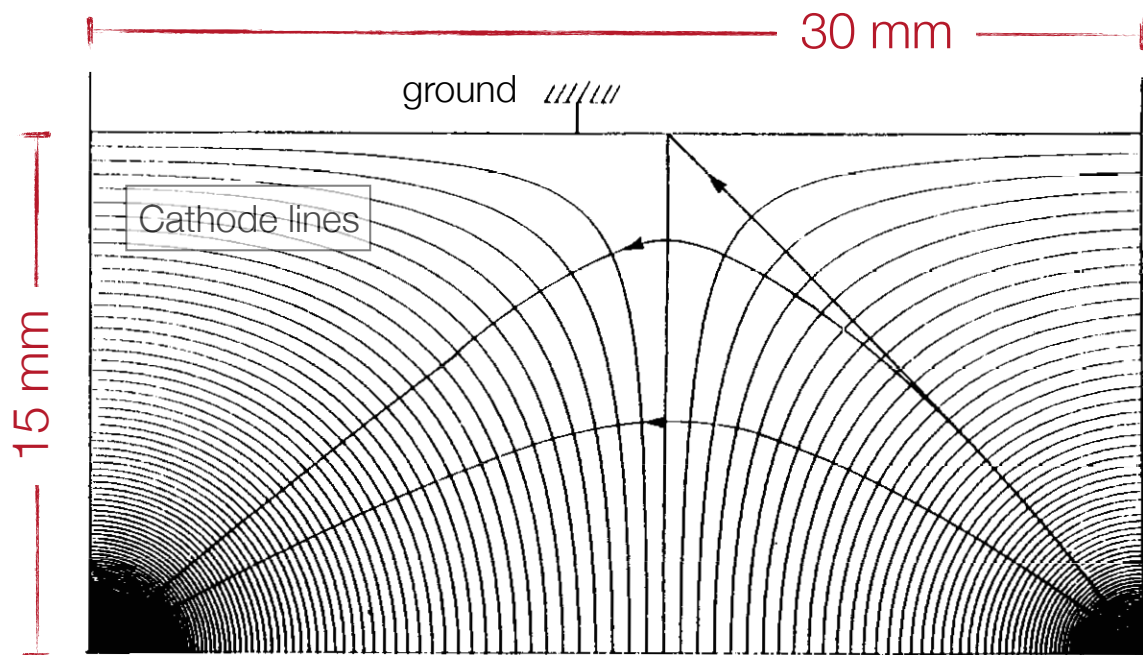
Introduce field wires to avoid low field regions, i.e. long drift-times



Field wires are at negative potential ...

Anode wires are at positive potential ...

Cathode planes are at zero potential ...



NIM 141 (1977) 43
[G.Marcel et. al]

Anode
[3.5 kV, Ø 50 µm]

Cathode
[-2 kV, Ø 200 µm]

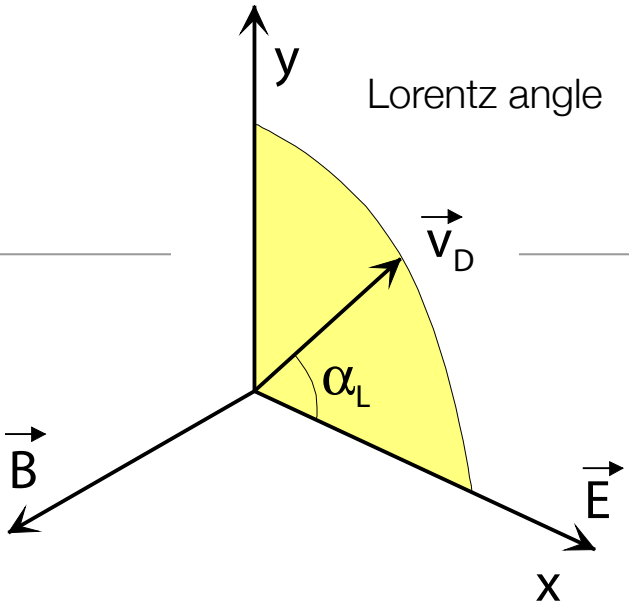
But:
Uniform drift field requires:
Gap length/wire spacing ≈ 1
i.e. for typical convenient wire spacing
one needs thick chambers ...

Drift Chambers – Lorentz Angle

Require B field for momentum measurement ...

In general drift field $E \perp$ to B field ...

→ Lorentz angle: $\alpha_L = \angle(\vec{v}_D, \vec{E}) \dots$



Reminder:

$$\vec{v}_D = \frac{\mu|\vec{E}|}{1 + \omega^2\tau^2} \left[\overbrace{\hat{E}}^{\text{Component } \perp \text{ to } E, B} + \omega\tau \overbrace{\hat{E} \times \hat{B}}^{\text{Component } \perp \text{ to } E, B} + \omega^2\tau^2 \overbrace{(\hat{E} \cdot \hat{B})\hat{B}}^{\text{Component in direction of } B} \right]$$

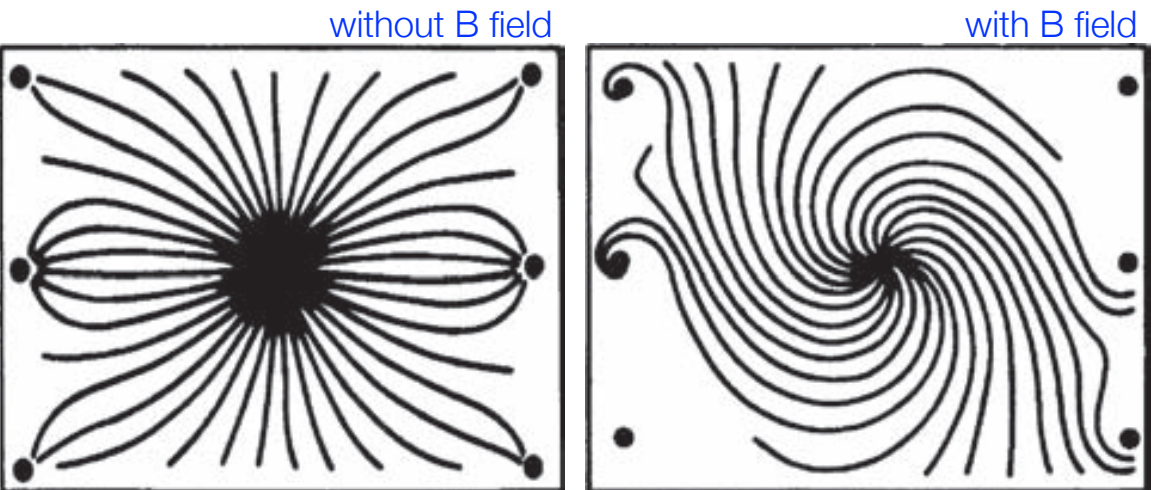
Using:

$$v_{D,x} = \frac{\mu E}{1 + \omega^2\tau^2}$$

$$v_{D,y} = \frac{\mu E}{1 + \omega^2\tau^2} \cdot \omega\tau$$

→ $\tan \alpha_L = \omega\tau$
 $= v_D \frac{B}{E}$

[with $\omega = \frac{eB}{m}$ and $\tau = \frac{mv_D}{eE}$]



Resolution determined by accuracy of drift time measurement ...

Influenced by:

Diffusion [$\sigma_{\text{Diff.}} \sim \sqrt{x}$]

see above: $\sigma^2 \sim 2Dt = 2Dx/v_D \sim x \dots$

δ -electrons [$\sigma_\delta = \text{const.}$]

independent of drift length; yields constant term in spatial resolution ...

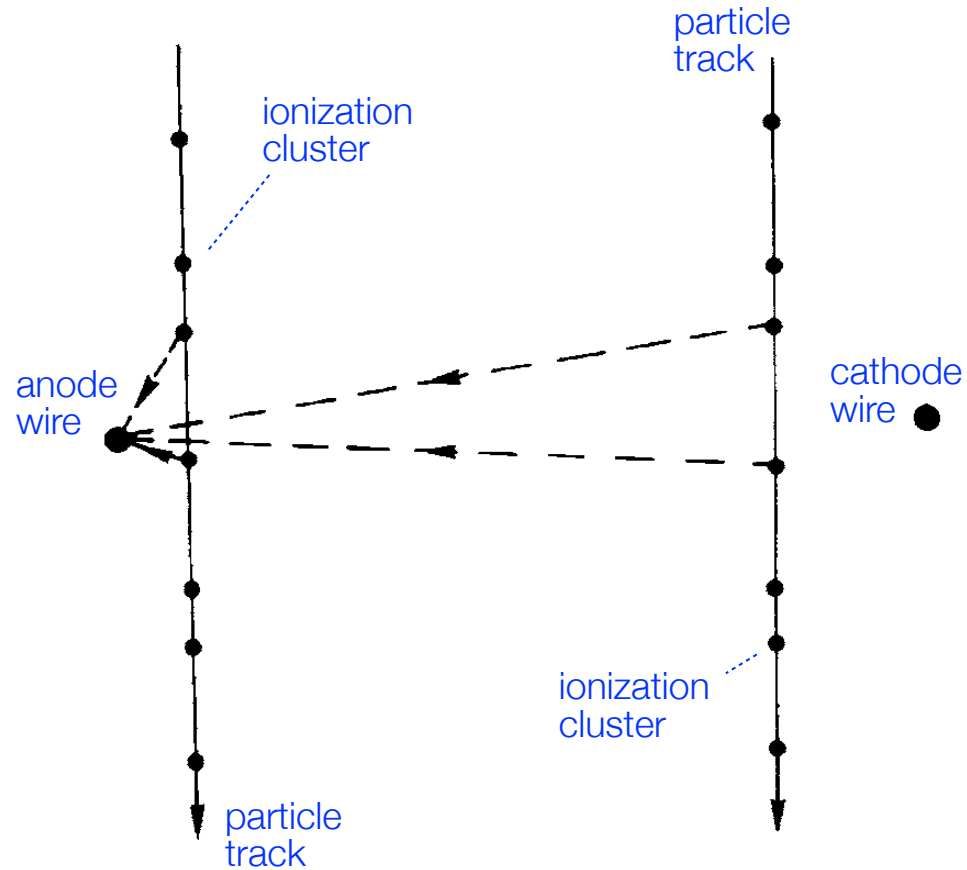
Electronics [$\sigma_{\text{electronics}} = \text{const.}$]

contribution also independent of drift length ...

Primary ionization statistics [$\sigma_{\text{prim}} = 1/x$]

Spatial fluctuations of charge-carrier production result in large drift-path differences for particle trajectories close to the anode ...

[minor influence for tracks far away from anode]



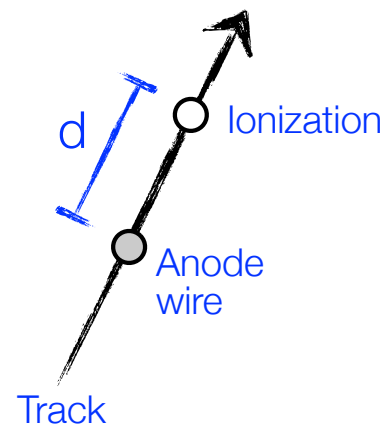
Primary ionization statistics:

Step 1: Consider a track passing through an anode wire ...

Probability of no ionization within distance d :

$$P_0(d) = e^{-2Nd}$$

with
 N : number of ionizations per unit length

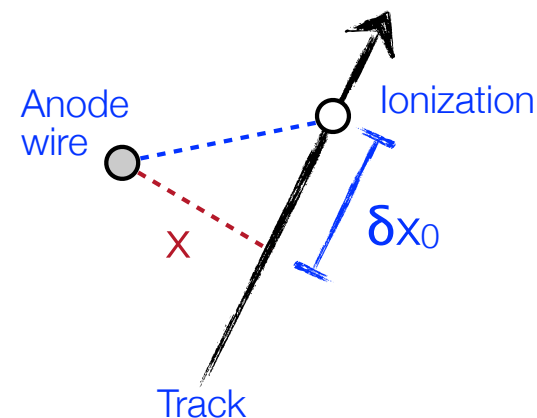


Average minimum distance of closest ionization cluster:

$$\delta x_0 = \langle d_{\min} \rangle = \int_0^{\infty} x e^{-2Nx} 2N dx = \frac{1}{2N}$$

Normalization

$$\sigma_{\langle d_{\min} \rangle}^2 = \int_0^{\infty} \left(x - \frac{1}{2N}\right)^2 e^{-2Nx} 2N dx = \frac{1}{4N^2}$$



Step 2: Track at distance x ...

$$\delta x = \sqrt{x^2 + (\delta x_0)^2} - x = x \left(\sqrt{1 + \left(\frac{\delta x_0}{x}\right)^2} - 1 \right) \approx \frac{x}{2} \left(\frac{\delta x_0}{x}\right)^2 \propto \frac{1}{x}$$

$$\sigma_x^2 = \underbrace{\left(\frac{1}{64N^2} \right) \cdot \frac{1}{x^2}}_{1^{\text{st}} \text{ ionization statistics}} + \underbrace{\frac{2D}{v_d} \cdot x}_{\text{diffusion}} + \underbrace{\sigma_{\text{const}}^2}_{\text{electronics } \delta\text{-electrons}}$$

Possible improvements:

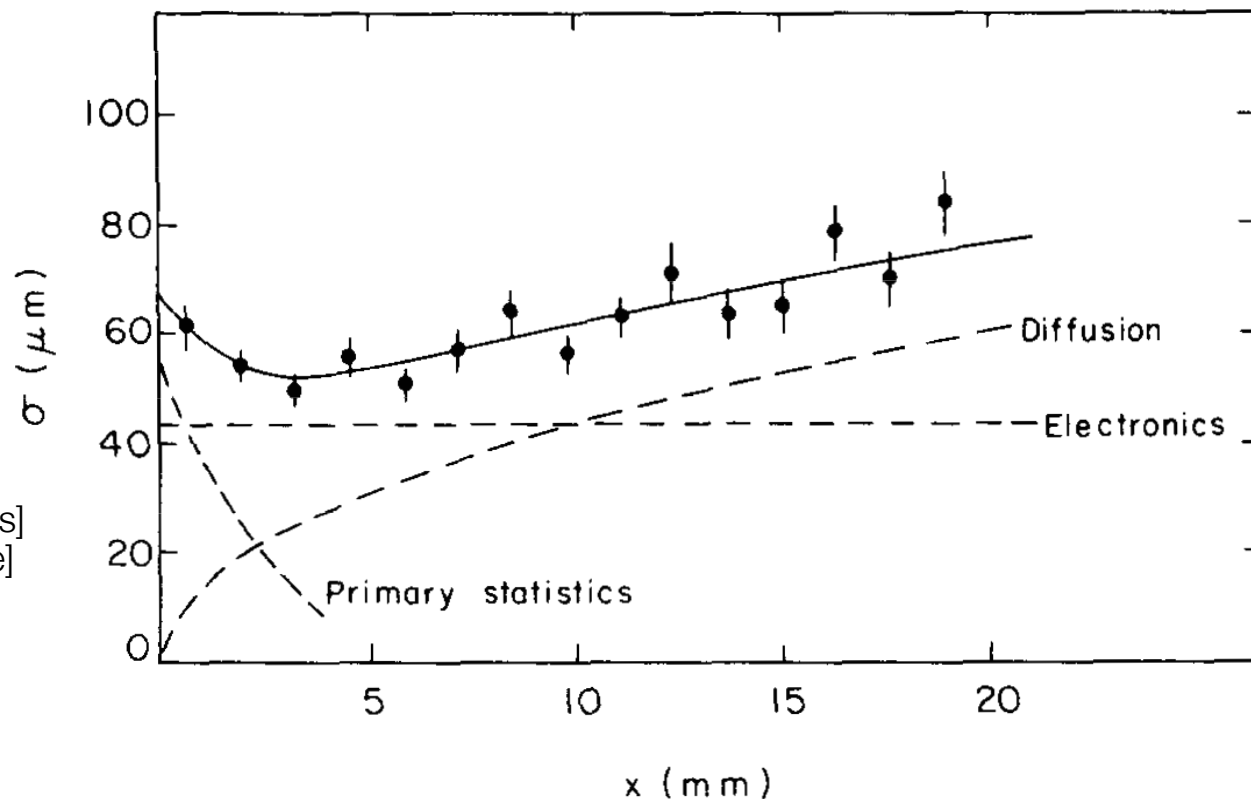
Increase N by increasing pressure ...

Decrease D by increasing pressure ...

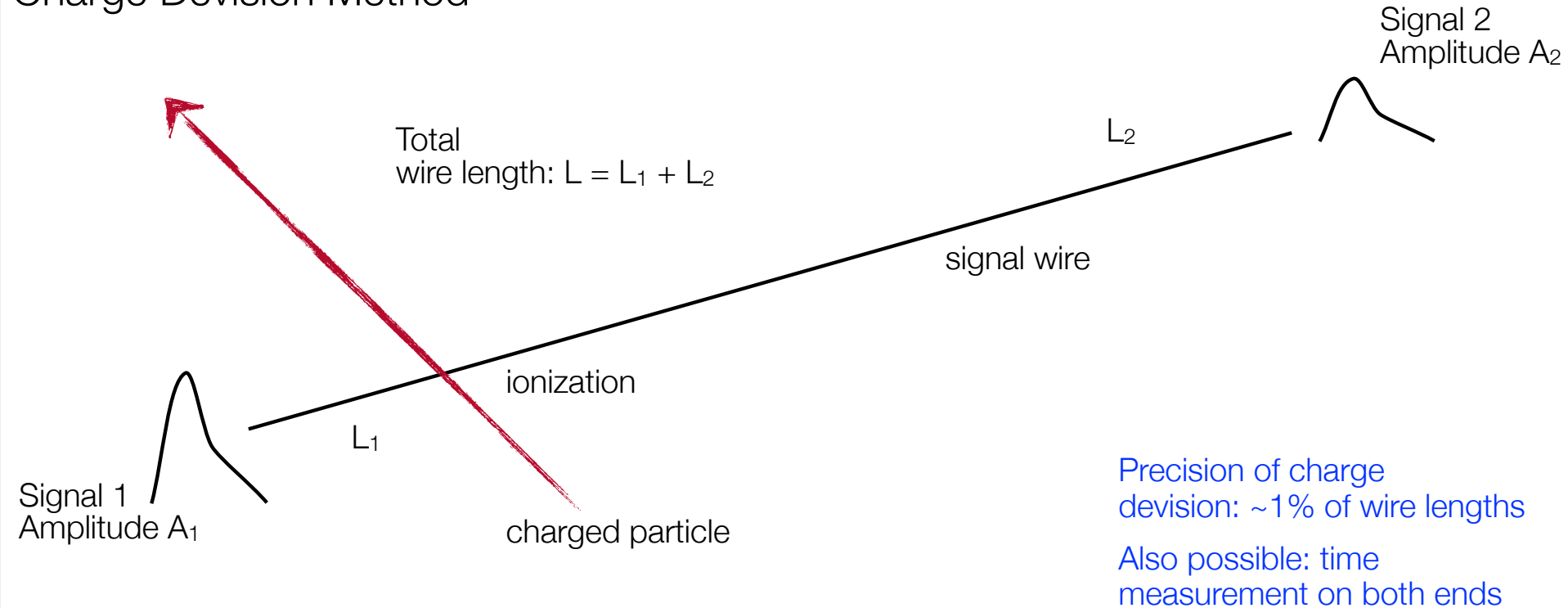
$$D \sim \frac{\lambda_0^2}{\tau} \sim \frac{1/n^2}{1/n} \sim \frac{1}{n}$$

[n: particle density in gas]
[increases with pressure]

i.e.: increase pressure ...
[up to 4 atm possible]



Principle of Charge Division Method



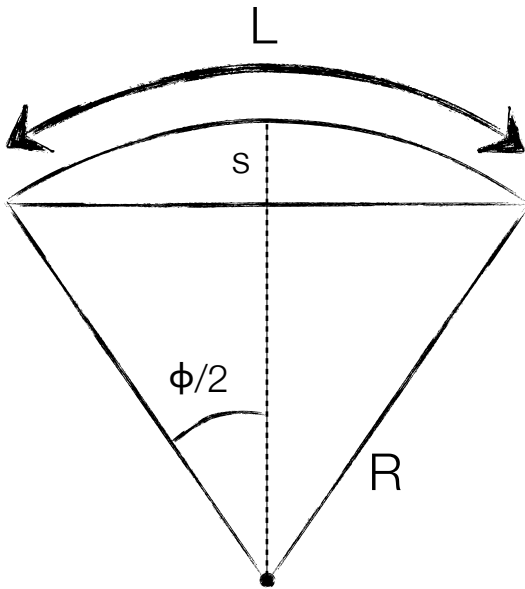
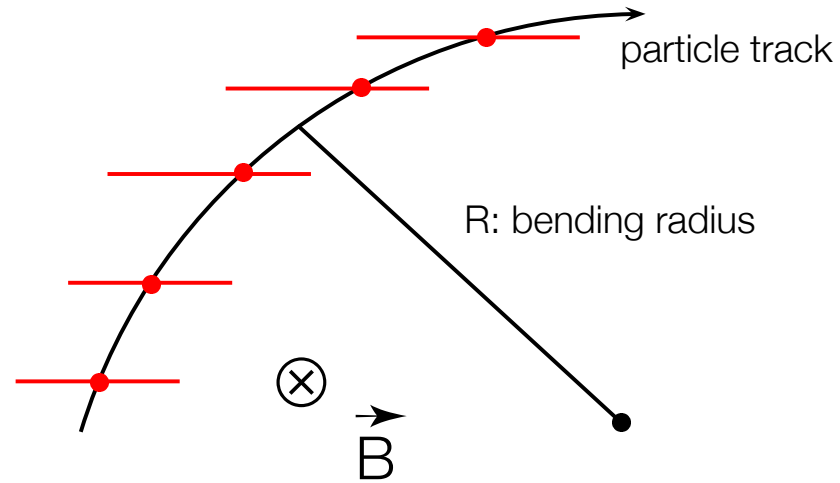
Determination of L_1, L_2 :

$$L_2 = \frac{A_1}{A_1 + A_2} \cdot L \quad L_1 = \frac{A_2}{A_1 + A_2} \cdot L$$

Momentum determination
in a cylindrical drift chamber ...

$$\frac{mv^2}{R} = evB \quad \rightarrow \quad p = eB \cdot R$$

$$p \left[\frac{\text{GeV}}{c} \right] = 0.3 B [\text{m}] \cdot R [\text{T}]$$



For Sagitta s :

$$s = R - R \cos \frac{\phi}{2} \approx R \frac{\phi^2}{8} \quad \text{with } \phi = \frac{L}{R}$$

$$s = R \frac{L^2}{8R^2} = \frac{L^2}{8R} \quad \text{and} \quad R = \frac{L^2}{8s}$$

$$\rightarrow \frac{\Delta p}{p} = \frac{\Delta R}{R} = \frac{L^2}{8Rs} \cdot \frac{\Delta s}{s}$$

Momentum measurement

uncertainty:

$$\frac{\sigma_p}{p} = \frac{L^2}{8Rs} \cdot \frac{\sigma_s}{s} = \frac{L^2}{8R} \cdot \frac{\sigma_s}{L^4/64R^2} = \frac{\sigma_s}{L^2} \cdot 8R = \frac{\sigma_s}{L^2} \cdot \frac{8p}{eB} \sim p \cdot \frac{\sigma_s}{BL^2}$$

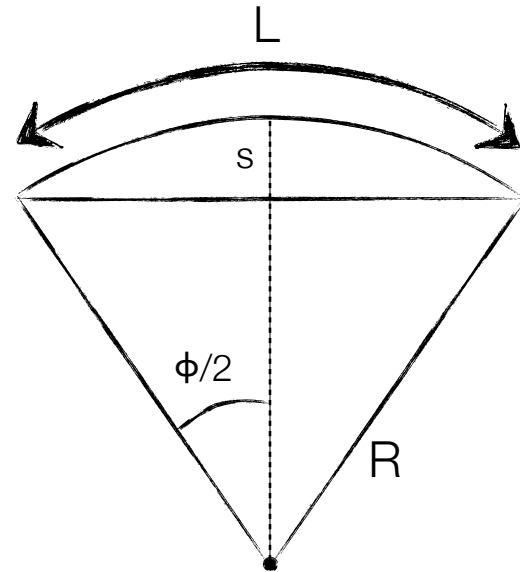
Uncertainty σ_s depends on number and spacing of track point measurements; for equal spacing and large N:

$$\sigma_s = \frac{\sigma_{r\phi}}{8} \sqrt{\frac{720}{N+5}}$$

see: Glückstern, NIM 24 (1963) 381 or Blum & Rolandi, Particle Detection ...

Good momentum resolution:

- large path length L
- large magnetic field B
- good Sagitta measurement



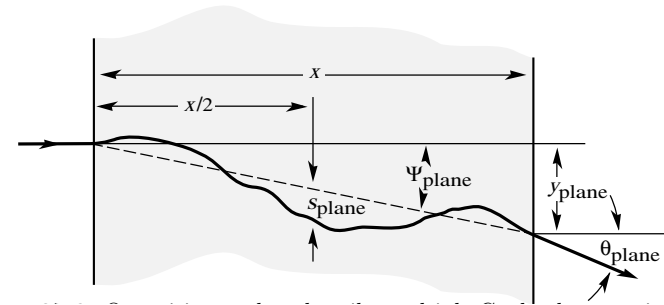
Multiple scattering contribution:

Reminder:

$$\sigma_\phi = \frac{13.6 \text{ MeV}}{\beta c p} z \sqrt{x/X_0} [1 + 0.038 \ln(x/X_0)]$$

$$\sigma_\phi \approx \frac{14 \text{ MeV}/c}{p} \sqrt{\frac{L}{X_0}} \quad \text{and} \quad \frac{\sigma_p}{p} = \frac{\sigma_R}{R} = \frac{\sigma_\phi}{\phi}$$

$$\text{as } R = \frac{L}{\phi}$$

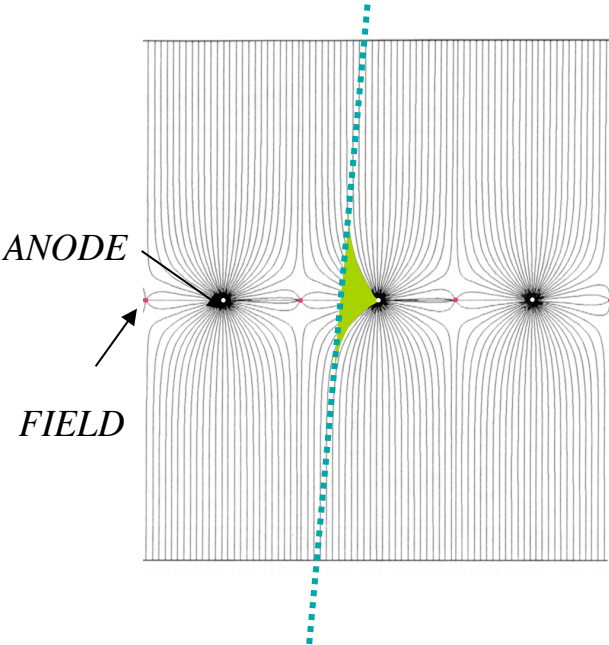


Drift Chambers

FIRST DRIFT CHAMBER OPERATION (H. WALENTA ~ 1971)

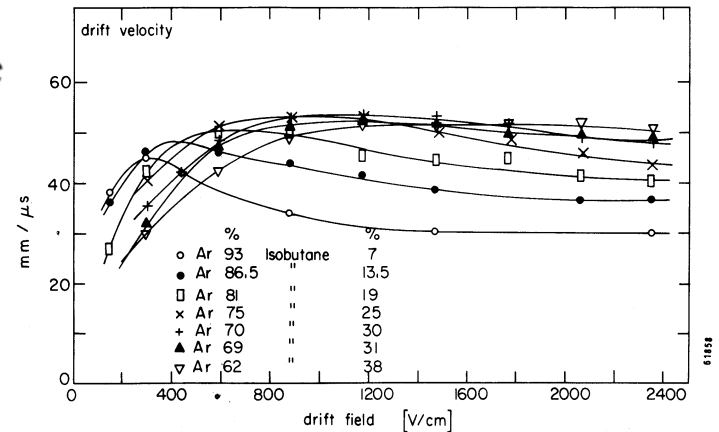
HIGH ACCURACY DRIFT CHAMBERS (Charpak-Breskin-Sauli ~ 1973-75)

THE ELECTRONS DRIFT TIME PROVIDES THE DISTANCE OF THE TRACK FROM THE ANODE:



HIGH AND UNIFORM ELECTRIC FIELD IN MOST OF THE VOLUME

Preferentially GAS MIXTURE WITH SATURATED DRIFT VELOCITY (linear space-time relation)

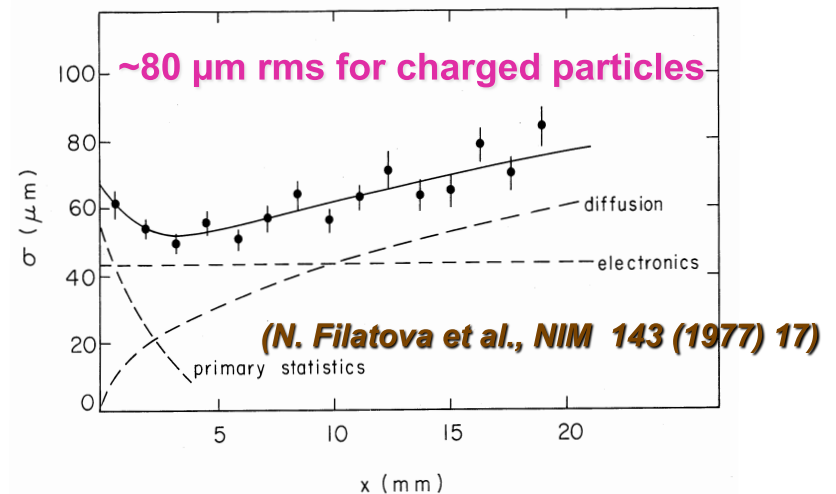


The spatial resolution is not limited to the cell size

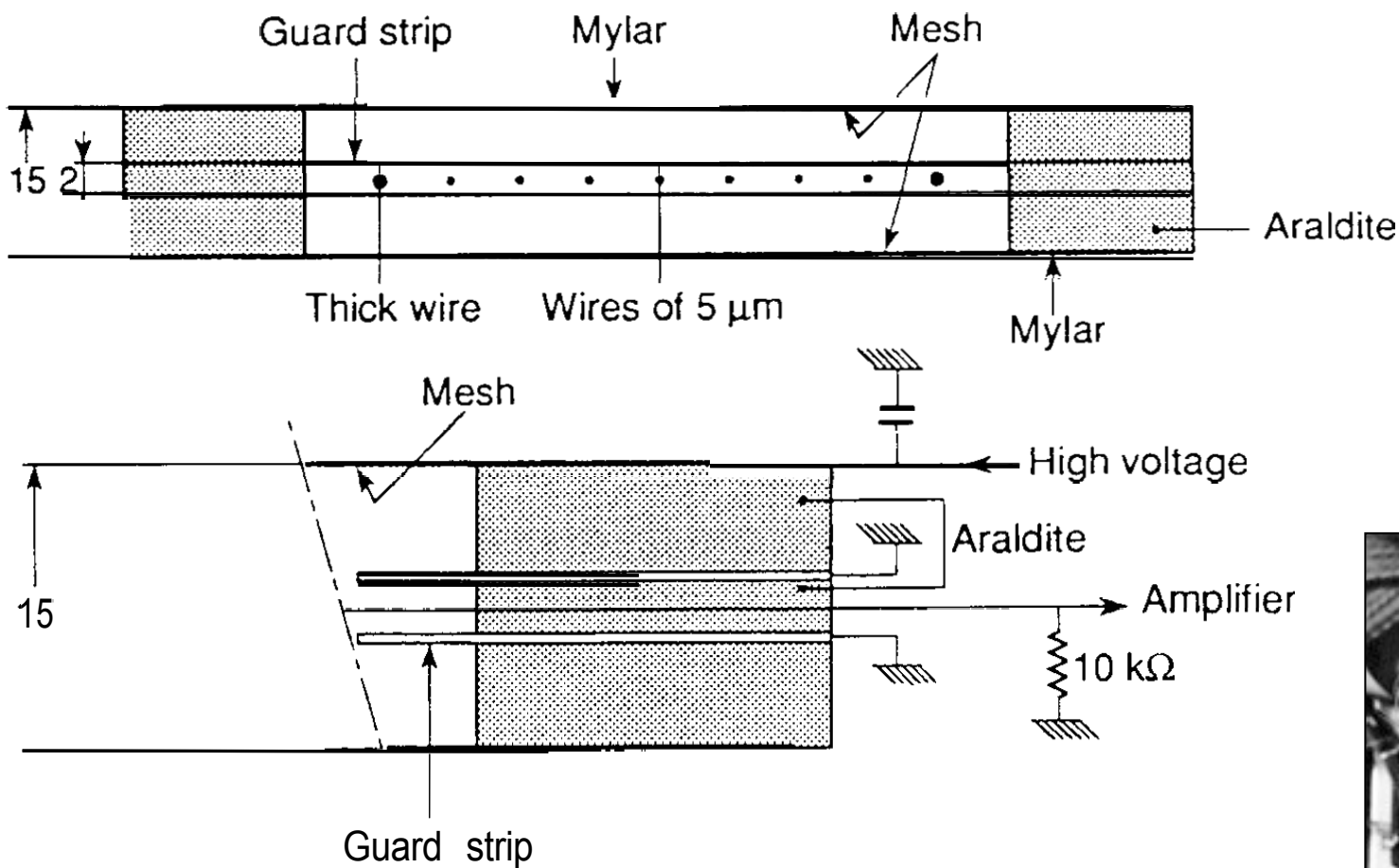
Space resolution determined by:

- Distribution of primary ionization
 - Diffusion
 - Readout electronics
- Electric field (gas amplification)
 - Range of 'delta electrons'

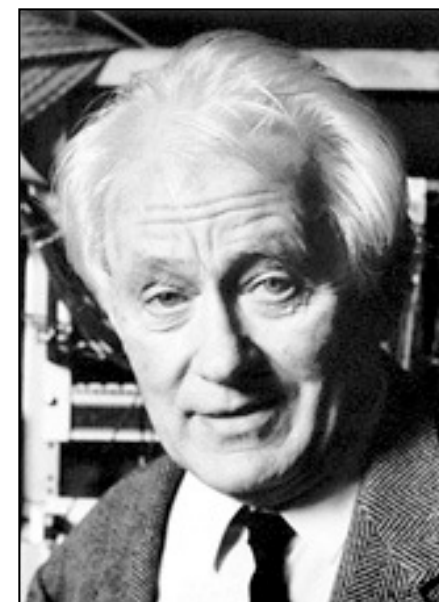
High accuracy drift chambers at low rates:



A. Breskin et al, Nucl. Instr. and Meth. 124(1975)189



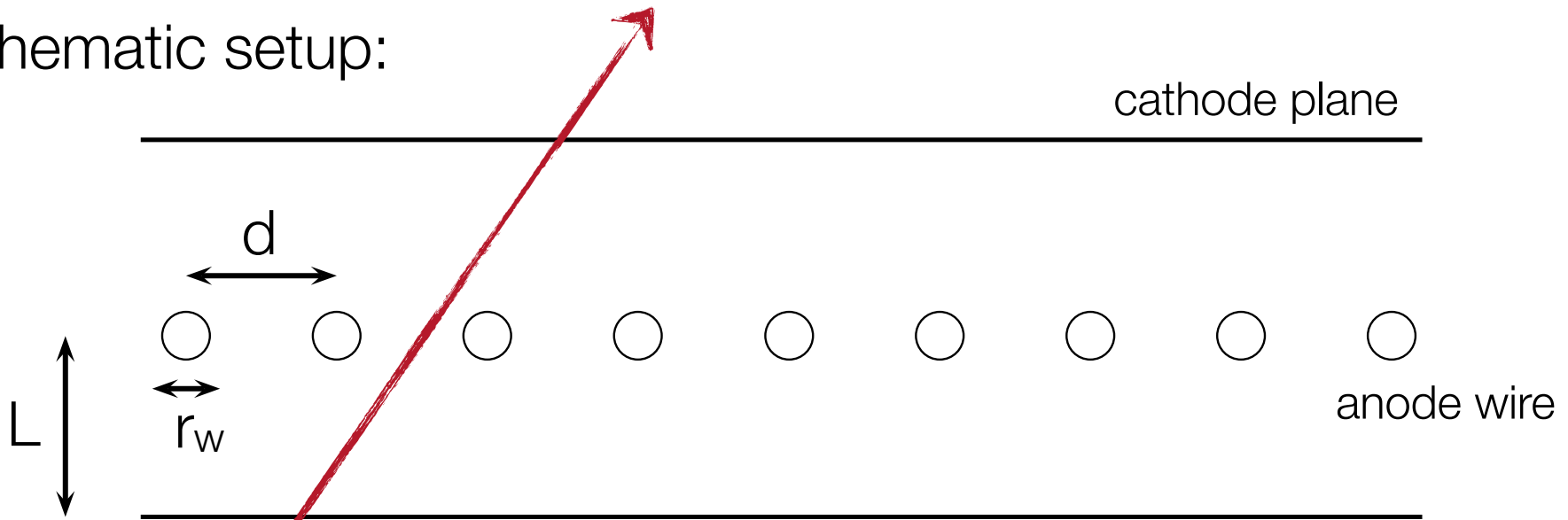
G. Charpak
Nobel Prize 1992



MWPC construction details
from Charpak's nobel lecture [1967 design]

Sense wires [$\varnothing = 20 \mu\text{m}$] separated by 2 mm; wires lie between two cathode meshes; edges of the planes are potted in Araldite ...

Schematic setup:



Parameters:

- $d = 2 - 4 \text{ mm}$
- $r_w = 20 - 25 \text{ }\mu\text{m}$
- $L = 3 - 6 \text{ mm}$
- $U_0 = \text{several kV}$
- Total area: $O(\text{m}^2)$

Features:

- Tracking of charged particles
- Some PID capabilities via dE/dx
- Large area coverage
- High rate capabilities

particle track

Signal generation:

Electrons drift to closest wire

Gas amplification near wire → avalanche

Signal generation due to electrons and slow ions ...

Timing resolution:

Depends on location of penetration

For fast response: OR of all channels ...

[Typical: $\sigma_t = 10$ ns]

Space point resolution:

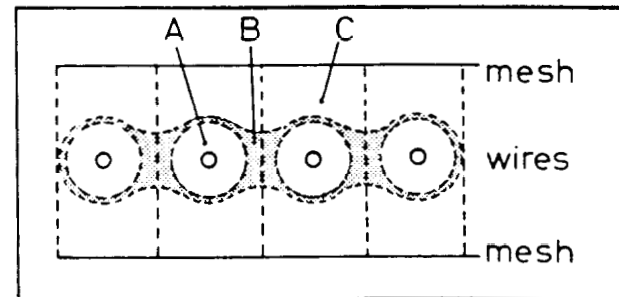
Only information about closest wire → $\sigma_x = d/\sqrt{12}$

[Not very precise and only one for one dimension ...]

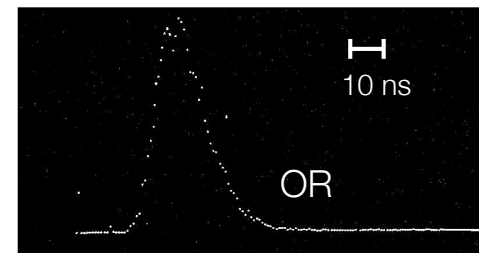
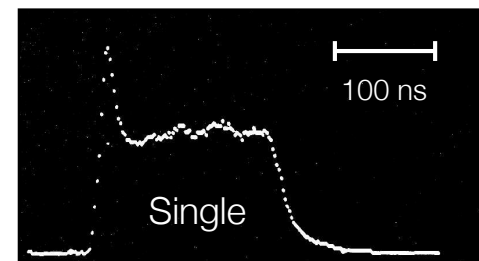
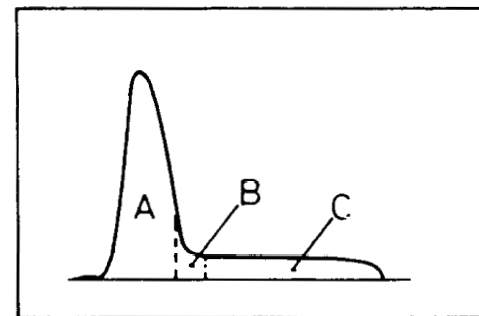
2-dim.: use 2 MWPCs with different orientation ...

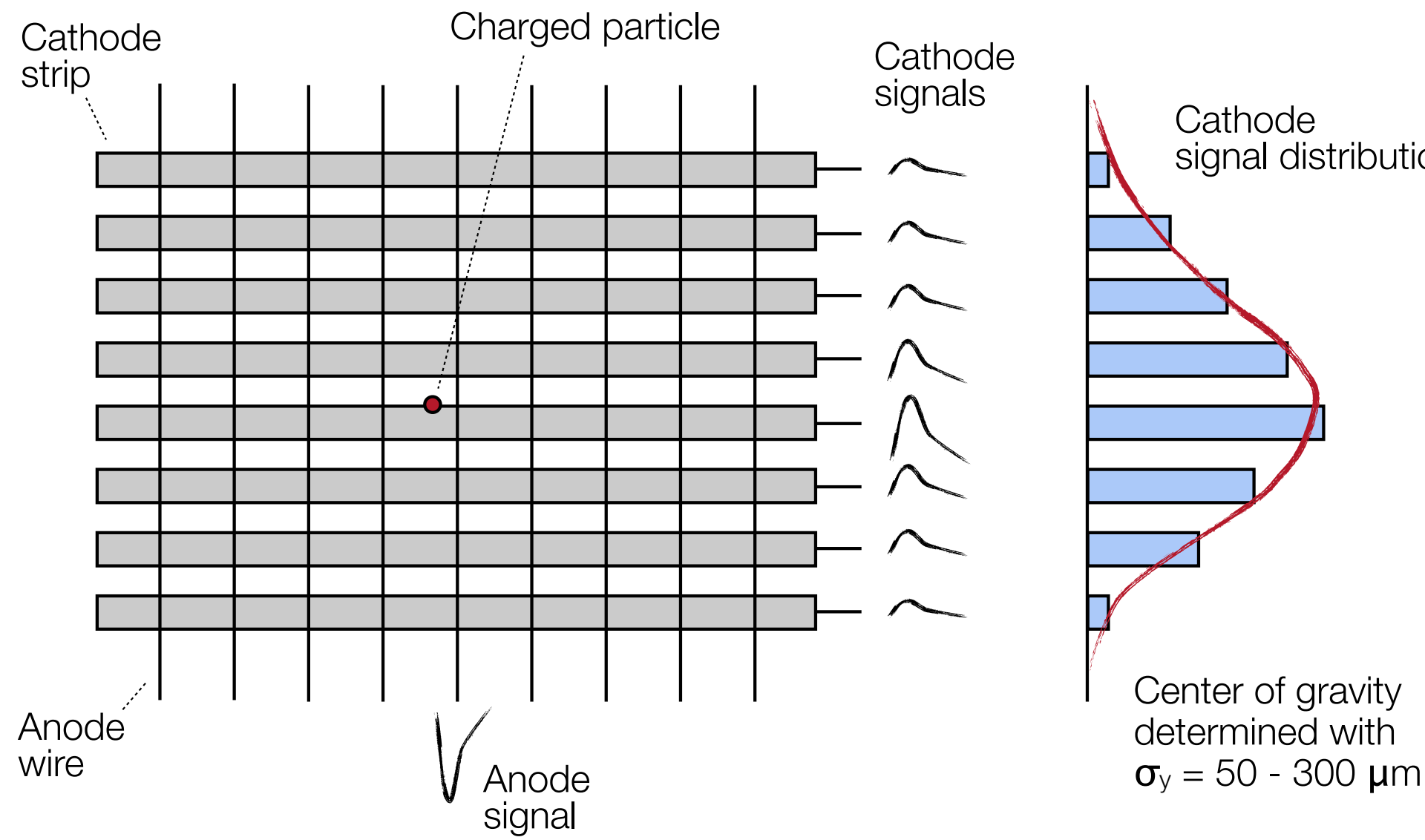
3-dim.: several layers of such X-Y-MWPC combinations.

Possible improvement: segmented cathode ...

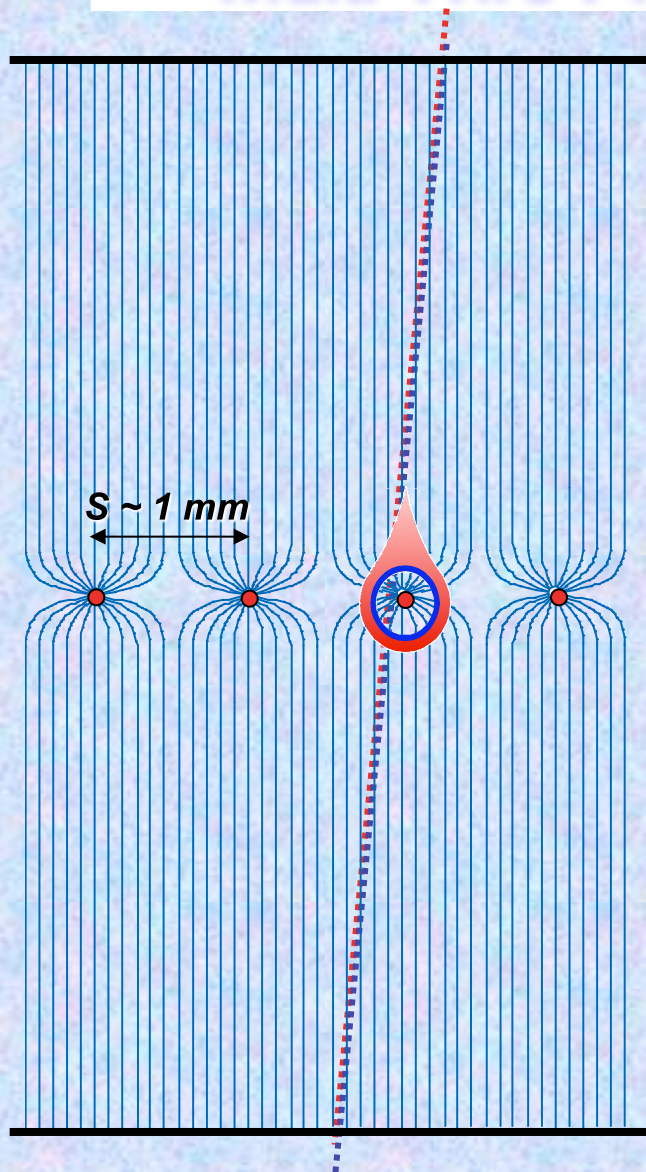


main contribution



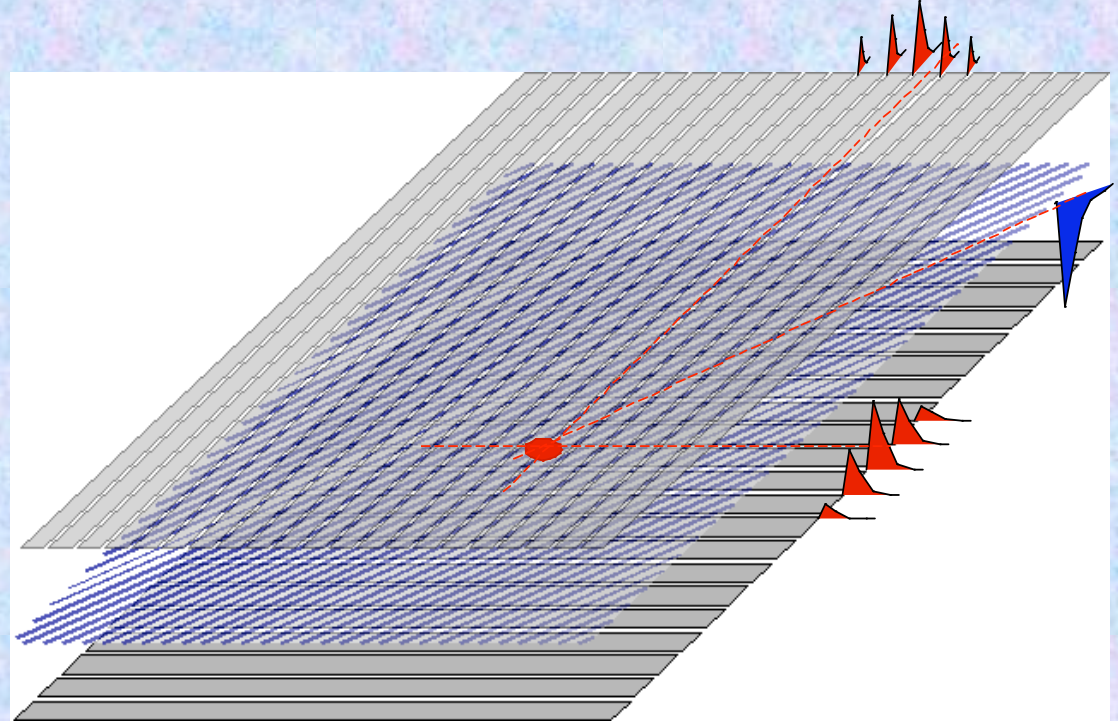


Multi-Wire Proportional Chamber (MWPC)



*High-rate MWPC with digital readout:
Spatial resolution is limited to $s_x \sim s/\sqrt{12} \sim 300 \mu\text{m}$*

**TWO-DIMENSIONAL MWPC READOUT CATHODE
INDUCED CHARGE (Charpak and Sauli, 1973)**



*Spatial resolution determined by: Signal / Noise Ratio
Typical (i.e. 'very good') values: $S \sim 20000$ e^- ; noise $\sim 1000e^-$
Space resolution $< 100 \mu\text{m}$*

**Resolution of MWPCs limited by wire spacing
better resolution \rightarrow shorter wire spacing \rightarrow more (and more) wires...**

Electronic 'bubble chamber' Full 3D reconstruction ...

xy : from wires and pads of MWPC ...
z : from drift time measurement

Momentum measurement ...
space point measurement
plus B field ...

Energy measurement ...
via dE/dx ...

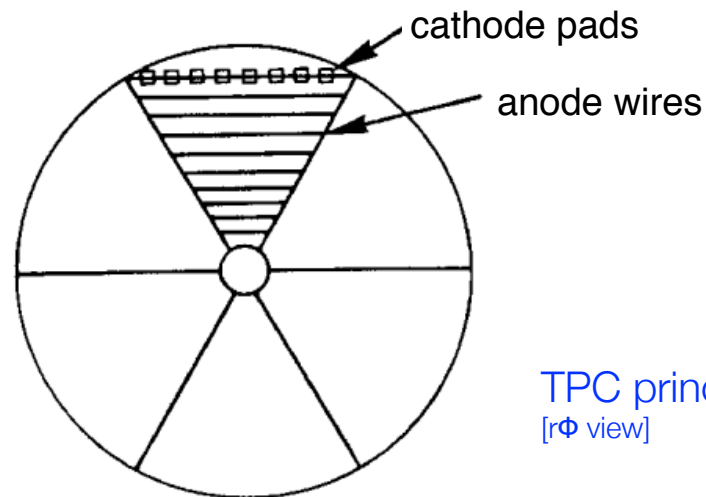
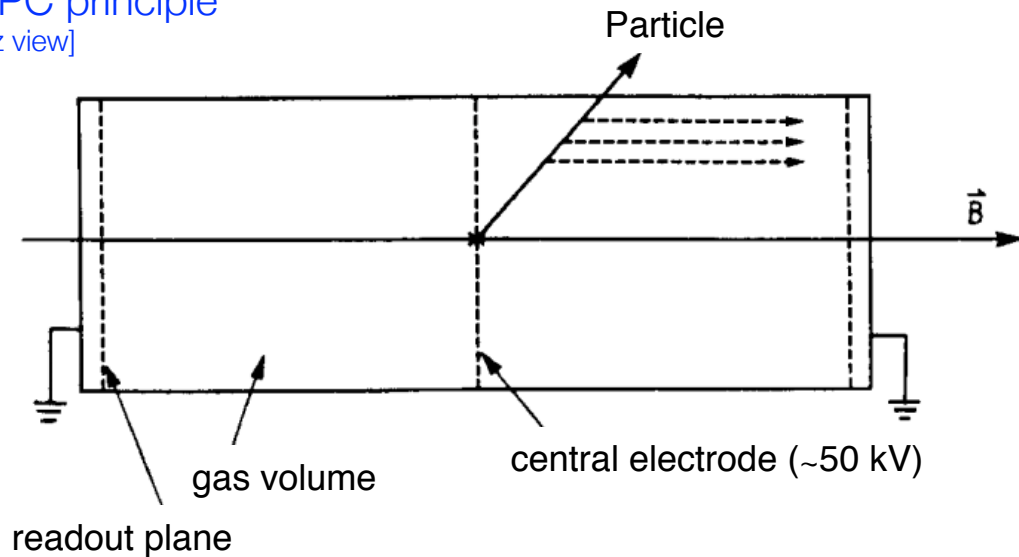
TPC setup:

(mostly) cylindrical detector
central HV cathode
MWPCs at end-caps of cylinder
 $B \parallel$ to $E \rightarrow$ Lorentz angle = 0

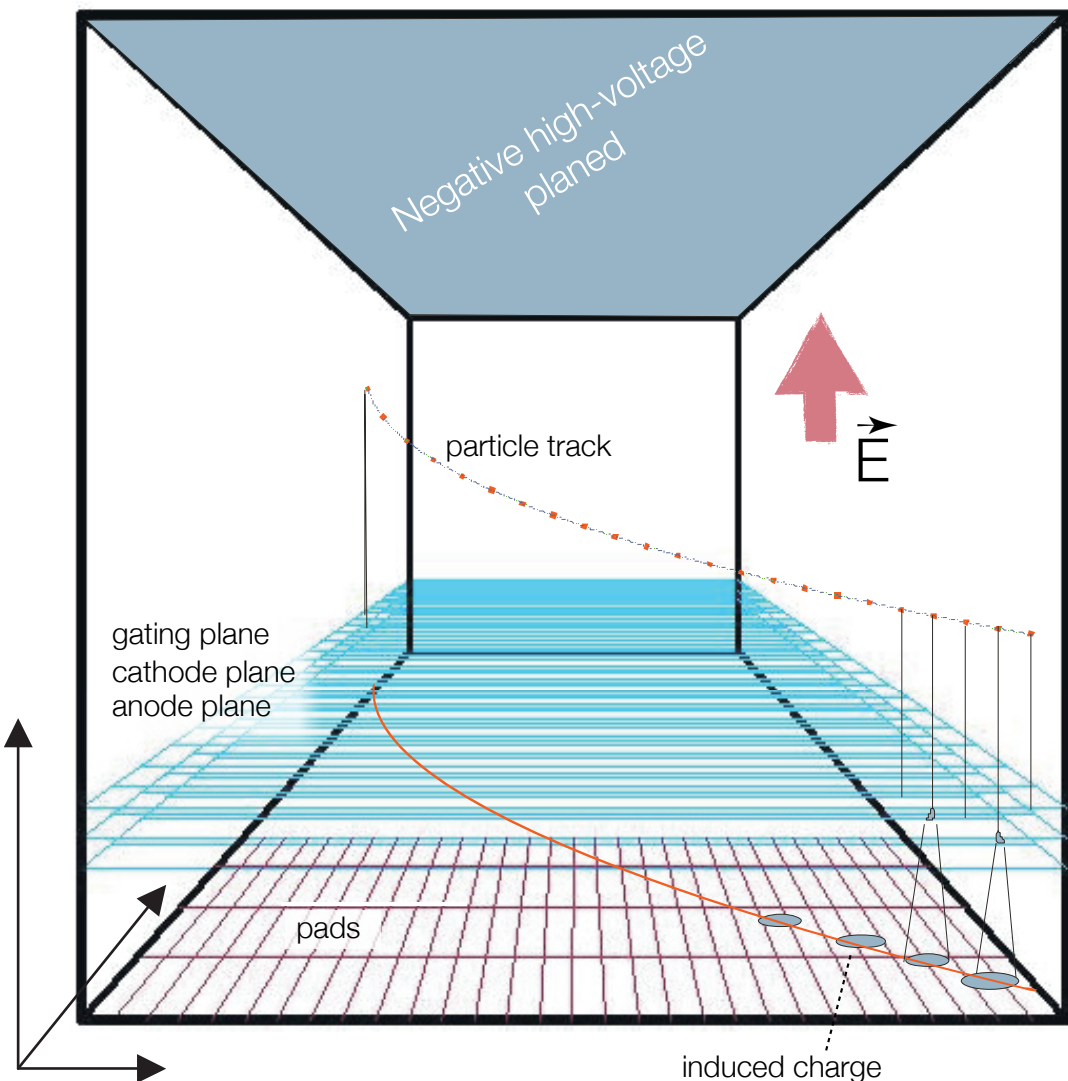
Charge transport :

Electrons drift to end-caps
Drift distance several meters
Continuous sampling of induced
charges in MWPC

TPC principle
[rz view]



TPC principle
[$r\phi$ view]



Advantages:

- Complete track within one detector yields good momentum resolution
- Relative few, short wires (MWPC only)
- Good particle ID via dE/dx
- Drift parallel to B suppresses transverse diffusion by factors 10 to 100

Challenges:

- Long drift time; limited rate capability [attachment, diffusion ...]
- Large volume [precision]
- Large voltages [discharges]
- Large data volume ...
- Extreme load at high luminosity; gating grid opened for triggered events only ...

Typical resolution:

z: mm; x: 150 - 300 μm ; y: mm
 dE/dx : 5 - 10%

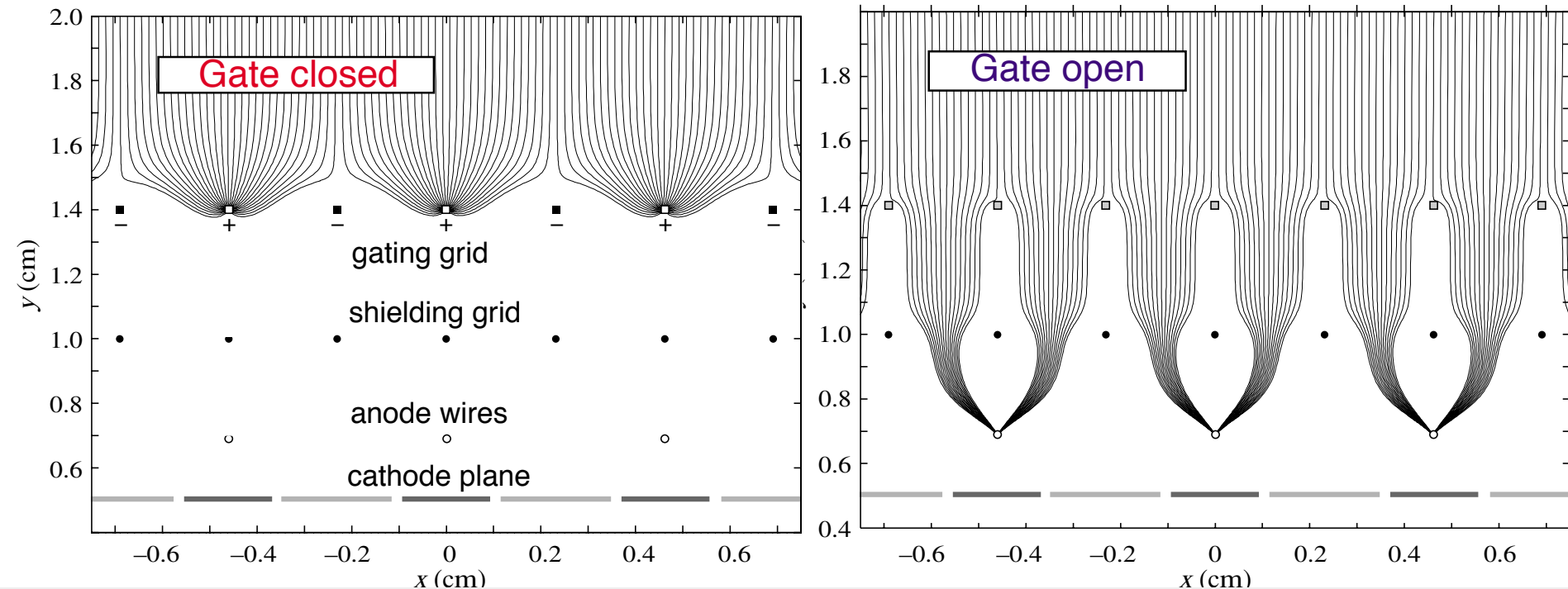
Difficulty: space charge effects due to slow moving ions
change effective E-field in drift region

Important: most ions come from amplification region

Solution: Invention of gating grid; ions drift towards grid ...

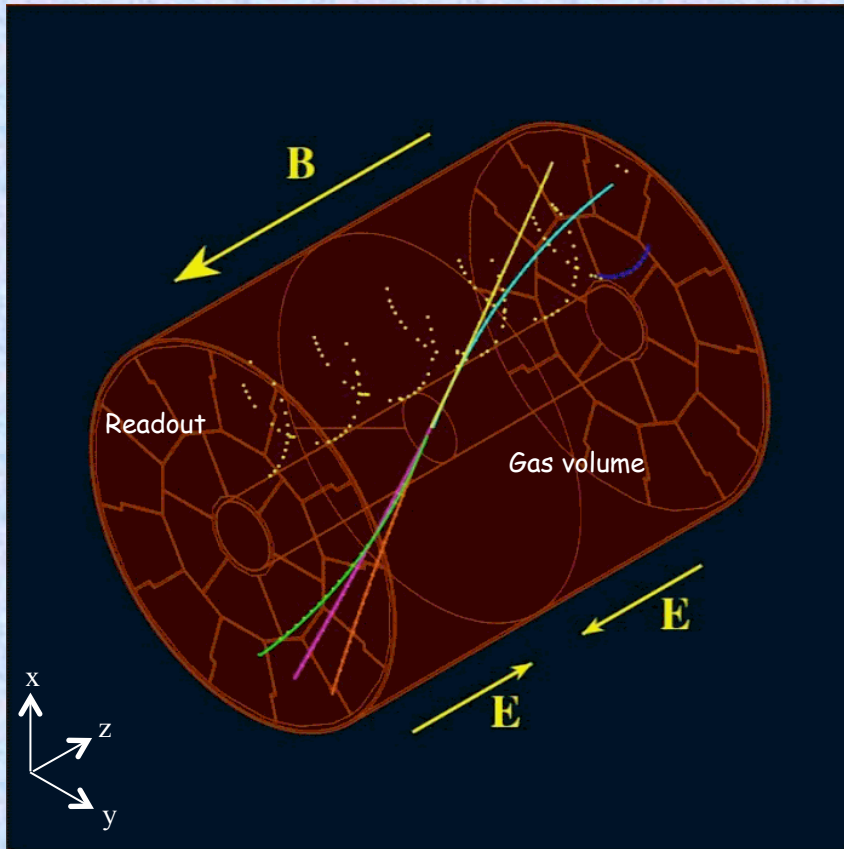
[Also: shielding grid to avoid sense wire disturbance when switching]

Requires external trigger to switch gating grid ...



Time Projection Chamber (TPC)

The TPC is a gas-filled cylindrical chamber with one or two endplates (D. Nygren, 1974)



Ingredients:

- Field cage for the E field
- Magnet for the B field
- Amplification system at the endplates
- Gating grid to suppress the ion feedback
- Laser calibration

1976: proposal for PEP4 at LBL
Proven technology: DELPHI, ALEPH (LEP), Ceres, NA49, STAR (heavy-ion experiments)
Future experiments: ALICE (LHC), ILC

	STAR	ALICE	ILC
Inner radius (cm)	50	85	32
Outer radius (cm)	200	250	170
Length (cm)	2 * 210	2 * 250	2 * 250
Charge collection	wire	wire	MPGD
Pad size (mm)	2.8 * 11.5 6.2 * 19.5	4 * 7.5 6*10(15)	2 * 6
Total # pads	140000	560000	1200000
Magnetic field [T]	0.5	0.5	4
Gas Mixture	Ar/CH4 (90:10)	Ne/CO2 (90:10)	Ar/CH4/CO2 (93:5:2)
Drift Field [V/cm]	135	400	230
Total drift time (μs)	38	88	50
Diffusion σ_T (μm/√cm)	230	220	70
Diffusion σ_L (μm/√cm)	360	220	300
Resolution in $r\phi$ (μm)	500-2000	300-2000	70-150
Resolution in r_z (μm)	1000-3000	600-2000	500-800
dE/dx resolution [%]	7	7	< 5
Tracking efficiency[%]	80	95	98

ALICE TPC:

Length: 5 meter

Radius: 2.5 meter

Gas volume: 88 m³

Total drift time: 92 μs

High voltage: 100 kV

End-cap detectors: 32 m²

Readout pads: 557568

159 samples radially

1000 samples in time

Gas: Ne/CO₂/N₂ (90-10-5)

Low diffusion (cold gas)

Gain: > 10⁴

Diffusion: $\sigma_t = 250 \mu\text{m}$

Resolution: $\sigma \approx 0.2 \text{ mm}$

$\sigma_p/p \sim 1\% p$; $\epsilon \sim 97\%$

$\sigma_{dE/dx}/(dE/dx) \sim 6\%$

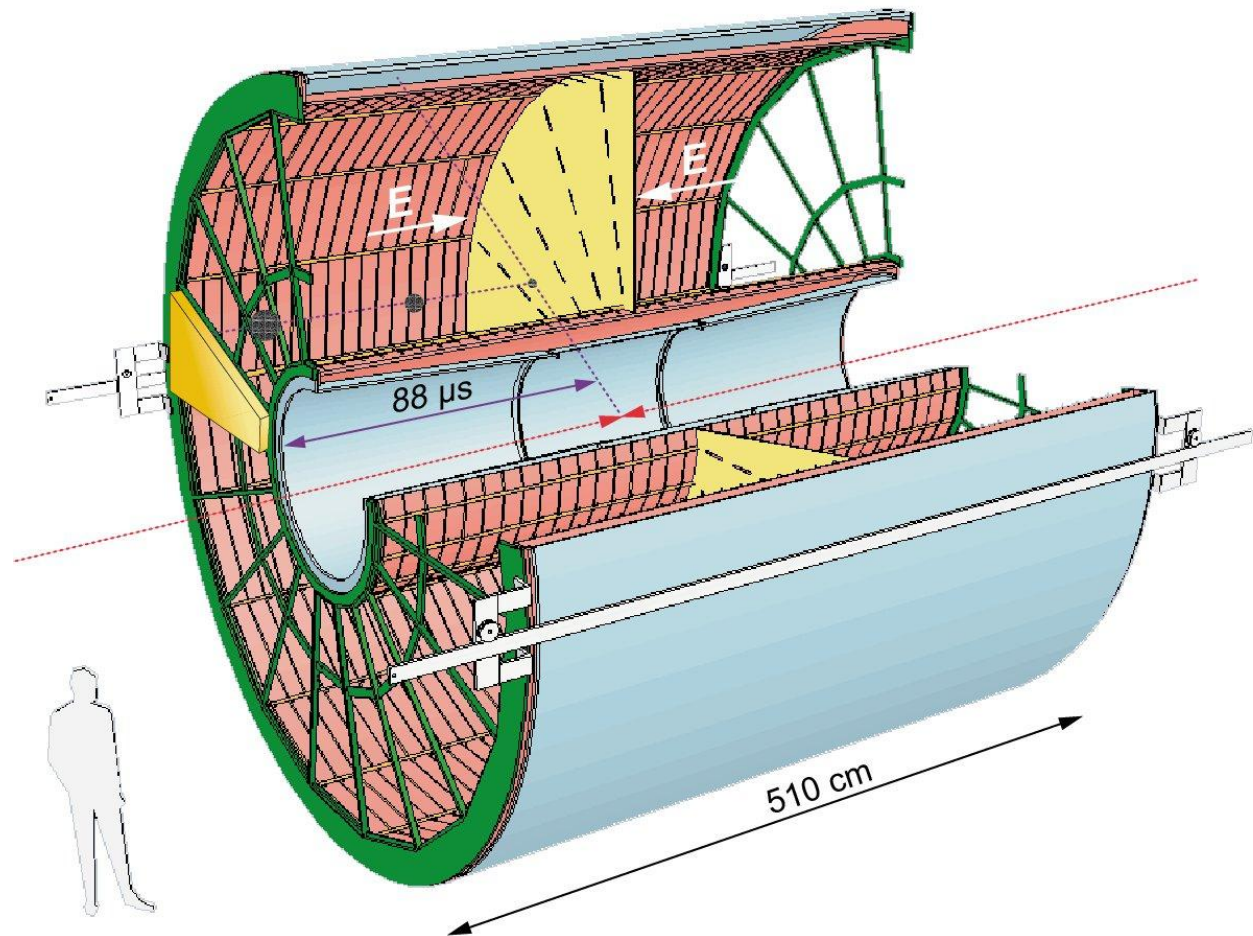
Magnetic field: 0.5 T

Pad size: 5x7.5 mm² (inner)

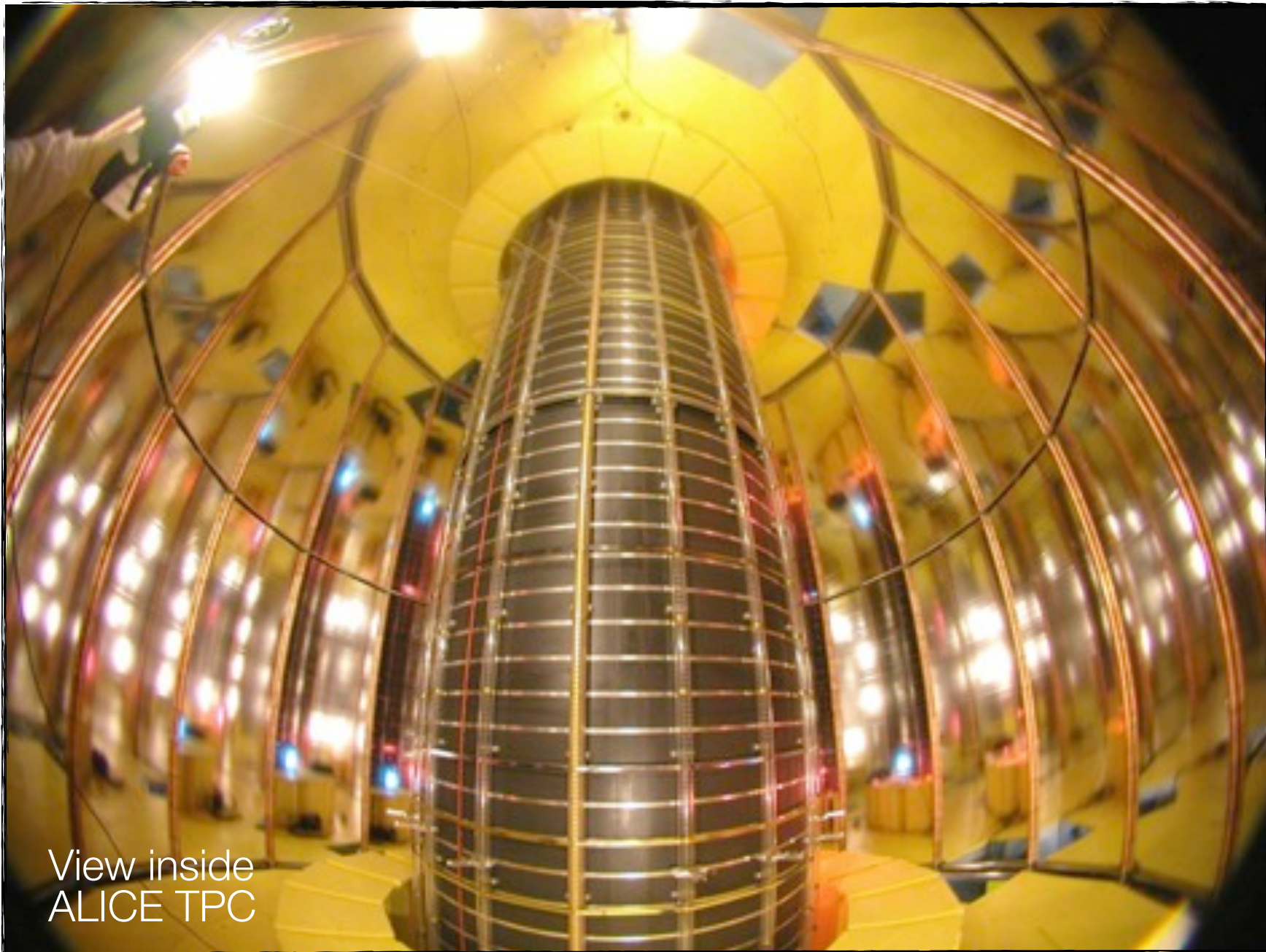
6x15 mm² (outer)

Temperature control: 0.1 K

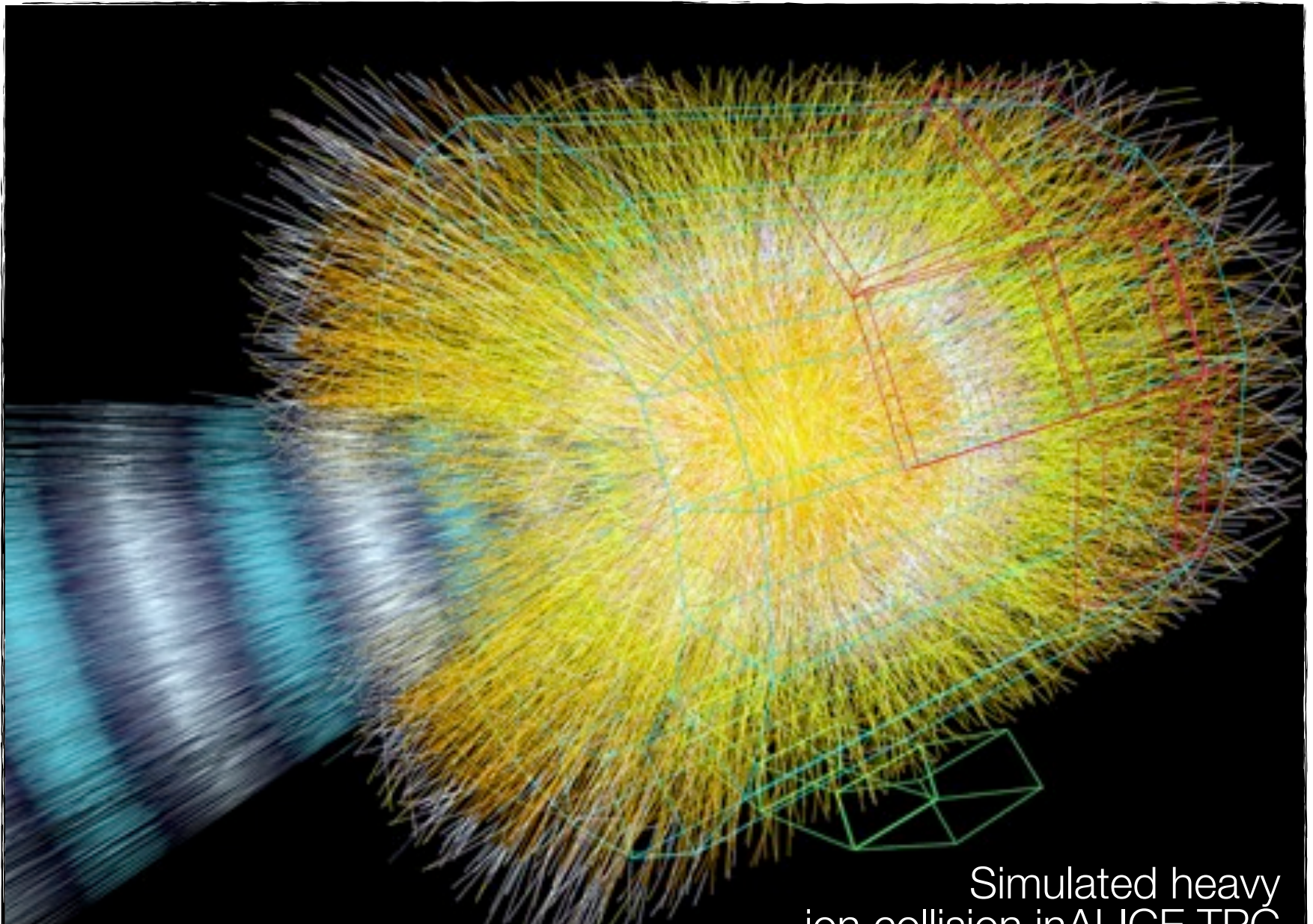
[also resistors ...]



Material: Cylinder build from composite material of airline industry ($X_0 = \sim 3\%$)

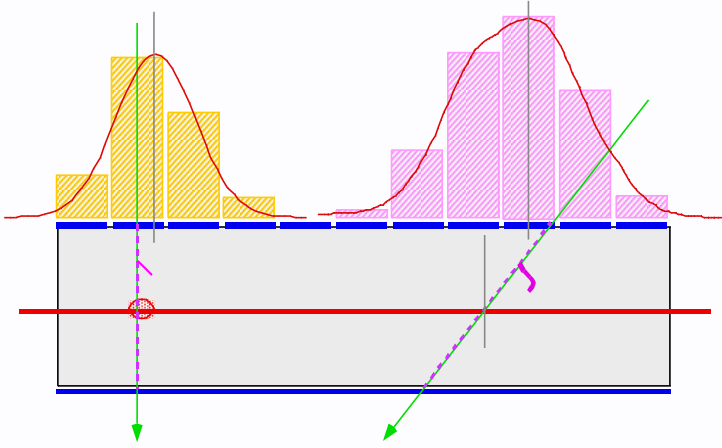


View inside
ALICE TPC

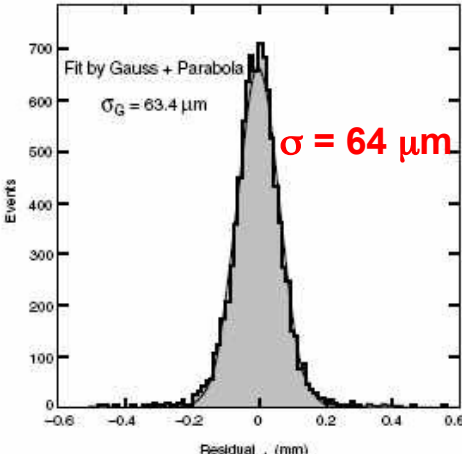
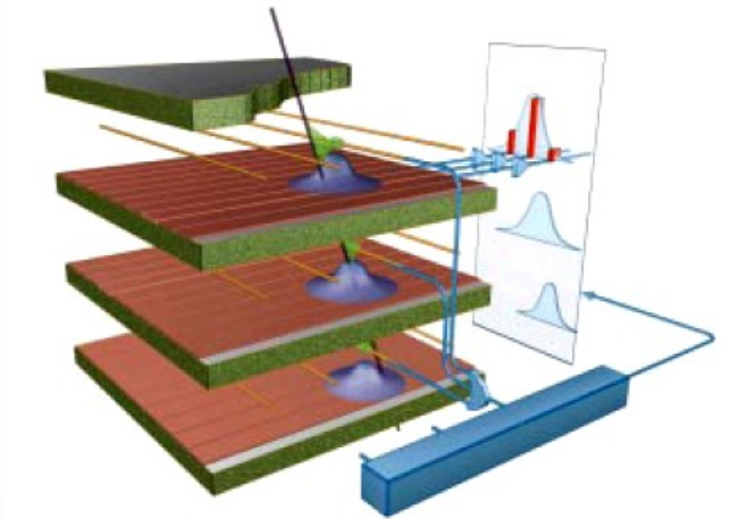


Simulated heavy ion collision in ALICE TPC

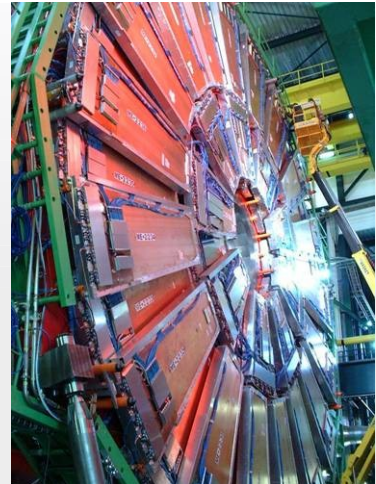
Precise measurement of the second coordinate by interpolation of the signal induced on pads.
 Closely spaced wires makes CSC fast detector.



Center of gravity of induced signal method.



Space resolution



CMS

Basic idea:

Use parallel plate chamber with high field ...

Electrons of ionization clusters start to produce an avalanche immediately ...

Induced signal = sum of all simultaneously produced avalanches ...

Signal: immediate ...

in contrast to e.g. wire chambers where avalanche only generated in vicinity of wire ...

But:

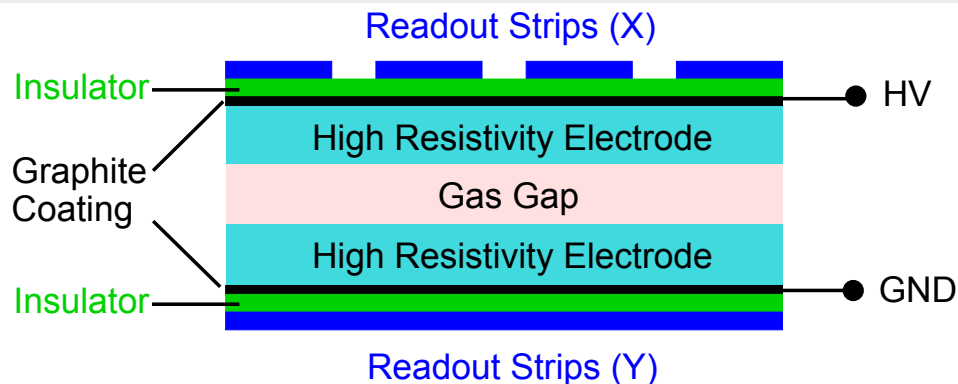
Electron avalanche develops according to Townsend [see above]:

$$n = n_0 e^{\alpha x}$$

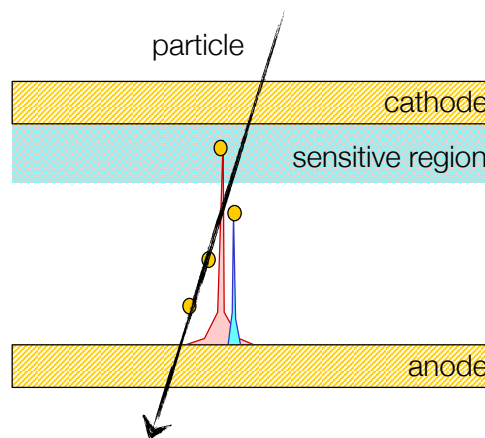
$$G = \frac{n}{n_0} = e^{\alpha x}$$

α : Townsend coefficient
 x : traversed path length
 G : amplification (gain)

Raether limit: $G \approx 10^8$; $\alpha x = 20$; then sparking sets in ...



Schematic image of typical RPC geometry



Schematic view of avalanche process

Gap size matters!
 [the smaller the better]

Thus: only avalanches traversing full gas gap produce detectable signal, i.e. limited signal region close to cathode ...

As maximum gain $< 10^8$; sensitive region limited to 25% of gap ...
 Time jitter: \sim time to cross sensitive region ...

Pestov chamber [1970]

[First example of resistive plate chamber]

Glass electrode (Pestov glass) + metal electrode

Operated at very high gas pressure: 12 atm

[For large density of primary ionization i.e. good detection efficiency]

Gas gap of 100 μm ; time resolution: 50 ps

Disadvantages:

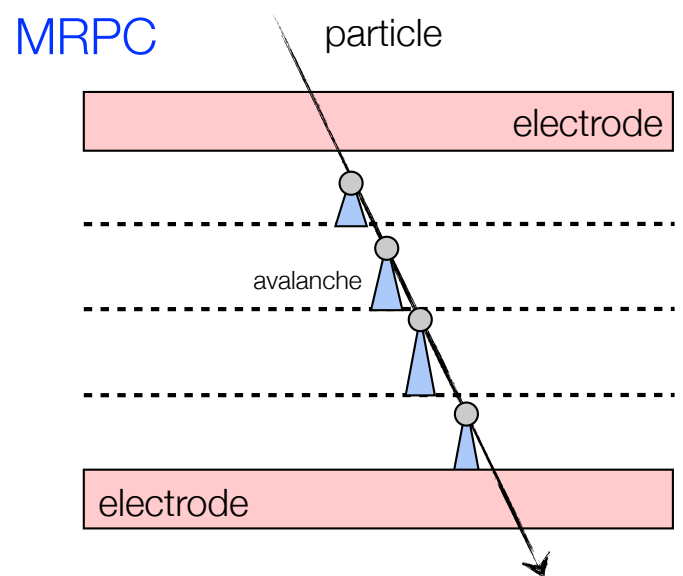
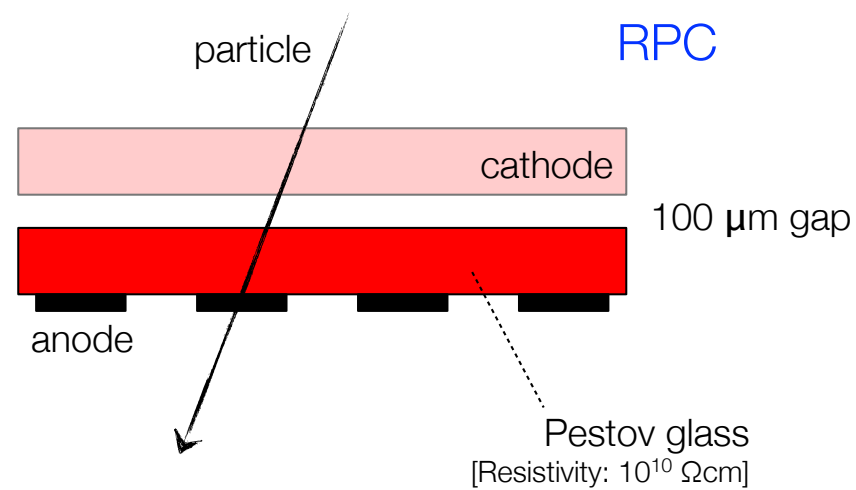
- Mechanical constraints high pressure
- Non-commercial glass (high resistivity)
- Limited sensitive volume
- Long tails of late events

Multi-gap RPC

[Developed for ALICE particle ID]

Idea: very high gas gain for immediate avalanche production, but mechanism to stop avalanche growth before sparking

Solution: add boundary layers invisible to fast induced signal; external electrodes sensitive to any of the initiated avalanches



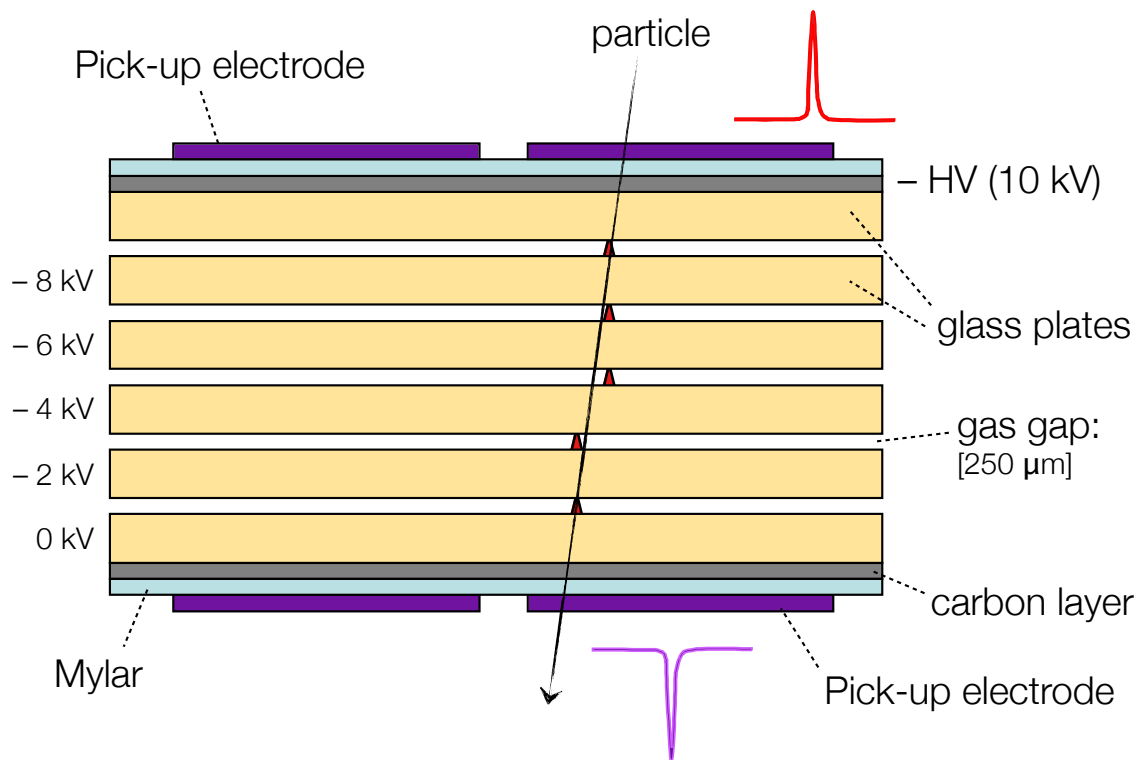
Multi-gap Resistive Plate Chamber

Stack of equally spaced resistive plates with voltage applied to external surfaces ...

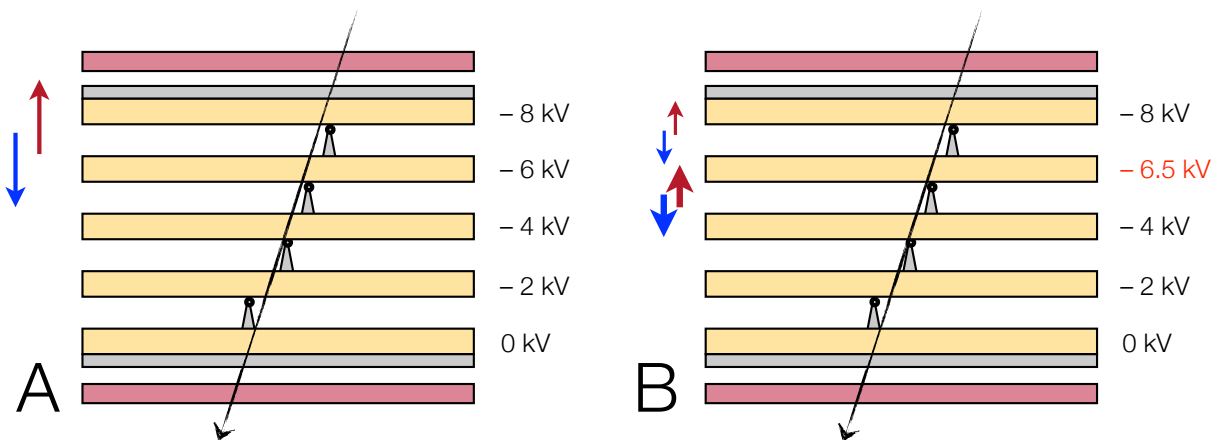
Internal plates electrically floating ...

Electrodes on external surfaces ...
[Resistive plates transparent to induced signal]

Internal plates take correct voltage ...
[Feedback due to electron/ion flow]



Feedback principle:



- ➔ Flow of electrons
- ➔ Flow of positive ions

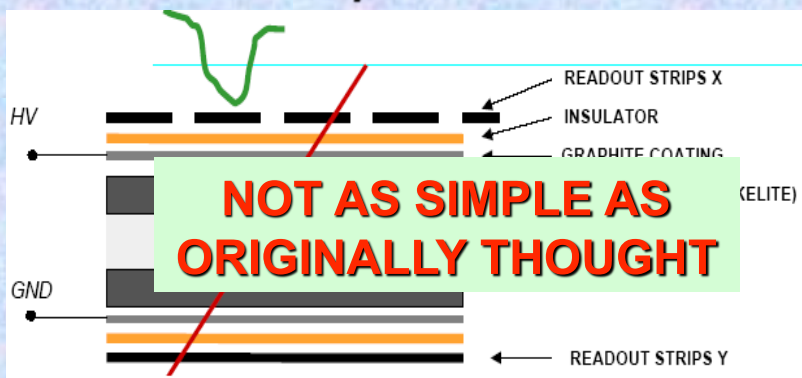
A: Same 2 kV across each gap; same gain, i.e. same charge flow ...

B: Flow to layer with 6.5 kV not symmetric; flow decreased for electrons and increased for ions ...

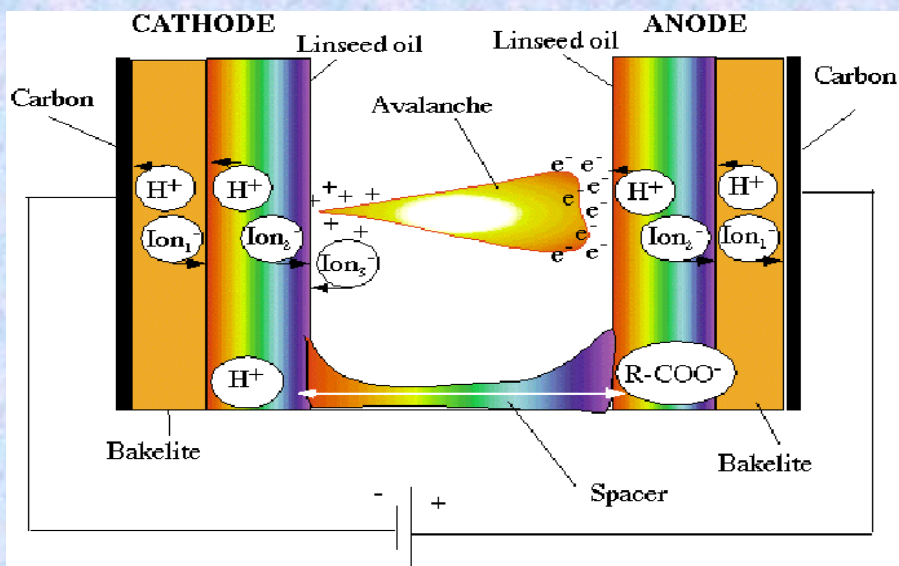
➔ System will go back to symmetric state with 2kV for all gaps ...

Conceptual View of a Resistive Plate Chamber (RPC)

RPC: Resistive Plate Chamber
Parallel-Plate capacitor: $E > 100\text{kV/cm}$



- Resistive plate: Oiled bakelite or ionic-conductive glass
- High electrode resistivity ($10^9\text{-}10^{12} \Omega \text{ cm}$) limits energy contained in charge avalanche
- Resistivity limits the rate capability
- Major advantages: good time resolution ($\sim 1 \text{ ns}$), With multi-gap RPC ($\sim 50 \text{ ps}$) large area coverage at affordable cost



Ionic conduction model of RPC:

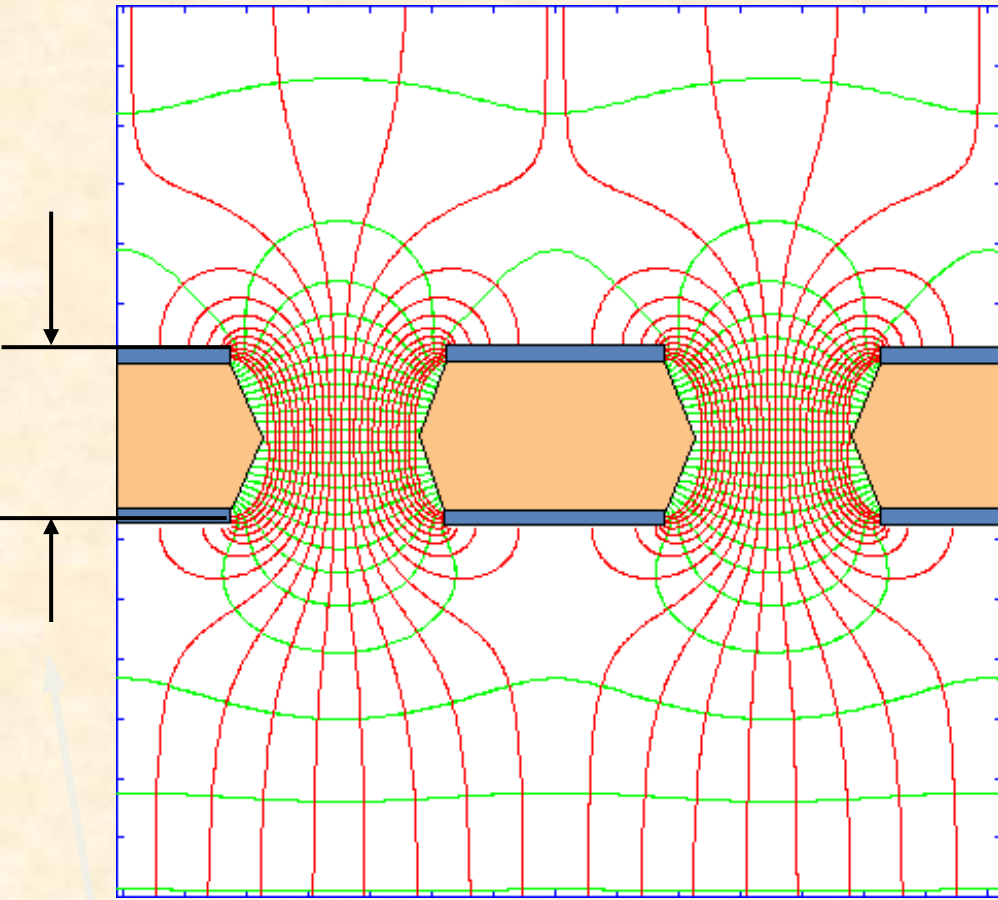
There are several ions involved in the current flow.

The charge exchange has to work well to prevent charging effects at various boundaries: gas, the linseed oil, the Bakelite and the graphite.

If a resistivity buildup occurs at some boundary, there may be a charging effect \rightarrow subsequent 'RPC death'

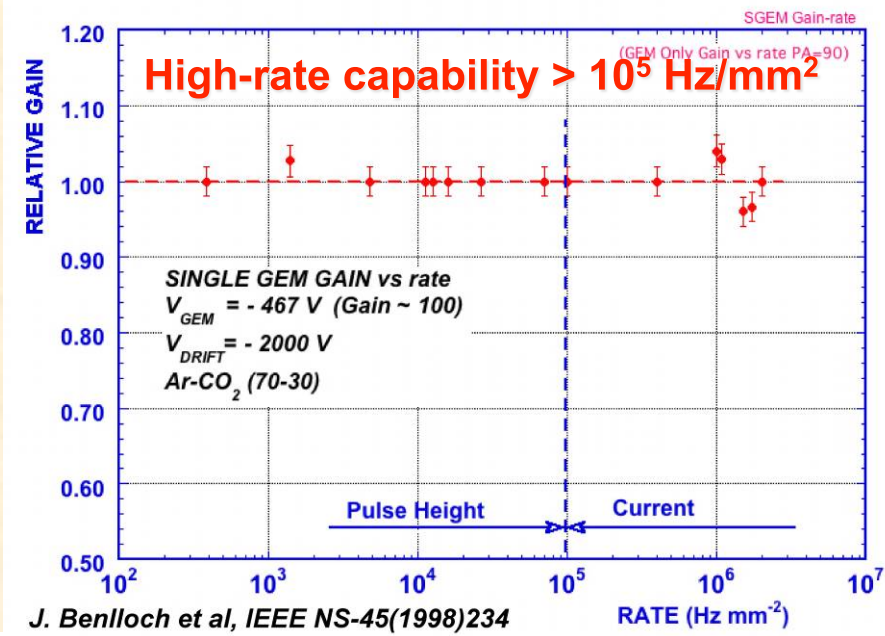
R. Santonico, Nucl. Instr. and Meth. A 187(1981)377
 R. Santonico, Nucl. Instr. and Meth. A 263(1988)20
 J. Va'vra, Nucl. Instrum. Methods A515(2003)1

Gas Electron Multiplier (GEM)

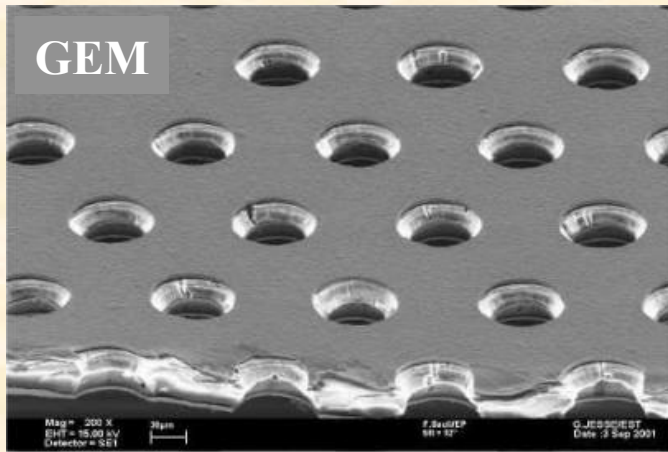


Thin metal-coated polymer foil chemically pierced by a high density of holes. Upon applying a voltage gradient, electrons released on top side, drift into the hole, multiply in avalanche and transfer the other side. Proportional gains $>10^3$ obtained in most common gases.

- Thickness: $\sim 50 \mu\text{m}$
- ΔV : 400 - 600 V
- Hole Diameter: $\sim 70 \mu\text{m}$
- Pitch: $\sim 140 \mu\text{m}$



GEM



Gas Electron Multiplier (GEM):

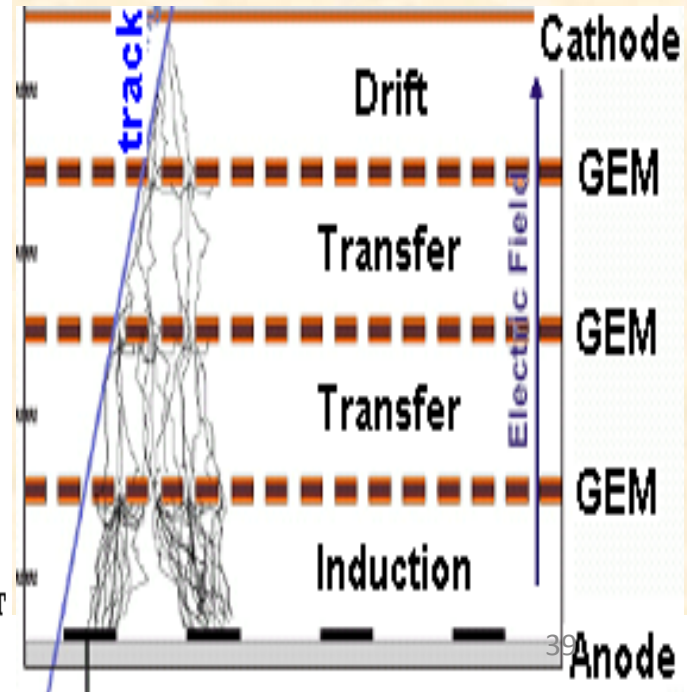
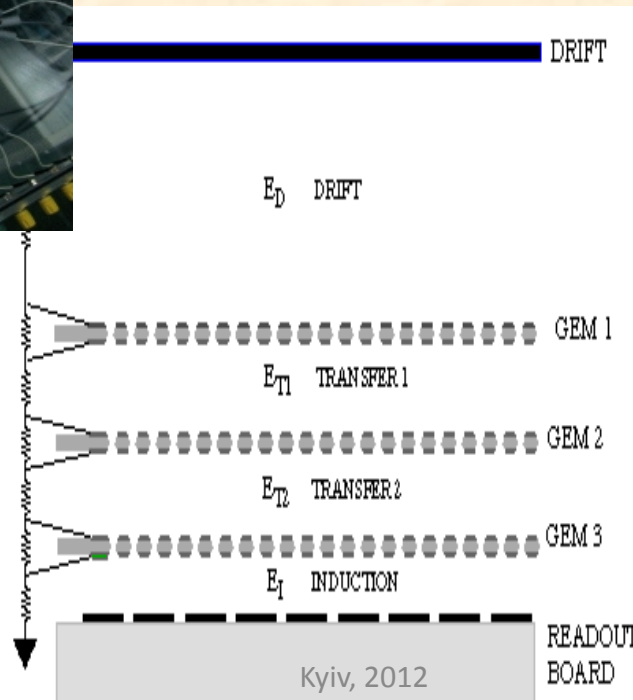
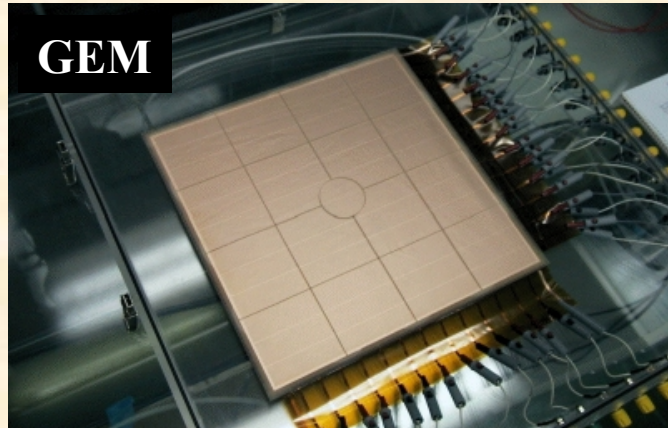
F. Sauli, NIM A386(1997) 531;

F. Sauli, <http://www.cern.ch/GDD>

Separation of amplification stage (GEM) and readout stage (PCB, anode)



GEM

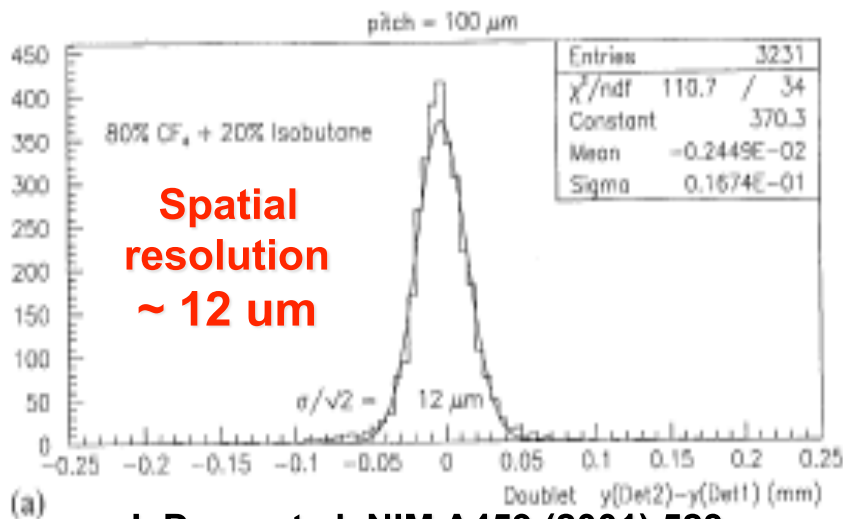


Parallel plate multiplication in thin gaps
between a fine mesh and anode plate

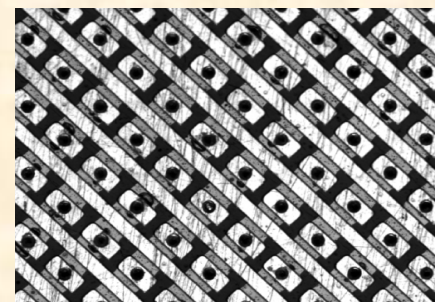
Y. Giomataris,
NIM A376(1996) 29

CAST readout:

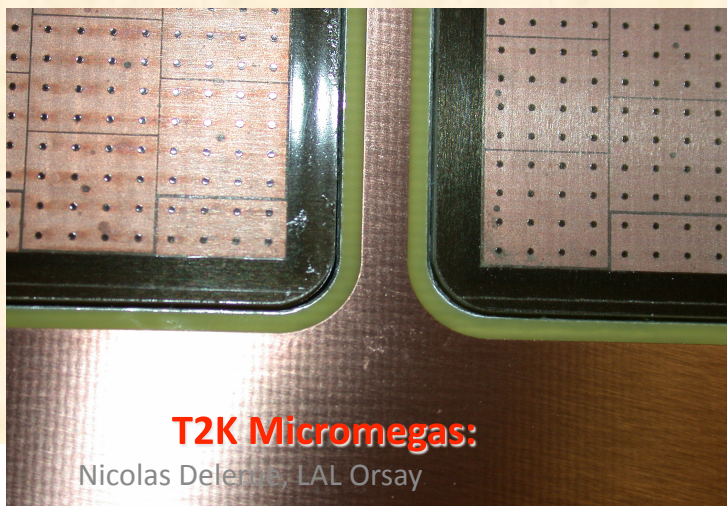
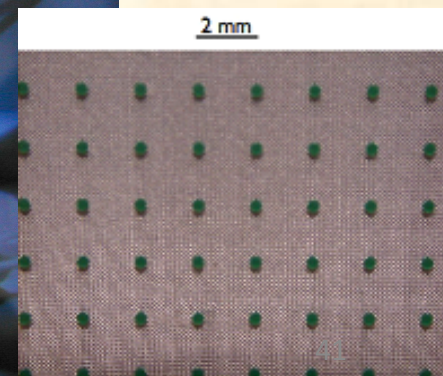
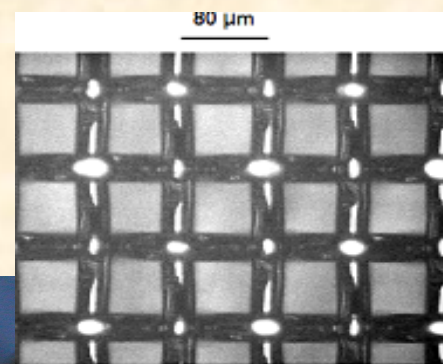
Small gap \rightarrow good energy resolution



J. Derre et al, NIM A459 (2001) 523



"Bulk" Micromegas:



T2K Micromegas:

Nicolas Delerue, LAL Orsay



**Piccolo Micromegas
in Casaccia Reactor**

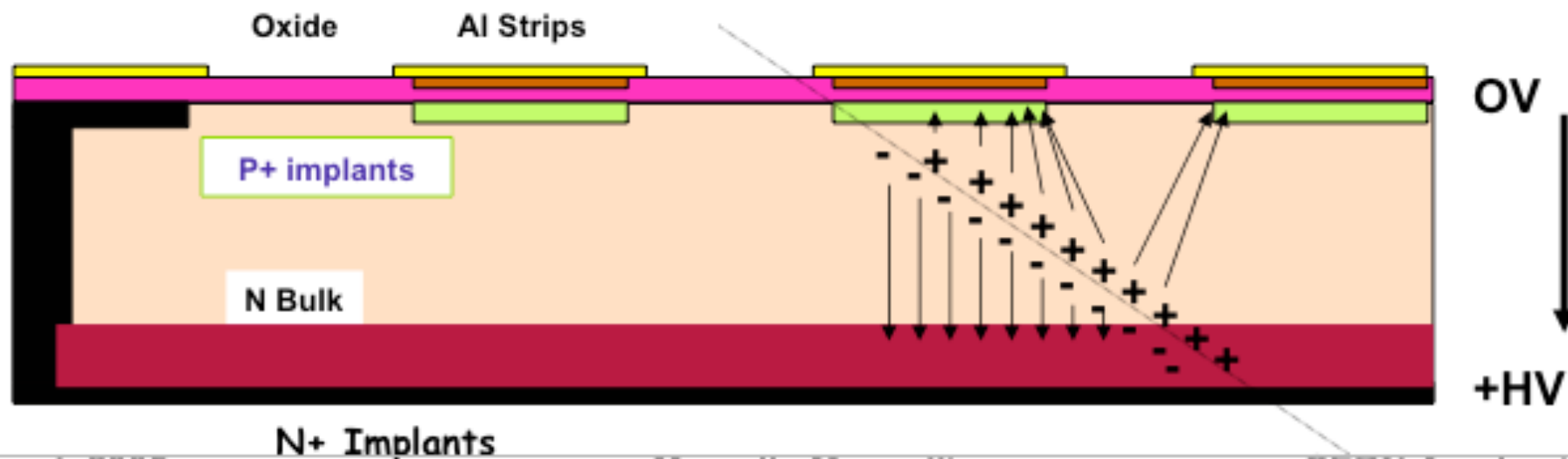
Kyiv, 2012

Bulk depletes from P+ implants, “front-side“ to N+ implant, “back-side“

Electron-hole pairs generated in the depleted region drift to the N+ and P+ electrodes respectively and generate a signal \sim to the depleted sensor thickness

Electron-hole pairs generated in the (conductive) un-depleted region recombine locally, and generate no signal

Even in a partially depleted sensor, the signal on the “front-side“ is localized



Electrical characteristics of strip detectors

Sensor thickness & bulk resistivity: determines depletion voltage

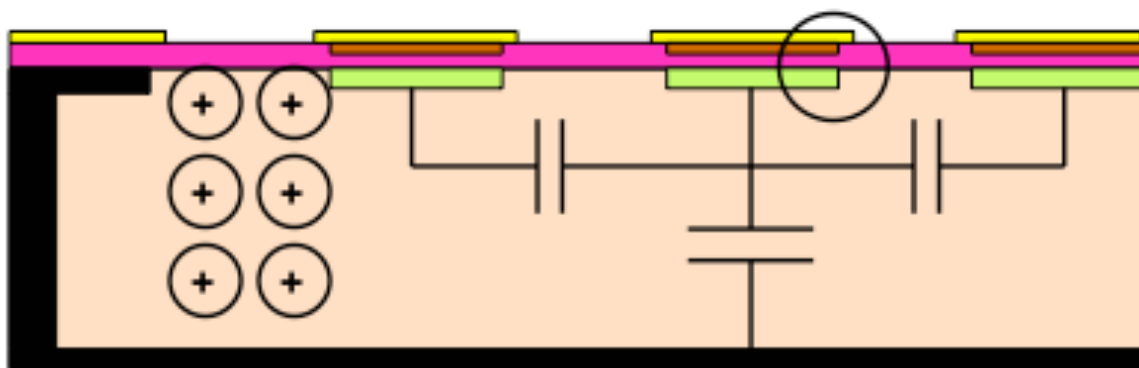
$$(V_{\text{depletion}} \sim N_{\text{eff}} * \text{Thickness}^2)$$

Strip Pitch / Width ratio: determines strip capacitive couplings & electronic noise

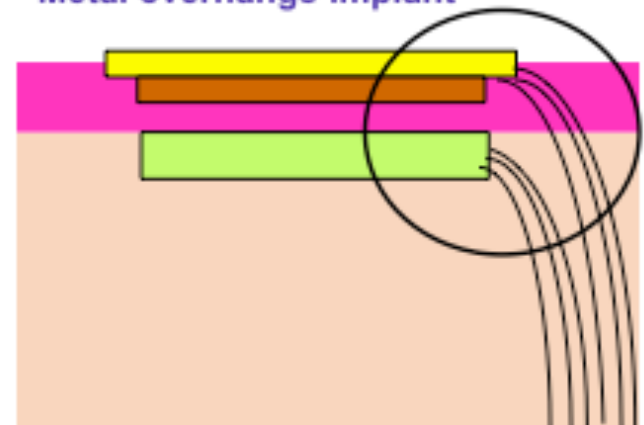
Strip Pitch & Width; Width of metal vs. implant: determine Electric field geometry, in particular high field region at strip edges & sensor breakdown characteristics

Nb. Breakdown voltage in Silicon Oxide $\sim 30 *$ breakdown voltage in Silicon bulk

Single-Sided Lithographic Processing (AC, Poly-Si biasing)



Metal overhangs implant



Radiation damage eventually results in “type inversion”

The initially N bulk undergoes “type inversion” and becomes P

The depletion voltage decreases and then increases again with higher fluence

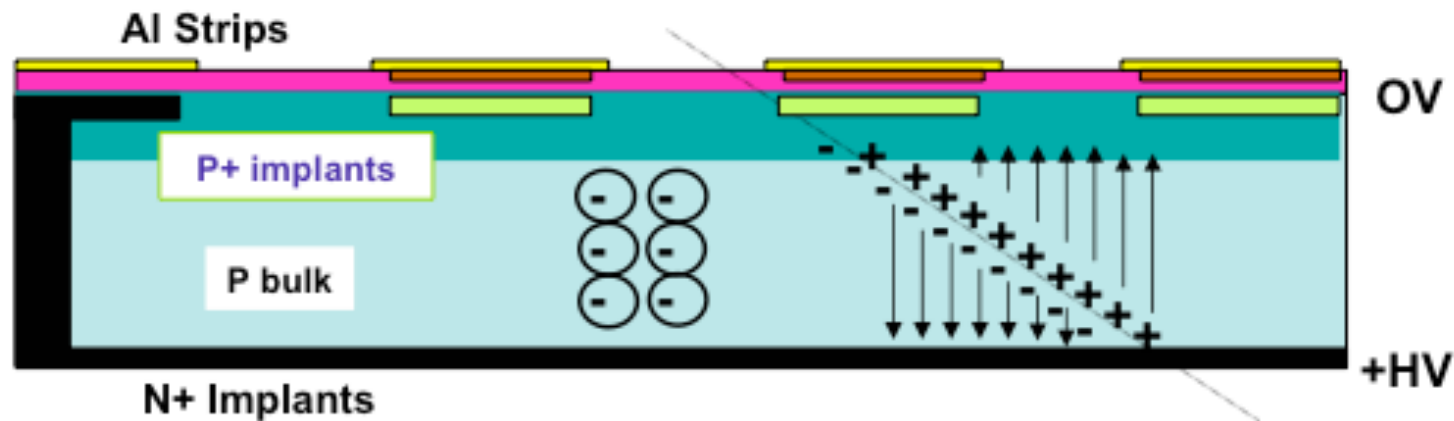
The effectively P bulk depletes from N+ implants, “back-side”, to P+ implant, “front-side”

Electron-hole pairs generated in the depleted region drift to the N+ and P+ electrodes respectively and generate a signal \sim to the depleted sensor thickness

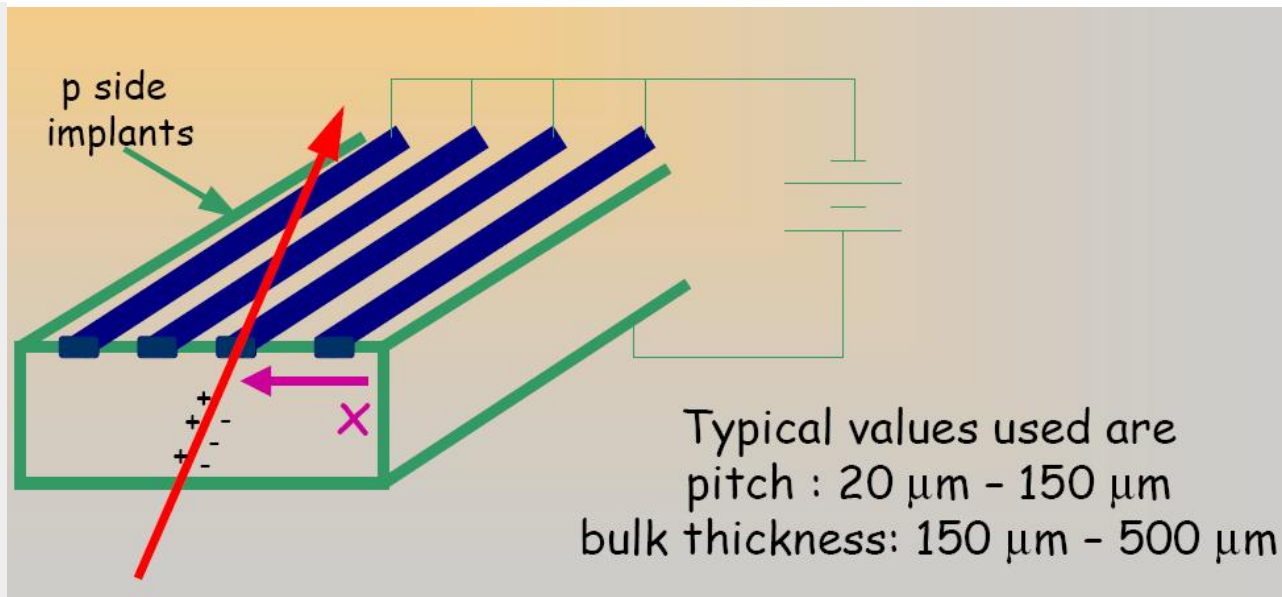
Radiation induced defects trap charge, leading to a loss of signal unless high fields

In the partially depleted sensor, the signal on the “front-side” is no longer localized

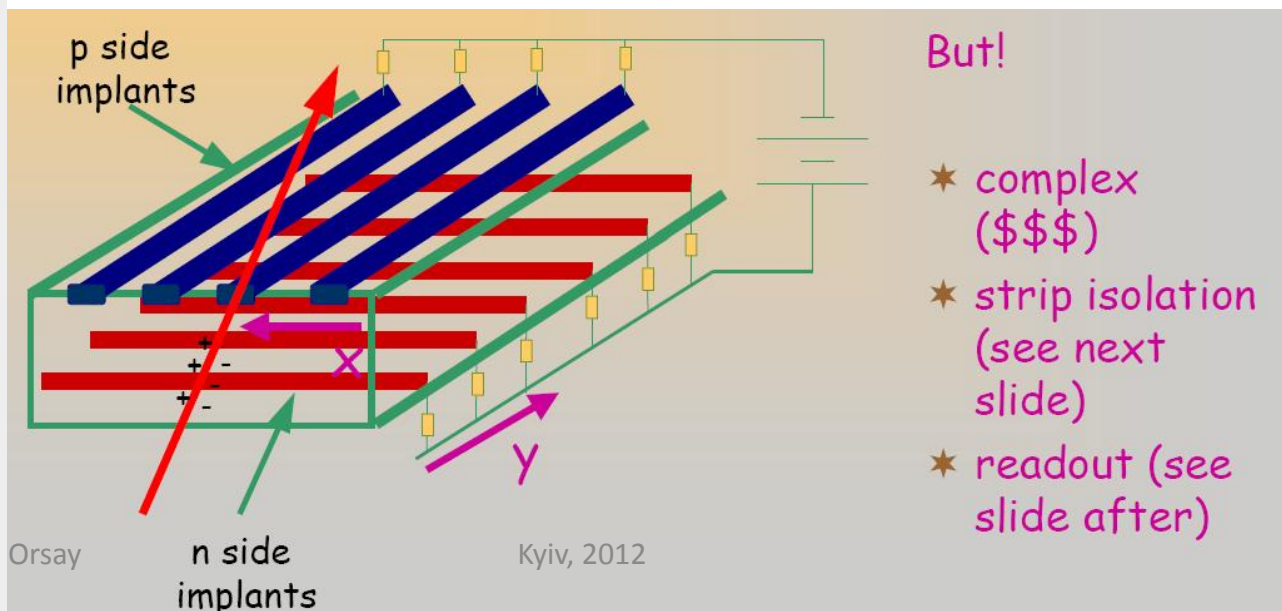
Sensor leakage current increases linearly with fluence (by \sim 3 orders of magnitude)



Measure coordinate → strips

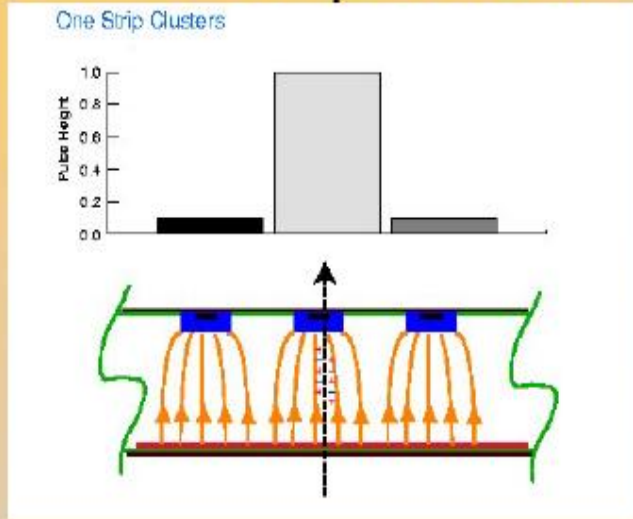


Strips on both sides → 3D measurement



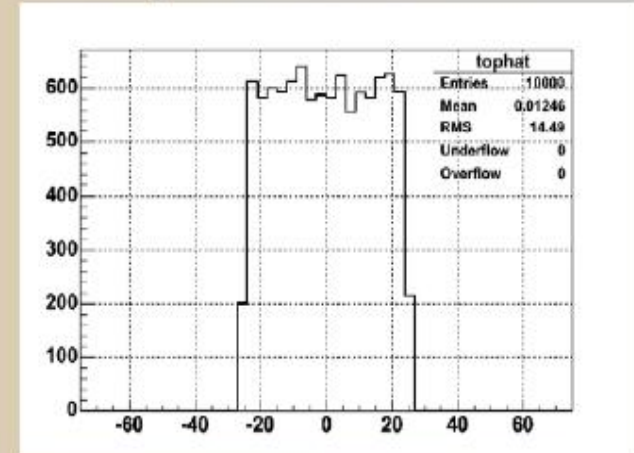
Resolution is the spread of the reconstructed position minus the true position

For one strip clusters

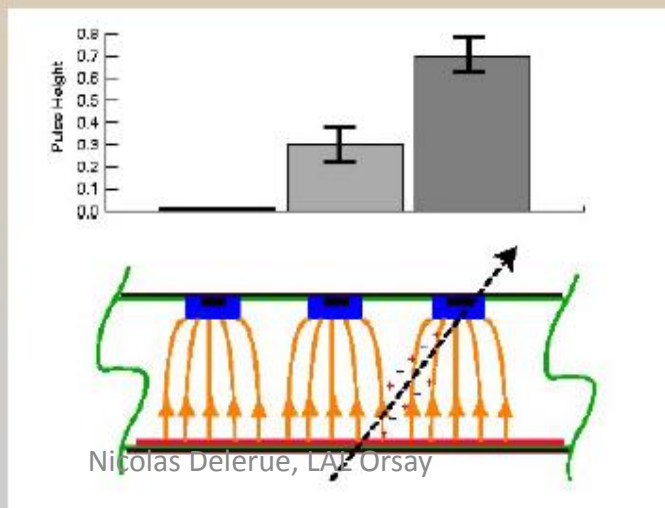


$$\sigma = \frac{\text{pitch}}{\sqrt{12}}$$

"top hat" residuals

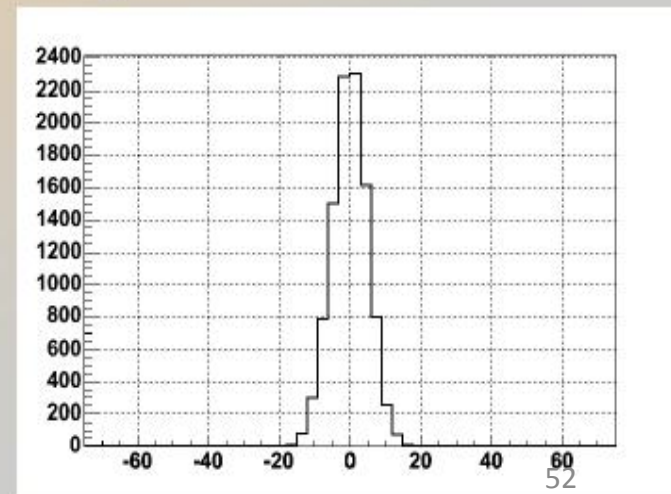


For two strip clusters



$$\sigma \approx \frac{\text{pitch}}{1.5 * (S/N)}$$

"gaussian" residuals



SILICON DETECTORS

Elemental semiconductors

★ Germanium:

Used in nuclear physics, due to small band gap (0.66 eV) needs cooling (usually done with liquid nitrogen at 77 K)

★ Silicon:

Standard material for vertex and tracking detectors in high energy physics, can be operated at room temperature, synergies with micro electronics industry.

★ Diamond (CVD or single crystal):

Large band gap, requires no depletion zone, very radiation hard, drawback is a low signal and high cost!

Compound semiconductors

Compound semiconductors consist of two (binary semiconductors) or more atomic element.

- GaAs: Faster and probably more radiation resistant than Si.
- CdTe: High atomic numbers (48+52) hence very efficient to detection

The ideal semiconductor detector

One of the most important parameter of a detector is the signal to noise ratio (SNR). A good detector should have a large SNR. However this leads to two contradictory requirements:

✗ **Large signal**

→ low ionisation energy → small band gap

✗ **Low noise**

→ very few intrinsic charge carriers

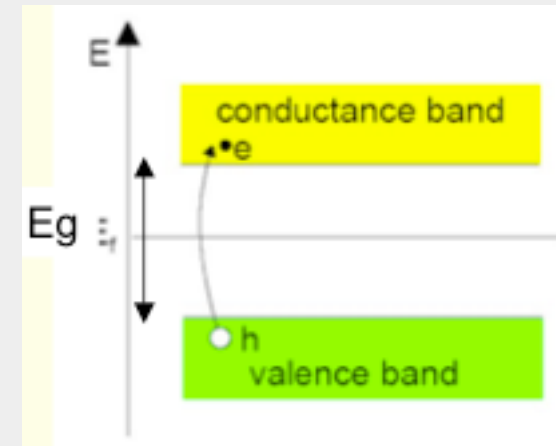
→ large band gap

An optimal material should have $E_g \approx 6 \text{ eV}$.

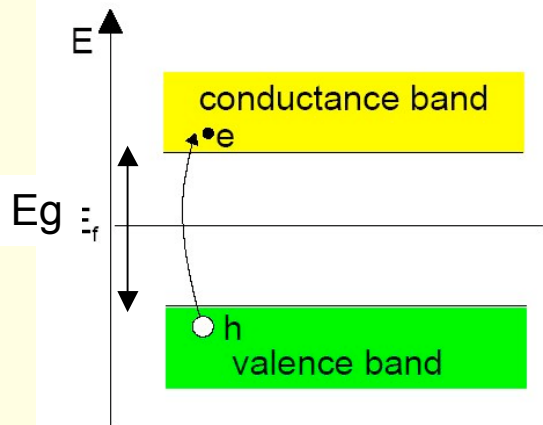
In this case the conduction band is almost empty at room temperature and the band gap is small enough to create a large number of e-h⁺ pairs through ionisation.

Such a material exist, ==> **Diamond**.

However even artificial diamonds (e.g. CVD diamonds) are too expensive for large area detectors.



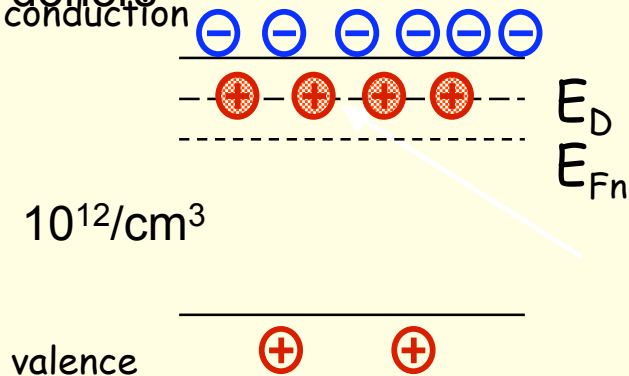
Solid state detectors



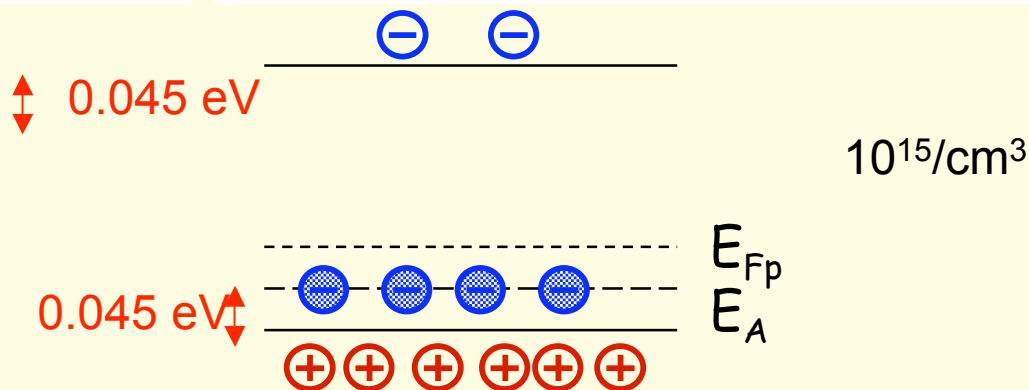
At $T=0$ Semi Conductor is an insulator but when $T \nearrow$
 electron density (n) = Hole density (p) = n_i
 $1.45 \cdot 10^{10}/\text{cm}^3$ for silicon (given by $\exp(-E_g/kT)$)

In a $1\text{cm} \times 1\text{cm} \times 300\mu\text{m}$ detector already $4.5 \cdot 10^8$ free charges
 against $3.2 \cdot 10^4$ e/h produced for a mip particle
 $\rightarrow S/\sqrt{N} = 1$ no chance to see signal
 \rightarrow Should reduce the number of free charge carriers
 \rightarrow Depletion of detector using doping

Doping type N with As,P acts as donors



Doping type P with B ,Ga, AL, In as acceptors



Electrons are the majority carriers

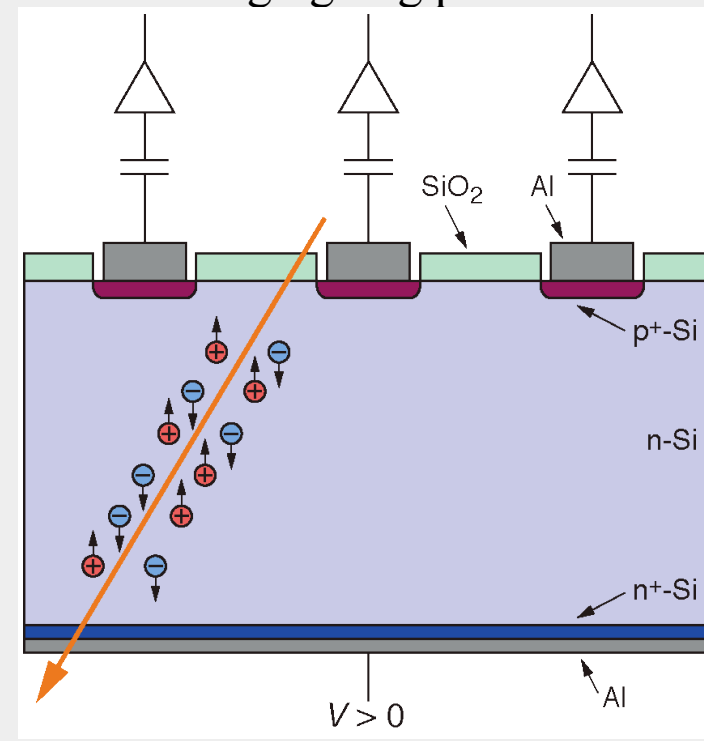
holes majority carriers

DC coupled strip detector

- Through going charged particles create e-h⁺ pairs in the depletion zone (about 30.000 pairs in standard detector thickness).
- These charges drift to the electrodes.
- The drift (current) creates the signal which is amplified by an amplifier connected to each strip.
- From the signals on the individual strips the position of the through going particle is deduced.

A typical n-type Si strip detector:

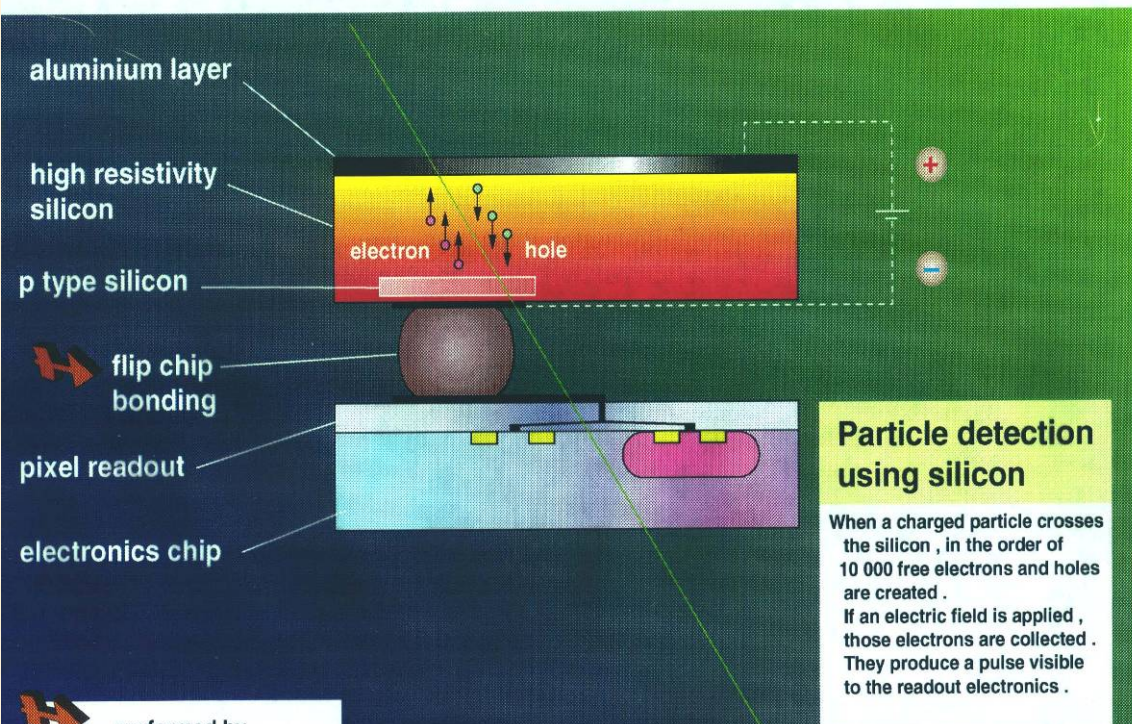
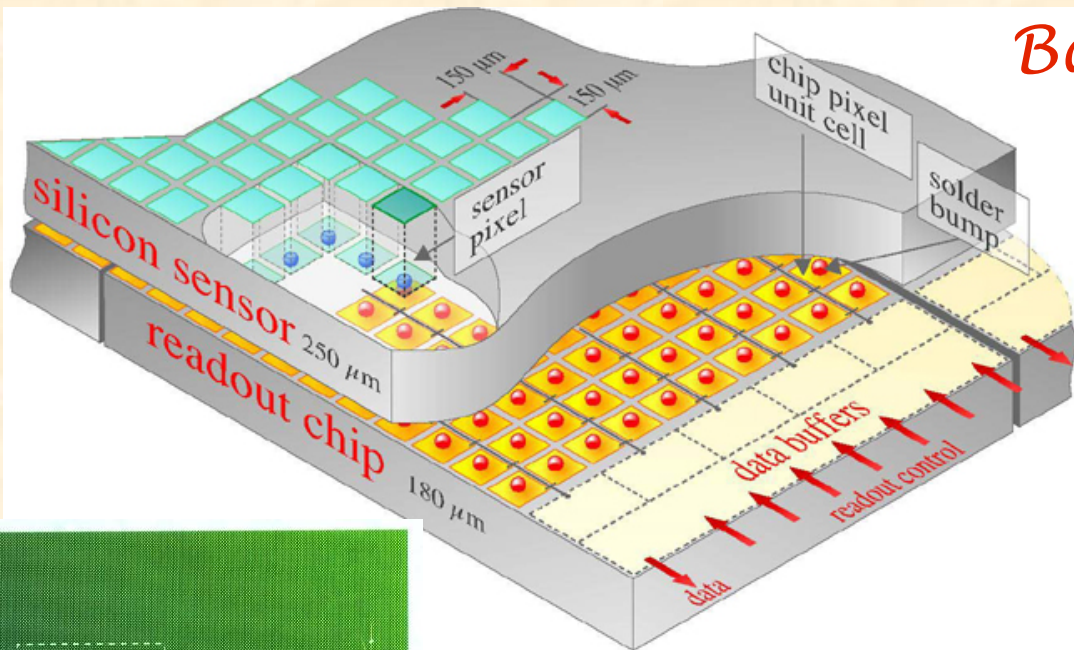
- ★ n-type bulk: $\rho > 2 \text{ k}\Omega\text{cm}$
- thickness 300 μm
- ★ Operating voltage $< 200 \text{ V}$.
- ★ n⁺ layer on backplane to improve ohmic contact
- ★ Aluminum metallization



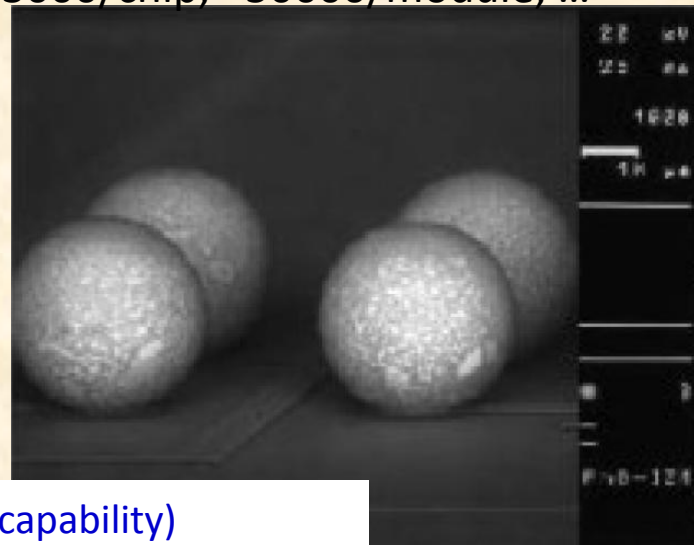
From strips to pixels

Flip-chip assembly

Pixel detector bump bonded to a read-out chip

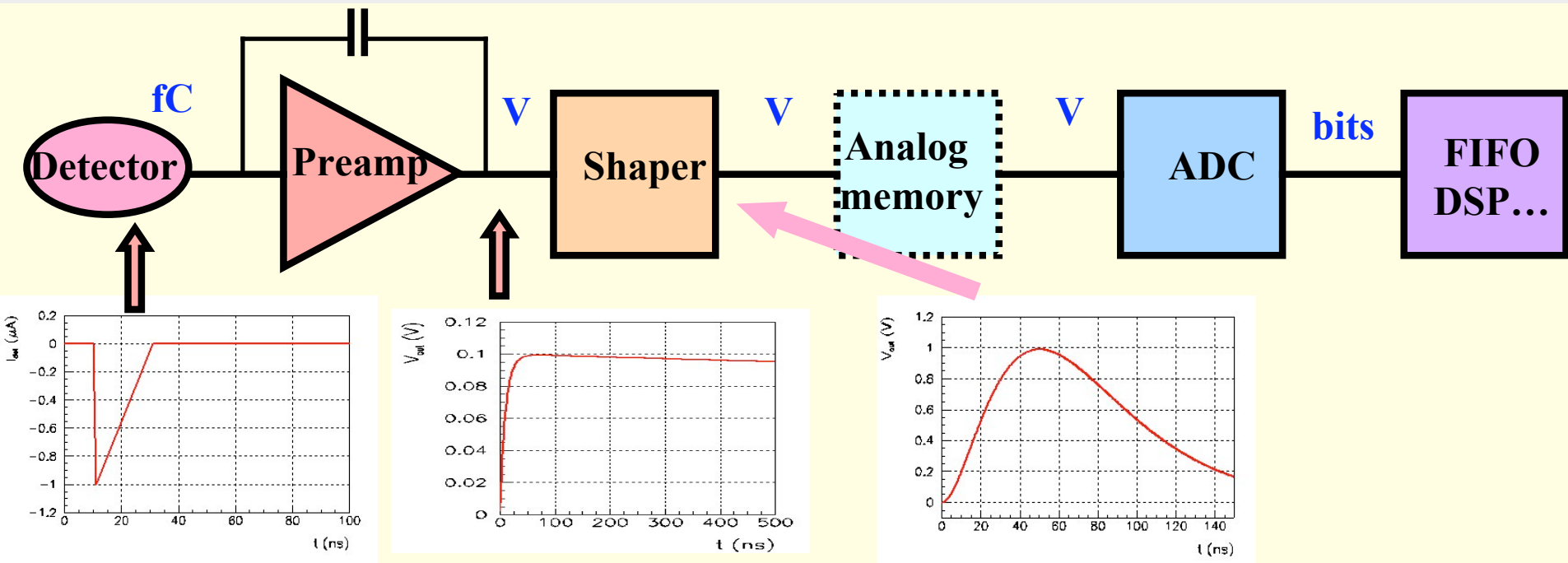


PbSn or In, 6-20 μm
~3000/chip, ~50000/module, ...



performed by
GEC
Marconi Materials LTD
Caswell UK

- Truly 2D event image (high rate capability)
- High granularity of readout plane (~50 μm)
- No long signal routine lines (low noise)



Most front-ends follow a similar architecture :

- Very small signals (fC) -> need **amplification** and **optimisation of S/N (filter)**
- Measurement of **amplitude** and/or **time** (ADCs, discris, TDCs)
- Several thousands to millions of channels
- Needs time to decide to keep or not the event : memory

Constraints as seen by a Electronics engineer (From C. de La Taille / LAL)

